
Theses and Dissertations

Summer 2014

Population pharmacokinetics of artesunate and dihydroartemisinin in children and pregnant women with malaria

Carrie Ann Morris
University of Iowa

Copyright 2014 Carrie Ann Morris

This dissertation is available at Iowa Research Online: <http://ir.uiowa.edu/etd/1367>

Recommended Citation

Morris, Carrie Ann. "Population pharmacokinetics of artesunate and dihydroartemisinin in children and pregnant women with malaria." PhD (Doctor of Philosophy) thesis, University of Iowa, 2014.
<http://ir.uiowa.edu/etd/1367>.

Follow this and additional works at: <http://ir.uiowa.edu/etd>



Part of the [Pharmacy and Pharmaceutical Sciences Commons](#)

POPULATION PHARMACOKINETICS OF ARTESUNATE AND
DIHYDROARTEMISININ IN CHILDREN AND PREGNANT WOMEN WITH
MALARIA

by
Carrie Ann Morris

A thesis submitted in partial fulfillment
of the requirements for the Doctor of
Philosophy degree in Pharmacy
in the Graduate College of
The University of Iowa

August 2014

Thesis Supervisor: Professor Lawrence Fleckenstein

Graduate College
The University of Iowa
Iowa City, Iowa

CERTIFICATE OF APPROVAL

PH.D. THESIS

This is to certify that the Ph.D. thesis of

Carrie Ann Morris

has been approved by the Examining Committee
for the thesis requirement for the Doctor of Philosophy
degree in Pharmacy at the August 2014 graduation.

Thesis Committee: _____
Lawrence Fleckenstein, Thesis Supervisor

Maureen Donovan

Jennifer Fiegel

Daryl Murry

Erika Ernst

ACKNOWLEDGMENTS

I am extremely grateful to my mentor Dr. Larry Fleckenstein for the extraordinary research opportunities I have had these past five years. I want to thank him for sharing his extensive knowledge of this research field, as well as for providing valuable advice and support regarding my long term plans, even as those plans substantially evolved.

I would also like to extend my gratitude to my committee members, Dr. Maureen Donovan, Dr. Jennifer Fiegel, Dr. Erika Ernst, and Dr. Daryl Murry, for providing helpful advice and useful insights.

Additionally, I would like to express my sincere thanks to Mark Schmidt for the innumerable engaging conversations which always brightened my day, as well as for offering me unwavering support throughout my time in the graduate program.

Finally, I would like to thank Amal Ayyoub and Youwei Bi for the valuable discussions about numerous aspects of pharmacokinetics and population modeling. These discussions aided my understanding of these domains.

ABSTRACT

Artemisinin derivatives are key to the current global treatment approach for malaria. However, much remains unknown regarding the pharmacokinetics of these agents, particularly in children and pregnant women, two groups highly vulnerable to development of severe malaria infection. In this thesis, nonlinear mixed effects modeling is used to characterize the pharmacokinetics of the artemisinin derivative artesunate and its active metabolite, dihydroartemisinin (DHA), in children and in pregnant women.

Chapter 1 of this thesis contains a general review of the clinical pharmacokinetic findings for artesunate and DHA following artesunate administration by the intravenous, intramuscular, oral and rectal routes. Chapter 2 presents a population pharmacokinetic model utilizing both pediatric and adult data from one Phase II and four Phase III clinical trials evaluating the combination agent pyronaridine tetraphosphate/artesunate. The focus of the modeling described in this chapter is the evaluation of the effects of body size and gender on the pharmacokinetics of artesunate and DHA in pediatric patients with uncomplicated malaria. Chapter 3 consists of a population pharmacokinetic model built utilizing plasma artesunate and DHA concentrations from 26 parasitemic second and third trimester pregnant women and 25 parasitemic non-pregnant female controls in the Democratic Republic of Congo who received 200 mg oral artesunate.

The model described in Chapter 2 is a simultaneously implemented parent-metabolite model consisting of a one compartment model for artesunate, a one compartment model for DHA, and first-order artesunate absorption. Various approaches for incorporating body size on artesunate and DHA apparent clearance and volume of distribution parameters were evaluated, with a linear body surface area model and an allometric scaling model both proving satisfactory. The effect of gender was modeled on artesunate and DHA apparent clearance and volume terms. Only the effect of gender on DHA apparent clearance could be estimated with reasonable precision, with the 95%

confidence interval for the effect being almost wholly contained within the predefined 0.75 to 1.25 no relevant clinical effect interval. The model described in Chapter 3 consists of a one compartment model for artesunate, a one compartment model for DHA, and mixed zero-order, lagged first order absorption of artesunate. In this model, pregnancy was found to have a marked effect on DHA apparent clearance, with a pregnancy-associated increase in DHA apparent clearance of 42.3%.

The models described in this thesis indicate that, for a given mg/kg dose of artesunate, both young children and pregnant women would be expected, on average, to display lower DHA concentrations than would be observed following administration of the same mg/kg dose to non-pregnant adults. Suboptimal dosing has clinical implications for the individual as well as potential implications regarding parasite susceptibility. Given this, the findings of the research described in this thesis highlight the necessity of investigations designed to comprehensively characterize the pharmacokinetics of artesunate and DHA in these two highly susceptible populations.

TABLE OF CONTENTS

LIST OF TABLES	viii
LIST OF FIGURES	ix
INTRODUCTION	1
Malaria infection.....	1
Transmission regions.....	2
High risk groups	3
Malaria in children	3
Malaria in pregnant women.....	4
Prevention of malaria in children and pregnant women.....	5
Artemisinin derivatives.....	5
Artesunate pharmacokinetics in children and pregnant women.....	7
Overview of thesis.....	8
CHAPTER 1 REVIEW OF ARTESUNATE PHARMACOKINETICS.....	9
Objectives of literature review.....	9
Artesunate and DHA properties.....	10
Sources of variation introduced by study methodology	10
Artesunate and DHA protein binding.....	10
IV administration: Artesunate pharmacokinetics	11
IV administration: DHA pharmacokinetics	12
IV administration: Bioassay results.....	12
IM administration: Artesunate and DHA pharmacokinetics	13
Oral administration: Artesunate pharmacokinetics	14
Oral administration: DHA pharmacokinetics	16
Oral administration: bioassay results.....	17
Oral administration: Population pharmacokinetics	17
Rectal administration: Artesunate and DHA pharmacokinetics.....	19
Rectal administration: Population pharmacokinetics	20
Artesunate and DHA pharmacokinetics in pediatric patients.....	21
Artesunate and DHA pharmacokinetics in pregnant women	22
Disease effects on artesunate and DHA pharmacokinetics	25
Drug-drug interactions.....	26
Summary and conclusions	29
CHAPTER 2 EFFECT OF BODY SIZE AND GENDER ON ARTESUNATE PHARMACOKINETICS IN PEDIATRIC PATIENTS.....	57
Introduction.....	57
Methods	60
Data.....	60
Sample handling and analysis	62
Base model	63

Model selection	66
Covariate modeling: Body size descriptor	68
Covariate modeling: Full covariate model	71
Predictive checks	72
Covariate modeling: Exploring trends.....	73
Results.....	74
Data.....	74
Base model	74
Covariate modeling: Body size descriptor	76
Full covariate model.....	78
Covariate modeling: Exploring trends.....	81
Discussion.....	82
Physiologic basis for models	83
Covariate Model: Gender Effects.....	86
Pharmacokinetic Comparisons	87
Inclusion of adult data	88
Conclusions.....	89
CHAPTER 3 POPULATION PHARMACOKINETICS OF ARTESUNATE AND DIHYDROARTEMISININ IN PREGNANCY	109
Background.....	109
Methods	110
Study design	110
Sample analysis	112
Population pharmacokinetic analysis	112
Base model development.....	113
Covariate model building.....	115
Model evaluation	116
Results.....	117
Subject data	117
Model development.....	118
Model evaluation	119
Discussion.....	120
Limitations and Summary.....	126
CHAPTER 4 CLINICAL IMPLICATIONS AND CONCLUSIONS.....	135
Optimizing dose selection.....	135
Partner drugs in children and pregnant women	137
Pharmacokinetics and resistance	138
Needed future research	140
APPENDIX A CONTROL STREAM FOR LINEAR BSA MODEL IN CHAPTER 2	141

APPENDIX B	CONTROL STREAM FOR ALLOMETRIC SCALING MODEL IN CHAPTER 2	143
APPENDIX C	OUTPUT SUMMARY FOR LINEAR BSA MODEL IN CHAPTER 2	145
APPENDIX D	OUTPUT SUMMARY FOR ALLOMETRIC SCALING MODEL IN CHAPTER 2	146
APPENDIX E	CONTROL STREAM FOR MODEL IN CHAPTER 3.....	147
APPENDIX F	OUTPUT SUMMARY FOR MODEL IN CHAPTER 3.....	149
APPENDIX G	LIST OF PUBLICATIONS	151
REFERENCES	152

LIST OF TABLES

Table 1.1 Artesunate pharmacokinetic findings following IV administration.	31
Table 1.2 DHA pharmacokinetic findings following IV artesunate.	34
Table 1.3 Artesunate pharmacokinetic results following IM artesunate.	38
Table 1.4 DHA pharmacokinetic results following IM artesunate.	39
Table 1.5 Artesunate T_{max} and half-life means obtained following oral artesunate.	40
Table 1.6 Artesunate and DHA AUC and C_{max} means following oral artesunate.	44
Table 1.7 DHA half-life means obtained following oral artesunate.	50
Table 1.8 Artesunate pharmacokinetic results following rectal artesunate.	54
Table 1.9 DHA pharmacokinetic results following rectal artesunate.	55
Table 2.1 Summary of covariate data for patients in the five clinical trials from which the full and pediatric datasets were derived.	91
Table 2.2 Formulas for body size descriptors used in modeling.	92
Table 2.3 NONMEM estimates and relative standard errors (%RSE) for DHA apparent clearance (CLM/F) in various body size models implemented with the full and pediatric datasets.	93
Table 2.4 NONMEM estimates and relative standard errors (%RSE) for DHA apparent volume of distribution (V_3/F) in various body size models implemented with the full and pediatric datasets.	94
Table 2.5 A summary of the results from the final allometric scaling and linear BSA models implemented using the pediatric dataset.	95
Table 2.6 A summary of the results obtained from the allometric scaling model and linear BSA model as implemented with the full population dataset.	96
Table 2.7 Covariance estimates, with bootstrap relative standard errors and confidence intervals, for the final linear BSA and allometric scaling models.	97
Table 2.8 Results of stratified numerical predictive checks for DHA.	97
Table 3.1 Demographic and clinical data for study participants.	128
Table 3.2 Final model parameter estimates for model describing the pharmacokinetics of artesunate and DHA in pregnant and non-pregnant women.	129

LIST OF FIGURES

Figure 1.1 Structures of artesunate and dihydroartemisinin.	56
Figure 2.1 Plots of patient age vs. best-fit lines for population-predicted DHA apparent clearance (L/hr/kg) obtained from implementation of the weight and BSA body size models.	98
Figure 2.2 Plot of patient age vs. best-fit lines for population-predicted DHA apparent volume of distribution (L/kg) obtained from implementation of the weight and BSA body size models.	99
Figure 2.3 Covariate effect plots for the effect of male gender on DHA apparent clearance for the linear BSA and allometric scaling models as implemented with the pediatric or full dataset.	100
Figure 2.4 Covariate effect plots for the effect of male gender on DHA apparent volume of distribution for the linear BSA and allometric scaling models as implemented with the pediatric or full dataset.	101
Figure 2.5 Covariate effect plots for the effect of male gender on artesunate apparent clearance for the linear BSA and allometric scaling models as implemented with the pediatric or full dataset.	102
Figure 2.6 Covariate effect plots for the effect of male gender on artesunate apparent volume of distribution for the linear BSA and allometric scaling models as implemented with the pediatric or full dataset.	103
Figure 2.7 Goodness-of-fit plots for DHA for the final linear BSA model as implemented with the pediatric dataset.	104
Figure 2.8 Visual predictive check plots for DHA stratified by age for the final linear BSA model implemented with the full dataset.	105
Figure 2.9 Categorical visual predictive check for proportion of artesunate concentrations below the lower limit of quantification for the linear BSA model implemented with the full dataset.	106
Figure 2.10 Categorical visual predictive check for proportion of DHA concentrations below the lower limit of quantification for the linear BSA model implemented with the full dataset.	108
Figure 2.11 Plots of DHA Conditional Weighted Residuals (CWRES) vs. age for the final linear BSA and allometric scaling models implemented with the pediatric dataset.	108

Figure 3.1 Diagram of final structural model for artesunate and DHA pharmacokinetics as developed to model artesunate and DHA pharmacokinetics in pregnant and non-pregnant women with asymptomatic parasitemia.	130
Figure 3.2 Typical DHA concentration-time profiles for pregnant and non-pregnant women based on final model parameter estimates.....	131
Figure 3.3 Goodness-of-fit plots for artesunate for final model.....	132
Figure 3.4 Goodness-of-fit plots for DHA for final model.....	133
Figure 3.5 Visual predictive check plots for artesunate and DHA for the final model.	134

INTRODUCTION

Malaria infection

Malaria infection represents a profound global health threat, resulting in substantial morbidity and mortality. In 2012, there were approximately 207 million cases of malaria infection, resulting in an estimated 627,000 deaths (1). Malaria is caused by protozoa of the genus *Plasmodium*, with two species, *Plasmodium falciparum* and *Plasmodium vivax* being responsible for the vast majority of infections. *P. falciparum* infection predominates in Africa, with only 1% of African malaria cases being associated with *P. vivax* infection. Outside of Africa, *P. vivax* accounts for approximately half of the cases of malaria. Infection with *P. falciparum* results in severe illness in 5% of cases, with *falciparum* malaria being associated with a vast majority of deaths due to malaria. Severe illness and death resulting from *P. vivax* infection is less common, although not non-existent (1, 2).

For *P. falciparum* and *P. vivax*, human infection begins when a female Anopheles mosquito takes a blood meal and *Plasmodium* sporozoites are transferred from the mosquito's saliva into a person's capillary blood. The sporozoites migrate to the liver within hours of the blood meal being taken. The protozoa undergo asexual reproduction inside hepatocytes for approximately six to eight days, at which time merozoites are released into the bloodstream. It should be noted that *P. vivax*, but not *P. falciparum*, can cause repeated infections due to the ability of the parasite to remain in the liver in a dormant state for months to years (2).

Merozoites released into the bloodstream invade and subsequently reproduce inside red blood cells. Merozoites undergoing asexual reproduction inside red blood cells go through an initial ring stage, followed by subsequent trophozoite and schizont stages. This maturation occurs over approximately 48 hours, after which the schizonts burst to release multiple merozoites into the bloodstream. A portion of the merozoites invading

red blood cells do not undergo asexual reproduction, but rather develop into male and female gametocytes. These gametocytes can be taken up by a mosquito taking a blood meal. Inside the mosquito, these gametocytes further mature into gametes, which fuse into a diploid form; further replication and development inside the mosquito yields sporozoites which can be transmitted to another person, thereby continuing the infectious cycle (2).

The release of merozoites into the bloodstream every 48 hours elicits an immune response which generates symptoms of fever, rigors, nausea, and myalgia. Additionally, red blood cells infected with *P. falciparum* merozoites display the capacity to adhere to blood vessel walls, potentially contributing to organ damage due to occlusion; other *Plasmodium* species cannot cause vascular adherence. The spleen acts to remove infected red blood cells, which contributes to the anemia commonly resulting from malaria infection. Clinically, a case of malaria is considered severe when infection is accompanied by signs of vital organ dysfunction. Complications occurring in severe malaria include cerebral malaria, in which cerebral small blood vessels are packed with parasitized red blood cells, as well as severe anemia, pulmonary edema, acute kidney injury, acidosis, hypoglycemia, and respiratory distress (2). Even with treatment, the fatality rate of severe malaria is 10 – 20%; left untreated, severe malaria is almost always fatal (2, 3).

Transmission regions

Much of sub-Saharan Africa is considered a high malaria transmission region, with individuals being inoculated by a mosquito bite with the malaria parasite numerous times per year. Young children living in such high transmission regions experience repeated malaria infections in early childhood. Due to these repeated infections, these children acquire partial immunity to the parasite, which provides protection against development of severe disease, and, ultimately, some protection against symptomatic malaria infection as adults. Because of this partial acquired immunity, children in high

transmission areas display a decreasing risk for development of severe malaria as they age (1, 2, 4).

In most areas of Central America, South America, and Asia in which malaria infections are observed, malaria transmission is considered low, with individuals living in these regions typically being inoculated by a mosquito bite with the malaria parasite at most once per year. In these areas, *P. falciparum* and *P. vivax* infections are essentially equally common. In such low transmission regions, the inoculation rate is insufficient to allow for development of protective immunity during childhood, resulting in symptomatic malaria infection being observed more evenly across the age spectrum (1, 2).

High risk groups

Given that susceptibility to the development of severe malaria tracks closely with the degree of protective immunity an individual displays, it follows that among those considered at highest risk include individuals who have not had the opportunity to acquire sufficient protective immunity, such as young children and individuals migrating from low to high transmission regions, as well as individuals, such as pregnant women and HIV/AIDS patients, displaying altered immune functioning (1-3). Two of these high risk groups, children and pregnant women, are the focus of the research presented in this thesis.

Malaria in children

Young children living in high transmission regions but who have not yet acquired a reasonably robust partial protective immunity against malaria are at substantial risk of experiencing malaria-related morbidity and mortality. WHO estimates that in 2012 approximately 73% of deaths worldwide due to malaria occurred in African children under five years of age. Even among children treated for and surviving severe malaria,

long term sequelae, including neurological damage from cerebral malaria, may be observed (5). Approximately 3 – 15% of children surviving cerebral malaria display neurological deficits, including paralysis of one side of the body, cerebral palsy, deafness, cortical blindness, and impaired learning; these neurological sequelae are of varying duration (2). A crucial means of reducing pediatric morbidity and mortality from malaria is the prompt provision of effective antimalarial treatment to children with malaria infection. Optimally, a child with a malaria infection can receive antimalarial treatment before progression to severe malaria can occur (1, 5).

Malaria in pregnant women

Malaria infection during pregnancy represents a substantial global health problem, with malaria being responsible for approximately 10,000 maternal deaths every year (6). Compared to their non-pregnant counterparts, pregnant women are three times more likely to develop severe disease from a malaria infection (6). Furthermore, in high transmission areas, pregnant women experience higher rates of *falciparum* parasitemia and severe malaria-related anemia than their non-pregnant counterparts. This severe anemia in pregnancy increases the risk of development of congestive heart failure and hemorrhage during delivery (6). In these regions, placental malaria infection, characterized by *P. falciparum* sequestration in placental tissue, also represents a significant health threat. Placental malaria can increase the risk of miscarriage, intrauterine growth restriction, preterm birth, and low birth weights (6-9). Low birth weights, in turn, increase the risk of neonatal death, with malaria infection in pregnancy being responsible for an estimated 100,000 neonatal deaths each year (6, 7).

Prevention of malaria in children and pregnant women

For children and pregnant women, prevention of malaria infection is a critical concern. Sleeping under insecticide-treated bed nets or spraying the insides of dwellings with insecticide are WHO recommended methods for reducing the likelihood of mosquito bites. Implementation of one of these vector control strategies is critical in homes with a pregnant woman or young child. However, vector control alone is not sufficient protection for particularly high risk individuals. Therefore, WHO recommends intermittent preventative treatment (IPT) with the antimalarial sulfadoxine-pyrimethamine (SP). Per WHO recommendations, infants should be administered one dose of SP between 8 – 10 weeks, a second dose between 12 – 14 weeks, and a third dose at 9 months; this schedule is designed to align with the typical timing of infant vaccinations. In moderate to high transmission areas, IPT in infants has been shown to reduce clinical malaria by 30% (10). For pregnant women, the first SP dose is given as early as possible in the second trimester and subsequently at every antenatal care visit until delivery, provided that the visits are at least one month apart. Use of IPT in pregnant women has been shown to reduce the risk of maternal parasitemia, anemia, and death during delivery; additionally, mothers receiving IPT had infants with higher birth weights (6). It should be noted that although it is a powerful tool against malaria in infants and pregnant women, IPT only reduces, but does not eliminate, the risk of malaria infection and its complications.

Artemisinin derivatives

Derivatives of the naturally occurring endoperoxide antimalarial artemisinin are of central importance in the current global treatment approach to malaria. These derivatives, which include artesunate (AS), artemether and dihydroartemisinin (DHA), produce more profound reductions in parasitemia and more rapid symptom relief than agents from any other class of antimalarial. The precise mechanism of action of these

agents has not been fully elucidated, but may involve breakage of the peroxide bridge with subsequent production of reactive oxygen species which damage the parasite. All of these derivatives are rapidly eliminated from the body, with typical half-life values of less than three hours (11).

Among the artemisinin derivatives, only artesunate is sufficiently water soluble to allow for administration by the IV route for treatment of severe malaria. All of the derivatives can be administered orally as part of combination therapy to treat uncomplicated malaria. Specifically, when used for such treatment, an artemisinin derivative is paired with a partner drug with an alternative mechanism of action and a longer half-life. Such combination therapies, termed artemisinin-based combination therapies (ACTs), allow for treatment of uncomplicated malaria using only a three-day treatment course. Artesunate, for example, has been incorporated into combination therapy with partner drugs including mefloquine, amodiaquine, and pyronaridine. The artemisinin derivative in the combination allows for rapid reductions in parasite counts and dramatic symptom relief, while the partner drug serves to eliminate any residual parasitemia, reducing the risk of treatment failure and protecting against selection for parasites displaying lower artemisinin susceptibility (3).

Current WHO treatment guidelines recommend parenteral artesunate (IV or IM) as the first-line treatment for severe malaria in both children and adults. Furthermore, the guidelines recommend ACTs as first line treatment for uncomplicated malaria caused by *P. falciparum*, as well as *P. vivax* not sensitive to chloroquine. Due to concerns regarding embryotoxicity of the artemisinins in the first trimester of pregnancy, ACTs are not considered first-line therapy for uncomplicated malaria in first-trimester pregnant women. However, they are considered to be acceptable for treatment of uncomplicated malaria in the second and third trimesters of pregnancy. Furthermore, parenteral artesunate is recommended as the preferred treatment of severe malaria in the second and

third trimesters of pregnancy, and is even considered a reasonable treatment option for severe malaria in the first trimester (3).

Artesunate pharmacokinetics in children and pregnant women

Clearly, artesunate is a therapeutically versatile agent with extremely important clinical applications. However, much remains unknown regarding the pharmacokinetics of artesunate, and its active metabolite DHA, in children and pregnant women. There are physiological justifications for concerns regarding altered artesunate and DHA pharmacokinetics in these groups. Both artesunate and DHA are high extraction ratio drugs; that is, their clearance is dependent on hepatic blood flow. Hepatic blood flow, in turn, is proportional to liver volume. In young children, liver volume represents a greater proportion of body volume than it represents in older children and adults. Because of this, following administration of a given mg/kg dose of a high extraction ratio drug such as artesunate, blood levels of the drug would be expected to be lower in a young child than in an older child or adult. Artesunate dosing is conceptualized in terms of mg/kg doses, with WHO recommending a target dose for all individuals of 4 mg/kg/day. Since young children are at high risk for experiencing complications from malaria, clearly the possibility that such individuals would experience lower exposure than older children and adults when administered the same mg/kg dose deserves investigation.

Pregnant women display numerous physiologic changes which can markedly alter pharmacokinetics. As noted above, hepatic blood flow changes are of particular interest when considering artesunate and DHA exposure. Some studies have identified increases in hepatic blood flow in pregnant women, particularly in the third trimester, while other studies did not identify such changes. However, the clearance of multiple high extraction ratio drugs have been observed to be increased pregnancy, which does suggest the possibility of increased hepatic blood flow (12). Given this possibility, and the serious

consequences of malaria infection in pregnancy, artesunate pharmacokinetics in pregnant women should be fully elucidated.

Overview of thesis

The first chapter of this thesis reviews presently available studies describing the pharmacokinetics of artesunate, and its active metabolite DHA, across various routes of administration and populations. Chapter 2 describes a population pharmacokinetic analysis of artesunate in pediatric patients with malaria participating in a set of Phase II and Phase III clinical trial for an ACT combining artesunate with the partner drug pyronaridine. This analysis focuses on the effects of body size and gender on the pharmacokinetics of artesunate and DHA. Chapter 3 describe the population pharmacokinetics of artesunate and DHA in a group of pregnant and non-pregnant women with asymptomatic *falciparum* malaria in the Democratic Republic of Congo (DRC). The final chapter discusses potential clinical applications of the research findings described in this thesis.

CHAPTER 1

REVIEW OF ARTESUNATE PHARMACOKINETICS

Objectives of literature review

Given the therapeutic significance and versatility of artesunate, and the necessity of appropriate dosing to avoid suboptimal efficacy or encouragement of resistance, research defining the pharmacokinetics of artesunate, and its active metabolite DHA, is of substantial clinical relevance. The intent of this chapter is to examine clinical pharmacokinetic findings of artesunate and DHA following artesunate administration by the intravenous (IV), intramuscular (IM), oral and rectal routes. To this end, an extensive literature search was conducted utilizing the PubMed database and the bibliographies of identified articles in order to locate artesunate clinical pharmacokinetic studies in which parameter estimates for artesunate and/or DHA are reported. The PubMed database was searched using combinations of the following search terms: artesunate, dihydroartemisinin, artemisinin, and pharmacokinetics. Conference abstracts and non-English language articles were not considered for inclusion in the review. Finally, it should be noted that much of the content presented in this chapter in the form of both text and tables was published previously in *Malaria Journal* in 2011 (13).

To facilitate comparison of results among various studies, units for these parameters were converted, as necessary, to a uniform scale as noted in the tables included at the end of this chapter. Additionally, individual pharmacokinetic analyses and population pharmacokinetic analyses are described separately for each route of administration, where applicable, to enable adequate description of the findings from each analysis method; only non-compartmental results are described in the tables. Additionally, in the tables, unless otherwise specified, parameter estimates are means and presented AUC values are estimates of area under the curve from time zero extrapolated to infinity ($AUC_{0-\infty}$).

Artesunate and DHA properties

Figure 1.1 displays the chemical structures of artesunate and DHA. With a pKa of artesunate of 4.6 (14), the extent of artesunate solubility is pH dependent. Specifically, artesunate solubility is 0.25 mg/mL and 0.3 mg/mL at pH 5 and 7, respectively, whereas DHA is a neutral compound which is practically insoluble in water (15).

Sources of variation introduced by study methodology

Multiple factors complicate comparison and summation of artesunate/DHA pharmacokinetic findings across multiple studies, including differences in assay sensitivities, sampling schedules, and choice of anticoagulant for blood sample collection. Differences in sampling schedules are of particular importance in comparisons of artesunate pharmacokinetic parameters; a relative lack of sampling points in the early post-dose period can result in much of subjects' artesunate exposure being missed. With regard to choice of anticoagulant, if fluoride-oxalate, rather than heparin, is included as the anticoagulant in blood sample collection tubes, ex vivo plasma esterase degradation of artesunate to DHA is greatly inhibited (16). This inhibition allows for greater preservation of a subject's artesunate concentrations at the time of blood sample collection. However, fluoride-oxalate may also result in greater erythrocyte shrinkage than heparin, and therefore increased plasma volume (16). Given these sources of variation, differences in pharmacokinetic findings among the studies described in this chapter cannot necessarily be regarded as solely related to whatever specific demographic or clinical features characterize the study subjects.

Artesunate and DHA protein binding

Binding of artesunate to human plasma proteins has been investigated utilizing equilibrium dialysis with [¹⁴C] artesunate. Artesunate was determined to be 75% protein bound at plasma concentrations less than 125 ng/mL, and 62% protein bound at higher

concentrations (17). DHA plasma protein binding, when measured by similar means, was determined to be 82% at plasma concentrations less than 25 ng/mL and 66% at higher concentrations (18). DHA percent bound was also assessed by ultrafiltration in patients with malaria infection (*falciparum* or *vivax*), Vietnamese healthy volunteers, and Caucasian volunteers and determined to be 93%, 88%, and 91%, respectively (19). However, as artesunate and DHA are both high extraction ratio drugs (20), any alterations in patients' protein binding capacity would not be expected to produce clinically relevant changes in the clearance of either agent.

IV administration: Artesunate pharmacokinetics

The pharmacokinetic results of the identified studies in which intravenous artesunate pharmacokinetics were assessed are presented in Tables 1.1 and 1.2 (21-32). In clinical settings, IV artesunate is administered as a bolus injection (33). As the identified IV artesunate studies utilized this administration method, very high artesunate maximum concentrations (C_{max}) were observed. Artesunate is metabolized through esterase-catalyzed hydrolysis to yield its active metabolite, DHA (11); conversion of artesunate to DHA occurs quickly following IV artesunate administration, as indicated by the rapid decline in artesunate concentrations in the early post-dose period. In six of the eleven IV artesunate studies in which artesunate pharmacokinetics were assessed, average artesunate half-life following IV artesunate was determined to be less than five minutes in at least one study cohort. In all of the studies, average artesunate half-life was determined to be fifteen minutes or less. Finally, per the findings of Li et al. (28), artesunate was determined to display dose linearity following IV administration across a dosage range of 0.5 – 8 mg/kg.

Examination of the artesunate clearance and volume estimates summarized in Table 1.1 indicates that the parameters obtained by Newton et al. (32) are dissimilar from the parameters obtained in other studies, likely due to a lack of sampling prior to 15

minutes post-dose. The remaining studies have somewhat more consistent clearance and volume estimates, with averages ranging from 1.16 - 5.05 L/hr/kg and 0.08 – 1.18 L/kg, respectively. A majority of the estimates range between 2 - 3 L/hr/kg for clearance and 0.1 – 0.3 L/kg for volume.

IV administration: DHA pharmacokinetics

DHA pharmacokinetic findings associated with IV artesunate administration are summarized in Table 1.2. In the IV artesunate studies, the time to maximum concentration (T_{max}) of DHA following IV artesunate administration generally occurred within 25 minutes post-dose. DHA metabolism occurs through conjugation of DHA by the UDP-glucuronosyltransferase system, with UGT1A9 and UGT2B7 being the primary responsible isoforms (34). This DHA elimination process occurs somewhat more slowly than the esterase catalyzed artesunate elimination, with average half-life estimates for DHA following IV artesunate administration ranging from 18 minutes to 2.14 hours, with the majority of estimates falling between 30 – 90 minutes. DHA apparent clearance (Cl/F) and volume of distribution (V/F) averages ranged from 0.48 - 5.6 L/hr/kg and 0.55 – 2.525 L/kg, respectively, with a majority of the estimates averaging 0.5 – 1.5 L/hr/kg for clearance and 0.5 – 2.0 L/kg for volume. As with artesunate, DHA displayed dose-linearity across an IV artesunate dosage range of 0.5 – 8 mg/kg (28).

IV administration: Bioassay results

The antimalarial bioassay method for determination of artesunate/DHA plasma concentrations provides values in DHA equivalents reflecting the contribution of both artesunate and DHA present in the sample. An assessment of antimalarial bioactivity in patients with acute uncomplicated *falciparum* malaria administered 2 mg/kg IV artesunate yielded estimates for half-life, volume of distribution at steady state (V_{ss}), and clearance of 0.73 hours, 0.61 L/kg, and 0.83 L/hr/kg, respectively (35). Bioassay data

were also used to compute the pharmacokinetic parameters following administration of 2.4 mg/kg IV artesunate to thalassemic and healthy non-thalassemic adults. The reported half-life estimates for normal and thalassemic subjects were 1.37 and 1.95 hours, respectively, with T_{\max} for bioassay activity occurring by the first sampling point (15 minutes) (36). As would be expected given the more extended half-life of DHA, these bioassay results appear somewhat more reflective of the DHA results than the artesunate results derived from traditional analytical methods.

IM administration: Artesunate and DHA pharmacokinetics

Tables 1.3 and 1.4 (26, 31, 37) summarize the results of the identified studies examining artesunate and DHA pharmacokinetics following IM artesunate administration, respectively. Average estimates of the extent of absorption of IM artesunate, as determined by DHA exposure, were 86.4% (26) and 88% (31) in adult and pediatric *falciparum* malaria patients, respectively. The average time to maximum artesunate concentrations following IM administration ranged from 7.2 - 12 minutes; average artesunate half-life ranged from 25.2 – 48.2 minutes. This more extended artesunate half-life following IM, as compared to IV, artesunate administration presumably indicates that the artesunate elimination rate is limited by the rate of absorption from the site of injection. Average estimates for artesunate apparent clearance and volume of distribution ranged from 2.4 – 3.4 1.09 – 3.98 L/kg, respectively. As would be expected given the high extent of absorption of IM artesunate, these estimates for apparent clearance are not strikingly higher than those obtained following IV artesunate administration.

Maximum DHA concentrations following IM artesunate administration were observed, on average, within the first 45 minutes post-dose. Average estimates for DHA half-life, apparent clearance, and apparent volume of distribution following IM artesunate

ranged from 31.9 – 64 minutes, 0.73 – 2.16 L/hr/kg, and 1.1 – 1.7 L/kg, respectively; all of these values are quite similar to those obtained following IV artesunate administration.

Hendriksen et al. (38) performed a population pharmacokinetic analysis of IM artesunate in African children with severe malaria. Using 274 artesunate and DHA plasma samples obtained during the first 12 hours post-dose from a total of 70 pediatric patients receiving 2.4 mg/kg IM artesunate, these investigators developed a model which consisted of a one compartment model for artesunate, a one compartment model for DHA, and a fixed (i.e. not estimated) absorption rate. Body weight was incorporated into the model using allometric scaling with standard exponents (0.75 for clearance and 1 for volume). Hemoglobin was a significant covariate on DHA apparent clearance, with a 10.2% increase in DHA apparent clearance being associated with each unit (g/dL) decrease in hemoglobin. Mean post hoc empirical Bayes estimates for artesunate apparent clearance and volume of distribution were 4.27 L/hr/kg and 2.58 L/kg, respectively; for DHA, mean apparent clearance was 2.01 L/hr/kg and mean apparent volume was 1.24 L/kg. The artesunate and DHA apparent clearance and volume values are reasonably similar to those obtained from the non-compartmental analyses summarized in Tables 1.3 and 1.4.

Oral administration: Artesunate pharmacokinetics

Artesunate displays good oral absorption when assessed by exposure to its active metabolite DHA. In studies examining the proportion of the oral dose to which the subject is exposed, the AUC for DHA resulting from IV administration of artesunate is compared to the AUC for DHA resulting from oral administration of artesunate. Using this method, the proportion of the dose absorbed by the oral route is 82% in healthy adults (23), 85% in adults with uncomplicated *falciparum* malaria (22), and 80% in adults with *vivax* malaria (21). These estimates are obtained assuming complete conversion of artesunate to DHA and accounting for the differences in molecular weights between the

compounds. It should be noted, however, that these results may reflect both the absorption of artesunate, with subsequent conversion to DHA through first-pass or systemic metabolism, as well as direct absorption of DHA following its formation in the gut through acid-dependent chemical hydrolysis (39). The rate of this reaction is pH-dependent, with a reaction half-life of 26 minutes at a pH of 1.2 and half-life of 10 hours at a pH of 7.4 (40). Given the rapidity of this reaction at gastric pH, direct absorption of DHA in humans following hydrolysis of artesunate clearly represents an input mechanism for DHA following oral artesunate administration.

Non-compartmental pharmacokinetic findings associated with oral artesunate administration are summarized in Tables 1.5 – 1.7 (20-23, 29, 41-67). Following oral administration, artesunate concentrations are detectable early, often within 15 minutes post-dose. As shown in Table 1.5, peak artesunate concentrations also occur early, with artesunate T_{max} typically being detected within the first hour post-dose. These findings suggest that artesunate is absorbed quickly and without appreciable lag. Artesunate half-life estimates available in the literature are summarized in Table 1.5, with average artesunate half-life reported for any cohort in the identified studies ranging from 0.24 - 1.2 hours. All studies in which artesunate half-life was determined cite artesunate half-life values between 20 and 45 minutes for at least one study cohort.

There are few published estimates, obtained from non-compartmental analysis, of artesunate apparent clearance and volume of distribution assessed following oral artesunate administration. Teja-Isavadharm et al. (50) determined mean artesunate CL/F and V/F to be 20.6 L/hr/kg and 14.8 L/kg, respectively, in six healthy adult subjects. Karbwang et al. (43) determined average artesunate CL/F to be 19.2 L/hr/kg in 11 Thai adults during the acute phase of uncomplicated malaria infection and 9.6 L/hr/kg during the convalescent phase. Median artesunate V/F was 6.8 L/kg during both phases of infection. Finally, in pediatric Gabonese patients with acute *falciparum* malaria,

estimates for average artesunate CL/F and V/F were 25 – 30 L/hr/kg and 25 – 41 L/kg, respectively (49). Given that artesunate is a high extraction ratio drug, the substantial difference in magnitude of these artesunate apparent clearance and volume estimates for oral administration, as compared to IV or IM administration, most likely reflects the low bioavailability of artesunate due to the extensive conversion of artesunate to DHA during first-pass metabolism.

Oral administration: DHA pharmacokinetics

For studies defining both artesunate and DHA pharmacokinetics following oral artesunate administration, DHA C_{max} exceeds artesunate C_{max} , and DHA AUC exceeds artesunate AUC. Literature results exemplifying this relationship between artesunate and DHA pharmacokinetic exposure are summarized in Table 1.6. In many of these studies, DHA AUC exceeds artesunate AUC by more than 10-fold, when considered on either a nmol*hr/mL or ng*hr/mL basis. It is in part due to this disparity in exposure that artesunate is often considered essentially a pro-drug for DHA following oral artesunate administration. The maximum concentration for DHA typically occurs within two hours post-dose. DHA is eliminated more slowly than artesunate following oral artesunate administration. DHA half-life was determined to be longer than artesunate half-life for studies in which both parameters were assessed. For the studies in which DHA half-life was estimable (Table 1.7), the average DHA half-life ranged from 0.49 hours to 3.08 hours, with approximately one-half of the half-life estimates being less than one hour and the bulk of the remaining estimates being between 1- 2 hours. Overall, most of the half-life estimates fell between 0.5 – 1.5 hours.

DHA CL/F and V/F estimates obtained following oral artesunate administration are limited. Teja-Isavadharm et al.(50) determined DHA CL/F to be 3.35 L/hr/kg in six

healthy adults and 1.01 L/hr/kg in six parasitemic adults. DHA apparent volume of distribution values were 4.14 L/kg and 1.55 L/kg in healthy subjects and malaria patients, respectively. In Gabonese children with malaria, DHA CL/F and V/F averaged 2.3 – 2.7 L/hr/kg and 1.6 – 4.2 L/kg, respectively (49). Orrell et al. (48), Davis et al. (54), and Zhang et al. (60) computed DHA CL/F, but did not provide values adjusted for body weight. Adjusting CL/F using the average body weight in these studies yields apparent clearance estimates of 2.2 L/hr/kg (artesunate alone) and 2.7 L/hr/kg (with amodiaquine) for Orrell et al. (48), 1.4 – 1.7 L/hr/kg for Davis et al. (54), and 1.8 L/hr/kg for Zhang et al. (60). Adjusted DHA V/F values ranged from 1.6 – 2.6 L/kg (54).

Oral administration: bioassay results

As was previously observed for IV bioassay studies, pharmacokinetic parameters derived from bioassay data obtained following oral artesunate administration appear to more closely resemble DHA rather than artesunate parameters. For example, in the four identified studies including bioassay data following oral artesunate administration, the average T_{max} for bioactivity ranged from 0.75 – 1.7 hours and average half-life from 0.71 – 1.17 hours (35, 50, 68, 69).

Oral administration: Population pharmacokinetics

Four population pharmacokinetic analyses describing artesunate and/or DHA pharmacokinetics following oral artesunate administration were identified, including two conducted with data from pregnant women (described under *Artesunate and DHA pharmacokinetics in pregnant women*, below), as well as analyses conducted using data from healthy volunteers and from pediatric malaria patients. Specifically, Tan et al. (70)

modeled the pharmacokinetics of artesunate and DHA simultaneously utilizing extensive sampling data from 91 healthy Korean adults administered oral artesunate. The data were fit to a parent-metabolite model with first-order artesunate absorption, a one-compartment model for artesunate and a two-compartment model for DHA. Adjusting for the median weight of the study population (61.5 kg), the final estimates for artesunate CL/F and V/F were 19 L/hr/kg and 20 L/kg, respectively. Similarly adjusting for median weight, DHA central clearance and central volume of distribution were 1.52 L/hr/kg and 1.58 L/kg, respectively, with weight as a statistically significant covariate on DHA apparent clearance. The only other significant covariate-parameter relationship identified in the model was the effect of food intake on the artesunate absorption rate constant, with a reduction in absorption rate of 84% associated with administration of artesunate with a high fat, high calorie meal. Inter-individual variability was estimated on five of the modeled parameters, with the highest inter-individual variability observed for K_a (%CV = 112%) and artesunate V/F (%CV = 57.4%).

Stepniewska et al. (71) described the population pharmacokinetics of DHA following oral artesunate administration to children (6 months – 5 years) with uncomplicated *falciparum* malaria. Artesunate and DHA pharmacokinetic data were obtained from 70 children who received artesunate and amodiaquine, but only DHA data could be modeled. Samples were collected once in the first dosing interval and once in the third dosing interval. The authors modeled DHA data using a one-compartment model with first-order input. They estimated DHA CL/F as 0.636 L/hr/kg for the first dosing period, with a substantial additive increase of 0.760 L/hr/kg being associated with the third dosing period. The authors speculated that this modeled increase in clearance

reflected pharmacokinetic changes related to resolution of acute illness. DHA apparent volume of distribution, which was not modeled as varying between dosing periods, was estimated as 2.285 L/kg, with age modeled as a covariate on volume. The authors noted that either age or weight explained a significant portion of the variability on volume, but that the two covariates appeared to exert overlapping effects. Inter-individual variability was modeled on DHA apparent volume of distribution (%CV = 47%), but no other parameter.

Rectal administration: Artesunate and DHA
pharmacokinetics

The bioavailability of rectally administered artesunate suppositories, as assessed by exposure to DHA, in pediatric patients with moderately severe malaria was estimated to be 23% in patients administered a dose of 20 mg/kg and 58% in patients administered 10 mg/kg (27). In one rectal-oral crossover study in healthy volunteers, the mean bioavailability of rectal artesunate relative to oral artesunate, as assessed by exposure to DHA, was 54.9% (51). However, in a study of similar design, no statistically significant differences in DHA AUC_{0-t} following oral and rectal artesunate administration were observed, although artesunate AUC was significantly larger and DHA C_{max} significantly smaller following rectal, as compared to oral, administration (45). The inconsistent findings of these two studies may relate to the difficulty of defining a sampling schedule able to optimally capture the unique concentration-time profiles associated with different routes of administration.

Tables 1.8 and 1.9 (27, 45, 51, 72, 73) summarize the pharmacokinetic findings of the identified rectal artesunate administration studies. T_{max} for artesunate following rectal

administration occurred on average between 0.58 – 1.43 hours. Artesunate half-life was estimated in only two studies, with half-life estimates of 0.9 – 0.95 hours. These longer half-life estimates may reflect absorption rate-limited elimination of artesunate.

Following rectal administration of artesunate, DHA concentrations peaked between 1.13 – 2.0 hours, and DHA was eliminated with a half-life averaging 0.79 – 1.8 hours. Only one non-population pharmacokinetic study (27) reported estimates of DHA apparent clearance and volume following rectal artesunate; those values were 2.6 – 3.9 L/hr/kg and 4.4 – 5.9 L/kg, respectively. As would be expected given that rectal artesunate administration largely avoids first-pass metabolism, the discrepancy in artesunate and DHA AUC values is not as striking with rectal, as compared with oral, administration of artesunate.

Rectal administration: Population pharmacokinetics

Two population pharmacokinetic analyses of data obtained following rectal artesunate administration were identified. Simpson et al. (74) described the population pharmacokinetics of DHA following rectal artesunate administration to adult and pediatric patients with moderately severe *falciparum* malaria. Patients were administered a single dose of 10 mg/kg artesunate with follow-up treatment administered orally. Artesunate concentrations could not be successfully modeled, since no clear pharmacokinetic profile for the obtained concentrations was apparent. DHA concentrations (424 levels) obtained from 164 patients were fit to a one-compartment model with fixed, lagged, first-order input (DHA appearance rate: 0.2/hr; lag: 0.14 hr). Gender and weight were identified as important covariates in the model, with DHA CL/F of 3.17 L/hr/kg for males and 2.03 L/hr/kg for females. DHA V/F was estimated as

increasing from 1.81 L/kg for a 15 kg subject to 6.34 L/kg for a 70 kg subject. Estimated inter-individual variability was 62% for CL/F and 75% for V/F.

Karunajeewa et al. (75) conducted a population pharmacokinetic analysis of artesunate and DHA data derived from samples collected following administration of 10 – 15 mg/kg rectal artesunate (2 doses, 12 hours apart) to 47 pediatric uncomplicated *falciparum* or *vivax* malaria patients in Papua New Guinea. Artesunate data and DHA data were each fit to a one compartment model; first-order AS absorption was specified. Due to identifiability issues, the volume of distribution estimates for artesunate and DHA were set equal (41.8 L). Weight was an influential covariate on volume. The artesunate CL/F (mean \pm SD) was determined to be 121.2 ± 35.4 L/hr and DHA CL/F to be 44.9 ± 13.0 L/hr. Average artesunate and DHA half-life estimates were 0.27 and 0.71 hours, respectively. The absorption half-life was estimated as 2.3 hours. The model included a bioavailability term for the second dose relative to the first dose (72%). The authors conjectured that higher core body temperature when the first dose was administered may have resulted in enhanced rectal blood flow and, therefore, absorption.

Artesunate and DHA pharmacokinetics in pediatric patients

The two previously described population pharmacokinetic models describing artesunate/DHA pharmacokinetics following rectal artesunate administration were conducted using data from a mixed adult and pediatric population (74) or an exclusively pediatric population (75); in both of these analyses, weight represented a significant covariate on DHA apparent volume of distribution. In the population pharmacokinetic analysis of DHA following oral artesunate administration to young children, Stepniewska et al. (71) determined that either weight or age could explain a significant portion of the

between subject variability in DHA volume of distribution. These findings suggest that weight, or a highly correlated covariate such as age, is an important predictor variable for DHA pharmacokinetics in pediatric patients. However, further study would be required in the pediatric population to assess if patient age is an important source of variability beyond that explained by body weight alone. Such a study would optimally focus on infants and very young children since the most marked differences in drug metabolism and other physiologic processes would be expected in this patient population.

Artesunate and DHA pharmacokinetics in pregnant women

A limited number of pharmacokinetic trials have been conducted to characterize artesunate/DHA pharmacokinetic changes that may be associated with the physiologic changes of pregnancy. McGready et al. (2006) (55) modeled the pharmacokinetics of DHA following oral administration of artesunate to 2nd and 3rd trimester pregnant women with acute uncomplicated malaria. Population modeling yielded DHA CL/F and V/F estimates of 1.77 L/hr/kg and 4.63 L/kg. Non-compartmental analysis of their data yielded estimates of 4.0 L/hr/kg for CL/F and 3.4 L/kg for V/F. The authors noted that exposure to DHA following oral artesunate administration to the pregnant women in the study was substantially lower than that observed in non-pregnant subjects in previous studies.

A more complex analysis was subsequently conducted in 20 second and third trimester pregnant women with uncomplicated *falciparum* malaria in Thailand (29). One cohort of women received IV artesunate at 4 mg/kg on day 0 followed by oral artesunate at 4 mg/kg/day for six additional days; the second cohort received 4 mg/kg oral artesunate on day 0, 4 mg/kg IV artesunate on day 1, and then 4 mg/kg/day oral

artesunate for five days. Extensive sampling for artesunate and DHA concentrations were obtained on days 0 and 1. A limited set of day 6 samples were also collected. At three months postpartum the women returned and were administered the regimen they had been administered while pregnant. The authors did not identify statistically significant differences in artesunate or DHA pharmacokinetics between pregnant and postpartum women when examining parameters derived from concentrations observed following IV artesunate administration. However, following oral artesunate administration, median AUC values for artesunate and DHA were both significantly higher in pregnant women as compared to the same women postpartum. Furthermore, estimated bioavailability was significantly higher in pregnancy for artesunate (21.7% pregnant vs. 9.9% postpartum) and DHA (77.0% pregnant vs. 72.7% postpartum). When considering oral dosing, DHA exposure was significantly lower on day 6 as compared to day 0 or 1, an effect which was observed with pregnant, but not postpartum women, and which the authors speculate reflects a disease effect. Finally, authors identified significantly higher combined artesunate+DHA drug exposure, regardless of route of administration, in patients classified as moderately unwell as compared to those classified as mildly unwell. The overall conclusions of the authors were that acute malaria appears to result in increased oral bioavailability of artesunate and DHA.

Onyamboko et al. (64) examined the pharmacokinetics of DHA following the oral administration of 200 mg artesunate to 26 second and third trimester pregnant women with asymptomatic *falciparum* parasitemia, the same women 3 months post-partum, and 25 matched asymptomatic parasitemia female controls in the Democratic Republic of Congo. The median DHA CL/F was 1.39 L/hr/kg, 1.26 L/hr/kg, and 1.07 L/hr/kg for

pregnant, post-partum, and non-pregnant control subjects, respectively. Median DHA V/F was 2.84 L/kg for pregnant, 3.00 L/kg for post-partum, and 2.45 L/kg for non-pregnant control subjects. DHA AUC was significantly different (geometric mean ratio: 0.68, 90% CI: 0.57 – 0.81) for the pregnant as compared to control subjects; however, DHA AUC values for pregnant women and the same women at three months post-partum were relatively similar.

In a recent analysis, Valea et al. (67) examined the pharmacokinetics of artesunate and DHA following oral artesunate+mefloquine administration once daily for three days to 24 pregnant and 24 paired non-pregnant women in Burkina Faso with uncomplicated *falciparum* malaria. Samples for artesunate/DHA concentration determinations were taken on the first day of study drug administration. Using non-compartmental analysis of the data, the authors obtained median artesunate CL/F estimates of 39.5 L/hr/kg and 60.0 L/hr/kg ($p < 0.05$), for pregnant and non-pregnant women, respectively. Artesunate V/F estimates were not significantly different, with median values of 19.3 L/kg in pregnant and 26.0 L/kg in non-pregnant women. DHA CL/F did not differ significantly between the groups, with a median CL/F for pregnant women of 2.1 L/hr/kg and for non-pregnant women of 2.0 L/hr/kg; DHA V/F estimates were also similar, with medians of 4.0 L/kg and 3.7 L/kg in pregnant and non-pregnant women, respectively. The authors note that the difference in artesunate kinetics observed in this study was unexpected and would require further investigation. They also note that the lack of a pregnancy-related effect on DHA apparent clearance could reflect the higher parasite density observed in the pregnant as compared to the non-pregnant women in the study. That is, the authors

speculated that a greater disease effect in the pregnant women in the study could have masked a pregnancy-related increase in DHA clearance.

Disease effects on artesunate and DHA pharmacokinetics

Multiple studies have attempted to investigate and characterize any changes in artesunate and DHA pharmacokinetics associated with malaria infection. Two of the studies described above, conducted by Stepniewska et al. (71) and Karbwang et al. (43), determined that the pharmacokinetics of orally administered artesunate may differ in the acute stage of infection as compared to the convalescent stage. Stepniewska et al. (71) determined that DHA clearance was substantially lower on the first day of treatment as compared to the third day. Karbwang et al. (43) determined that DHA C_{\max} was significantly decreased, and AUC not significantly changed, on the first day of treatment as compared to the fifth day. On the first day of treatment, higher artesunate clearance was also reported. Newton et al. (35) used bioassay data to investigate the antimalarial activity in patients with *falciparum* malaria during the patients' acute and convalescent phases. The analysis indicated that antimalarial activity AUC and C_{\max} were two-fold higher in the acute phase as compared to the convalescent phase for subjects administered the same dose of oral artesunate. Correspondingly, apparent clearance and volume of distribution of antimalarial activity were significantly smaller in the acute phase of infection. Finally, as noted above, an analysis in Thai pregnant women suggested increased artesunate and DHA bioavailability associated with acute illness (29). Although these studies do not fully align regarding the effect of disease resolution on artesunate and DHA pharmacokinetics, perhaps due to the use of differing populations, sampling time points, and time course of sampling, taken together these studies do

suggest that some alteration in pharmacokinetics occurs over the period of malaria resolution. It should be noted that changes over the course of treatment are likely not due to time-dependency of artesunate or DHA pharmacokinetics, as has been observed with various other artemisinin derivatives. Following oral administration of artesunate over a typical treatment course, time-dependent kinetics are not apparent (41).

A direct comparison of healthy and parasitaemic subjects was conducted by Teja-Isavadharm et al. (50), who studied the pharmacokinetics of DHA following oral artesunate administration to six healthy adults and six adult *falciparum* malaria patients. The investigators determined that AUC and C_{max} of DHA were significantly higher in subjects with malaria as compared to healthy subjects. Binh et al. (23) obtained similar results when comparing the pharmacokinetics in eight patients with *falciparum* malaria and ten healthy subjects. However, given the relatively small size of both the Binh et al. (23) and Teja-Isavadharm et al. (50) studies, drawing definitive conclusions regarding differences in pharmacokinetics between healthy and infected subjects is not possible at present. Nonetheless, as DHA clearance is dependent upon hepatic blood flow, a reduction in clearance, and consequently an increase in exposure, associated with acute infection would be consistent with the known pharmacokinetic properties of DHA.

Drug-drug interactions

Given the metabolic pathways of artesunate (esterase-catalyzed hydrolysis) and DHA (UGT-mediated conjugation), artesunate should not be susceptible to the many common drug-drug interactions involving CYP450 enzymes. Agents evaluated for their drug interaction potential with orally administered artesunate include atovaquone-proguanil (76), sulphadoxine-pyrimethamine (77), pyronaridine (70), mefloquine (54),

chlorproguanil-dapsone (56), artemisinin (60), amodiaquine (48), ritonavir (63), and the antiretroviral combination lamivudine/zidovudine/nevirapine (61). Artesunate co-administration does not appear to alter the pharmacokinetics of atovaquone-proguanil (76) or sulphadoxine-pyrimethamine (77). No significant change in DHA AUC was detected when artesunate was co-administered with mefloquine (54). In the population pharmacokinetic analysis of artesunate and DHA pharmacokinetics following oral artesunate administration by Tan et al. (described above), co-administration of artesunate with the Mannich-base derivative, pyronaridine, was not determined to significantly influence artesunate or DHA pharmacokinetics (70). Multiple dose administration of artesunate did not alter the pharmacokinetics of artemisinin; however, artemisinin co-administration with artesunate in ten healthy adults was associated with a more than two-fold increase in DHA AUC, a finding which led the authors to speculate that artemisinin may act as a UGT inhibitor (60). Finally, artesunate co-administration with chlorproguanil-dapsone did not produce significant alterations in chlorproguanil or dapsone pharmacokinetics, although moderate increases in exposure to the metabolites chlorcycloguanil and monoacetyl dapsone were detected. No clinically significant alterations of artesunate and DHA pharmacokinetics were found to be associated with artesunate-chlorproguanil-dapsone combination therapy (56).

Fehintola et al. (61) conducted a parallel group study evaluating the interaction potential of lamivudine/zidovudine/nevirapine therapy with artesunate+amodiaquine. The authors administered a three day regimen of artesunate+amodiaquine to HIV infected patients on no antiretroviral therapy (control group; n=11) or patients on long term lamivudine/zidovudine/nevirapine therapy (antiretroviral groups; n=10). They noted

significantly higher artesunate exposure and significantly shorter DHA half-life estimates in the antiretroviral group; however, DHA exposure was not significantly different between the groups. Ultimately, given the small number of subjects and the likely inherent clinical differences between the two groups, these results do not allow for any firm conclusions to be drawn.

An investigation of the effects of coadministration of low dose ritonavir with the artemisinin-based combination therapy pyronaridine tetraphosphate/artesunate (PA) has been conducted; healthy subjects were administered 100 mg ritonavir twice daily for 17 days, with PA given at standard treatment doses on days 8 – 10; samples for pharmacokinetic analysis were taken on day 10 (63). The comparison group of subjects was simply administered PA once daily for three days, with sampling on the third day. Per this analysis, the ritonavir/without ritonavir ratio of geometric means (90% CI) for DHA AUC_{0-t} was 0.6432 (0.4875, 0.8486) and for DHA C_{max} was 0.7348 (0.5500, 0.9815). These findings suggest the potential of ritonavir to induce metabolism of DHA, which the authors note likely reflects the capacity of ritonavir to induce glucuronidation. However, this interaction would need further evaluation in HIV infected patients in order to better gauge its true nature.

Orrell et al. (48) investigated the drug interaction potential of artesunate and amodiaquine. The authors conducted a crossover study in which 12 healthy African adults received 4 mg/kg artesunate on day 0 and either amodiaquine or amodiaquine+artesunate on day 7, with the alternative regimen administered on day 28. The investigators determined that when amodiaquine and artesunate were coadministered, the mean DHA AUC was approximately 33% lower, the mean DHA

C_{\max} was 49% lower, and the mean DHA half-life was 57% longer than when artesunate was administered alone (48). The AUC of the amodiaquine metabolite desethylamodiaquine was determined to be 45% lower when amodiaquine was coadministered with artesunate. However, the subject with the highest desethylamodiaquine AUC during amodiaquine+artesunate co-administration was excluded from the amodiaquine drug interaction analysis (48). Orrell et al. do not speculate on the source of the interaction. Given the small size of the study, and the lack of any clear physiologic basis for the observed interaction, further study would be needed to fully characterize this potential drug-drug interaction.

Summary and conclusions

Artesunate is a clinically versatile artemisinin derivative utilized for the treatment of mild to severe malaria infection. Given the therapeutic significance of artesunate, and the necessity of appropriate artesunate dosing, substantial research has been performed investigating the pharmacokinetics of artesunate and its active metabolite DHA. The results of the studies identified in this review indicate that administration of IV artesunate produces an artesunate C_{\max} of substantially greater magnitude than observed with any other route of administration. Following IV administration, artesunate hydrolysis to DHA occurs rapidly, producing DHA peak concentrations within 25 minutes post-dose. Artesunate and DHA display average clearance values of 2 – 3 L/hr/kg and 0.5 – 1.5 L/hr/kg, respectively, with volume estimates averaging 0.1 – 0.3 L/kg for artesunate and 0.5 – 1.0 L/kg for DHA. IM administration of artesunate is associated with high bioavailability, as assessed by DHA exposure. Although generally displaying similar pharmacokinetics to IV artesunate, IM artesunate does produce lower C_{\max} , higher V/F,

and longer half-life values for artesunate, as well as longer T_{max} values for DHA, than IV administration.

Following oral artesunate administration, peak artesunate concentrations are attained within an hour, with artesunate eliminated with a half-life of 20 - 45 minutes. DHA C_{max} values occur within two hours post-dose; DHA half-life values average 0.5 – 1.5 hours. A marked discrepancy in artesunate and DHA AUC values is apparent following oral artesunate administration, with DHA AUC values commonly determined to be more than 10-fold higher than corresponding artesunate AUC values. The pharmacokinetic parameters obtained in studies with rectal artesunate administration are generally similar to those obtained in studies with oral administration, although artesunate T_{max} is delayed and artesunate half-life extended. Population pharmacokinetic analyses of artesunate/DHA data following oral and rectal artesunate administration suggest that weight and pregnancy represent influential predictors of DHA pharmacokinetics following artesunate administration.

To date, drug interactions studies of artesunate with various other antimalarial agents have not yielded strong evidence of clinically relevant drug-drug interactions involving artesunate. Several relatively small studies examining the effects of infection on artesunate and DHA pharmacokinetics indicate that acute malaria infection may be associated with pharmacokinetic changes; most likely, such changes result in increased artesunate and/or DHA exposure during acute illness. With regard to pregnancy, present evidence indicates that further study will be required for complete description of any pregnancy-associated changes in artesunate and DHA pharmacokinetics..

Table 1.1 Artesunate (AS) pharmacokinetic findings following IV administration.

Ref.	Subjects & Regimen	C _{max} (ng/mL)	CL (L/hr/kg)	V (L/kg)	Half-life (min)	AUC (ng*hr/mL)
(21)	12 Vietnamese adults with <i>vivax</i> malaria 120 mg IV AS over 2 min	13685 ^{†a}	3.01	0.16	2.19	876 [†]
(22)	26 adult uncomplicated <i>falciparum</i> malaria patients in Vietnam 120 mg IV AS over 2 min		2.33 ^a	0.140 ^a	2.73	1146 [†]
(23)	17 healthy Vietnamese volunteers; subjects randomized into two groups, both receiving 120 mg IV AS over 2 min		3.0; 2.2	0.19; 0.16	2.6; 3.3	846; 1269 [†]
(25)	30 parasitemic adults with <i>falciparum</i> malaria Group 1: 12 with complications Group 2: 8 without complications Group 3: 10 with moderately severe complications Group 1 and 2: 120 mg IV AS over 2 min Group 3: 240 mg IV AS infused over 4 hours		Group 1: 1.63 Group 2: 2.49 Group 3: 3.07	Group 1: 0.08 Group 2: 0.24 Group 3: 0.23	Group 1: 2.3 Group 2: 4.3 Group 3: 3.2	

[†]Units converted to uniform scale a. Median

Table 1.1 Continued.

Ref.	Subjects & Regimen	Cmax (ng/mL)	CL (L/hr/kg)	V (L/kg)	Half-life (min)	AUC (ng*hr/mL)
(26)	23 Vietnamese adults with uncomplicated <i>falciparum</i> malaria; subjects randomized into two Groups, both receiving: 120 mg IV AS over 2 min	16146; 16530†	2.8; 2.1	0.22	3.2	1038; 1230†
(31)	28 pediatric Gabonese patients with severe malaria randomized into two groups Group 1: 2.4 mg/kg IV AS Group 2: 1.2 mg/kg IV AS	Group 1: 29677 ^a Group 2: 15369 ^a	Group 1: 3.12† ^a Group 2: 4.26† ^a	Group 1 Vss: 0.17† ^a Group 2 Vss: 0.44† ^a	Group 1: 1.5 ^a Group 2: 11.5 ^a	Group 1: 1042† ^a Group 2: 555† ^a
(28)	30 healthy volunteers 0.5, 1, 2, 4, or 8 mg/kg IV AS over 2 min	4797; 6128; 19420; 36100; 83340	1.3; 18; 1.3; 1.4; 1.6†	Vss: 0.092; 0.187; 0.106; 0.109; 0.165†	7.2; 8.4; 14.4; 9.0; 12.6†	386; 593; 1595; 3038; 6994†
(24)	14 Ugandan adults with severe malaria 2.4 mg/kg IV AS over 3 – 4 minutes	3260 ^a			15† ^a	AUC _{0-t} 727

†Units converted to uniform scale a. Median

Table 1.1 Continued

Ref.	Subjects & Regimen	C _{max} (ng/mL)	CL (L/hr/kg)	V (L/kg)	Half-life (min)	AUC (ng*hr/mL)
(29)	Thai women with uncomplicated <i>falciparum</i> malaria evaluated when pregnant (n=20) and again at 3 months postpartum (n=14) 4 mg/kg IV AS	Pregnant 15700 ^a Postpartum 12200 ^a	Pregnant 4.19 ^a Postpartum 5.05 ^a	Pregnant 0.76 ^a Postpartum 1.18 ^a	Pregnant 7.2 ^{†a} Postpartum 7.8 ^{†a}	Pregnant 955 ^a Postpartum 792 ^a
(30)	18 healthy adults (6 per dosing cohort) 2 mg/kg, 4 mg/kg, or 8 mg/kg IV AS administered over 2 minutes once daily x 3 days	Day 1 28411; 40574; 63677 Day 2 17920; 34387; 74588 Day 3 16487; 51164; 67613	Day 1 [†] 1.27; 1.16; 1.67 Day 2 [†] 1.77; 1.64; 1.60 Day 3 [†] 1.67; 1.38; 1.73	V _{ss} Day 1 [†] 0.10360; 0.10434; 0.18799 Day 2 [†] 0.18524; 0.13976; 0.12910 Day 3 [†] 0.12200; 0.12217; 0.16458	Day 1 [†] 9.6; 12.6; 12.0 Day 2 [†] 11.4; 13.8; 11.4 Day 3 [†] 9.0; 12.0; 12.0	Day 1 [†] 2051; 4640; 6022 Day 2 [†] 1410; 2628; 6669 Day 3 [†] 1270; 3518; 5916

†Units converted to uniform scale a.Median

Table 1.2 DHA pharmacokinetic findings following IV artesunate.

Ref.	Subjects & Regimen	C _{max} (ng/mL)	T _{max} (min)	CL/F (L/hr/kg)	V/F (L/kg)	Half-life (min)	AUC (ng*hr/mL)
(21)	12 Vietnamese adults with <i>vivax</i> malaria 120 mg IV AS over 2 min	2192 ^{†a}	8 ^a	1.10	0.92	36.7	1845 [†]
(22)	26 adult uncomplicated <i>falciparum</i> malaria patients in Vietnam 120 mg IV AS over 2 min	2648 ^{†a}	9.0 ^a	0.75 ^a	0.76	40.2	2377 [†]
(23)	17 healthy Vietnamese volunteers; subjects randomized into two groups, both receiving 120 mg IV AS over 2 min	1507; 1678 [†]	9; 16			53; 47	
(25)	30 parasitemic adults with <i>falciparum</i> malaria Group 1: 12 with complications Group 2: 8 without complications Group 3: 10 with moderately severe complications Group 1 and 2: 120 mg IV AS over 2 min Group 3: 240 mg IV AS infused over 4 hours	Group 1: 2417 [†] Group 2: 2531 [†] Group 3: 910 [†]	Group 1: 10.4 Group 2: 9.9 Group 3: NA	Group 1: 1.09 Group 2: 0.73 Group 3: 0.73	Group 1: 0.77 Group 2: 1.01 Group 3: 0.78	Group 1: 40.0 Group 2: 64.1 Group 3: 46.2	Group 1: 2078 [†] Group 2: 2559 [†] Group 3: 5573 [†]

[†]Units converted to uniform scale a.Median

Table 1.2 Continued

Ref.	Subjects & Regimen	C _{max} (ng/mL)	T _{max} (min)	CL/F (L/hr/kg)	V/F (L/kg)	Half-life (min)	AUC (ng*hr/mL)
(27)	34 Ghanaian children (8 months – 7 years) with moderate <i>falciparum</i> malaria Group 1 & 2: AS rectal suppository, IV AS 2.4 mg/kg 12 hr later Group 3: 2.4 mg/kg IV AS, AS rectal suppository 12 hr later	Group 1/2: 1280† ^a Group 3: 1592 † ^a	Group 1/2: 12† ^a Group 3: 12†	Group 1/2: 1.5 ^a Group 3: 1.0 ^a	Group 1/2: 0.6 ^a Group 3: 0.9 ^a	Group 1 & 2: 18† ^a Group 3: 31.8† ^a	Group 1/2: 1166† ^a Group 3: 1706† ^a
(26)	23 Vietnamese adults with uncomplicated <i>falciparum</i> malaria; subjects randomized into two groups, both receiving 120 mg IV AS over 2 min	2758; 2730† ^a	7; 9 ^a	0.64; 0.48	0.8; 0.55	59; 50	2872; 3298†
(31)	28 pediatric Gabonese patients with severe malaria randomized into two groups Group 1: 2.4 mg/kg IV AS Group 2: 1.2 mg/kg IV AS	Group 1: 3011† ^a Group 2: 1584† ^a	Group 1: 1: 0.5 ^a Group 2: 1.4 ^a	Group 1: 2.16† ^a Group 2: 1.08† ^a	Group 1 Vss: 0.75 ^a Group 2 Vss: 0.77 ^a	Group 1: 20.7 ^a Group 2: 32.0 ^a	Group 1: 923† ^a Group 2: 737† ^a

†Units converted to uniform scale a. Median

Table 1.2 Continued

Ref.	Subjects & Regimen	C _{max} (ng/mL)	T _{max} (min)	CL/F (L/hr/kg)	V/F (L/kg)	Half-life (min)	AUC (ng*hr/mL)
(32)	17 adults with severe <i>falciparum</i> malaria in Thailand 2.4 mg/kg IV AS over 2 min [2.1 (1.4 – 2.8 mg/kg)]	605 ^{†a}	T _{max} reached by 15 min	5.6 ^a	V _{ss} : 1.9 ^a	20.4 ^{†a}	418 ^{†a}
(28)	30 healthy volunteers 0.5, 1, 2, 4, or 8 mg/kg IV AS over 2 min	428; 802; 1286; 3148; 4744	9.6; 15; 9.6; 7.2; 24 [†]	1.3; 0.98; 1.1; 0.86; 0.82 [†]	V _{ss} : 1.734; 2.201; 1.860; 1.701; 2.403 [†]	57.6; 92.4; 69.0; 82.2; 128.4 [†]	385; 1082; 1850; 4886; 10410
(24)	14 Ugandan adults with severe malaria 2.4 mg/kg IV AS over 3 – 4 minutes	3140 ^a	8.4 ^{†a}			78.6 ^{†a}	AUC _{0-t} 3492 ^a

[†]Units converted to uniform scale a.Median

Table 1.2 Continued

Ref.	Subjects & Regimen	C _{max} (ng/mL)	T _{max} (min)	CL/F (L/hr/kg)	V/F (L/kg)	Half-life (min)	AUC (ng*hr/mL)
(29)	Thai women with uncomplicated <i>falciparum</i> malaria evaluated when pregnant (n=20) and again at 3 months postpartum (n=14) 4 mg/kg IV AS	Pregnant 3210 ^a Postpartum 2930 ^a		Pregnant 1.20 ^a Postpartum 1.35 ^a	Pregnant 1.76 ^a Postpartum 2.37 ^a	Pregnant 61.8 ^{†a} Postpartum 69 ^{†a}	Pregnant 2450 ^a Postpartum 2220 ^a
(30)	18 healthy adults (6 per dosing cohort) 2 mg/kg, 4 mg/kg, or 8 mg/kg IV AS administered over 2 minutes once daily x 3 days	Day 1 1735; 3015; 6056 Day 2 1710; 2923; 5943 Day 3 2358; 3018; 5762	Day 1 [†] 17.4; 15.0; 15.0 Day 2 [†] 12.0; 15.0; 13.2 Day 3 [†] 9.6; 17.4; 17.4	Day 1 [†] 0.9708; 0.9552; 0.9306 Day 2 [†] 1.053; 1.162; 1.018 Day 3 [†] 0.8778; 1.049; 0.9360	Vss Day 1 [†] 1.634; 2.377; 1.870 Day 2 [†] 2.224; 2.249; 2.525 Day 3 [†] 1.691; 1.895; 1.776	Day 1 [†] 71.4; 104.4; 85.2 Day 2 [†] 95.4; 85.2; 114.6 Day 3 [†] 78.6; 74.4; 80.4	Day 1 [†] 2121; 4391; 9697 Day 2 [†] 2012; 3740; 8732 Day 3 [†] 2385; 3960; 9205

†Units converted to uniform scale a. Median

Table 1.3 Artesunate pharmacokinetic results following IM artesunate.

Ref.	Subjects & Regimen	C _{max} (ng/mL)	T _{max} (min)	CL/F (L/hr/kg)	V/F (L/kg)	Half-life (min)	AUC (ng*hr/mL)
(26)	11 Vietnamese adults with uncomplicated <i>falciparum</i> malaria 120 mg AS administered by intramuscular injection	884 ^{†a}	12 ^a	2.9	2.6	41	999 [†]
(31)	28 pediatric Gabonese patients with severe malaria randomized into two Groups Group 1: 2.4 mg/kg IV AS, followed by 1.2 mg/kg IM AS 12 hours later Group 2: 2.4 mg/kg IM AS, followed by 1.2 mg/kg IV AS 12 hours later	Group 1: 615 ^{†a} Group 2: 661 ^{†a}	Group 1: 7.2 ^a Group 2: 8.0 ^a	Group 1: 2.4 ^{†a} Group 2: 3.48 ^{†a}	Group 1 Vss/F: 2.07 ^a Group 2 Vss/F: 3.98 ^a	Group 1: 25.2 ^a Group 2: 48.2 ^a	Group 1: 535 ^{†a} Group 2: 544 ^{†a}
(37)	9 Vietnamese adults with severe <i>falciparum</i> malaria 2.4 mg/kg AS administered by intramuscular injection	2195 ^{†a}		2.84 ^a	1.09 ^a	30 ^a	856 ^{†a}

[†]Units converted to uniform scale a.Median

Table 1.4 DHA pharmacokinetic results following IM artesunate.

Ref.	Subjects & Regimen	C _{max} (ng/mL)	T _{max} (min)	CL/F (L/hr/kg)	V/F (L/kg)	Half-life (min)	AUC (ng*hr/mL)
(26)	11 Vietnamese adults with uncomplicated <i>falciparum</i> malaria 120 mg AS administered by intramuscular injection	1166 ^{†a}	45 ^a	0.73	1.1	64	2474 [†] F: 88%
(31)	28 pediatric Gabonese patients with severe malaria randomized into two Groups Group 1: 2.4 mg/kg IV AS, followed by 1.2 mg/kg IM AS 12 hours later Group 2: 2.4 mg/kg IM AS, followed by 1.2 mg/kg IV AS 12 hours later	Group 1: 341 ^a Group 2: 626 ^a	Group 1: 25.9 ^a Group 2: 40.5 ^a	Group 1: 2.16 ^{†a} Group 2: 1.5 ^{†a}	Group 1: Vc/F: 1.2 ^a Vss/F: 1.32 ^a Group 2: Vc/F: 1.2 ^a Vss/F: 1.28 ^a	Group 1: 31.9 ^a Group 2: 40.2 ^a	Group 1: 396 ^{†a} Group 2: 1123 ^{†a} Combined Group F: 86.37% ^a
(37)	9 Vietnamese adults with severe <i>falciparum</i> malaria 2.4 mg/kg AS administered by intramuscular injection	870 ^{†a}	35 ^a	1.18 ^a	1.79 ^a	52.7 ^a	1496 ^{†a}

[†]Units converted to uniform scale a.Median

Table 1.5 Artesunate T_{max} and half-life means obtained following oral artesunate.

Ref.	Subjects	Regimen	T _{max} (hours)	Half-life (hours)
(52)	6 healthy adults in Geneva	200 mg AS once	0.25 (5/6 subjects) 0.5 (1/6 subjects)	
(43)	11 male Thai adults with uncomplicated <i>falciparum</i> malaria	200 mg AS once, followed by 100 mg 12 hours later, then 100 mg once daily for another 4 days	Acute: 0.5 ^a Convalescence: 1.0 ^a	Acute: 0.36 ^a Convalescence: 0.54 ^a
(44)	8 healthy male Thai adults	300 mg AS (Guilin or Arenco formulation)	Guilin: 0.25 ^a Arenco: 0.31 ^a	Guilin: 0.53 Arenco: 0.57
(45)	12 healthy male Malaysian adults	200 mg AS once	0.66	0.49
(50)	6 male Thai adults with uncomplicated <i>falciparum</i> malaria and 6 healthy male adults	100 mg AS once	Healthy: 0.71 Patients: not determined	Healthy: 0.41 Patients: not determined
(20)	8 healthy adults in Australia	150 mg AS once	0.65 (n=6) ^a	
(53)	15 healthy Cambodian male adults	4 mg/kg AS once with mefloquine	0.75 ^a	
(54)	20 healthy adult males in Australia	200 mg/day x 3 days alone (Period 1); repeated with mefloquine after washout (Period 2)	Period 1/Day 1: 0.6 ^b Period 1/Day 3: 0.6 ^b Period 2/Day 1: 0.5 ^b Period 2/Day 3: 0.6 ^b	

a. Median b. Geometric Mean

Table 1.5 Continued.

Ref.	Subjects	Regimen	T _{max} (hours)	Half-life (hours)
(41)	10 healthy male Vietnamese adults	200 mg AS once daily x 5 days	Day 1: 0.8 ^a Day 5: 0.8 ^a	Day 1: 0.43 ^a Day 5: 0.50 ^a
(48)	13 healthy adults in Africa	Mean dose: 4.26 mg/kg with (ACT) or without (AS only) amodiaquine as single dose	AS only: 0.62 ACT: 0.86	
(49)	57 children (2-14 years) with uncomplicated <i>falciparum</i> malaria in Gabon	AS dose (mg/kg/day) with pyronaridine Group A:2.1(1.4-2.4) Group B:3.3(2.4 – 3.9) Group C:4.8(3.0 – 6.1) Group D: 3.8(3.0-4.3)	Group A:0.6 Group B:0.7 Group C:1.0 Group D:0.5	Group A: 0.8 (n=12) Group B:1.1 (n=12) Group C:0.5 (n=10) Group D:1.2 (n=13)
(42)	40 children and adults with uncomplicated <i>falciparum</i> malaria in Pailin, Cambodia and 40 adults with uncomplicated <i>falciparum</i> malaria in Wang Pha, Thailand	At each site: Group 1: AS monotherapy: 2 mg/kg/day x 7 days Group 2: AS 4 mg/kg/day x 3 days + mefloquine	Thailand: Group 1: 0.38 ^a Group 2: 0.50 ^a Cambodia: Group 1:0.50 ^a Group 2: 1.00 ^a	Thailand: Group 1: 0.37 ^a Group 2: 0.58 ^a Cambodia: Group 1: 0.29 ^a Group 2: 0.29 ^a
(56)	86 acute uncomplicated <i>falciparum</i> malaria patients from Malawi and Gambia	1, 2, or 4 mg/kg AS with chlorproguanil and dapsone once daily x 3 days	1 mg/kg: 1.08 ^a 2 mg/kg: 0.55 ^a 4 mg/kg: 1.03 ^a	1 mg/kg: 0.515 ^b 2 mg/kg: 0.478 ^b 4 mg/kg: 0.467 ^b

a. Median b. Geometric mean

Table 1.5 Continued

Ref.	Subjects	Regimen	T _{max} (hours)	Half-life (hours)
(47)	23 healthy Malaysian adults	200 mg AS once with amodiaquine as fixed or non-fixed product	Fixed:0.26 Non-fixed:0.53	Fixed:0.63 Non-fixed:0.76
(66)	13 male and female adult patients in the DRC with acute uncomplicated <i>falciparum</i> malaria	200 mg AS once daily x 3 days with amodiaquine	1.4 (n=10)	
(46)	43 adults with uncomplicated <i>falciparum</i> malaria in Thailand	AS+mefloquine as fixed (200 mg AS) or non-fixed (4 mg/kg AS) combination	Fixed:0.833 (n=19) Non-fixed:0.925 (n=23)	
(62)	26 health male Indian adults	100 mg once with amodiaquine as fixed or non-fixed product given per crossover design	Fixed: 0.33 ^a Non-fixed: 0.50 ^a	Fixed: 0.59 ^a Non-fixed: 0.42 ^a
(61)	10 HIV-infected Nigerian adults receiving long term lamivudine/zidovudine/nevirapine therapy (ART Group) 11 HIV-infected Nigerian adults not receiving antiretroviral therapy (control Group)	200 mg AS with 600 mg amodiaquine daily x 3 days	Day 3 ART Group: 1.0 ^a Control Group: 1.0 ^a	Day 3 ART Group: 0.4 Control Group: 1.1

a. Median b. Geometric Mean

Table 1.5 Continued.

Ref.	Subjects	Regimen	T _{max} (hours)	Half-life (hours)
(29)	Thai women with uncomplicated <i>falciparum</i> malaria evaluated when pregnant (n=20) and again at 3 months postpartum (n=14)	4 mg/kg oral AS	Pregnant 1.00 ^a Postpartum 1.00	Pregnant 0.35 ^a Postpartum 0.24 ^a
(63)	Healthy adults randomized to Arm A (n=17) or Arm B (n=16)	Arm A: 100 mg ritonavir twice daily x 17 days with pyronaridine tetraphosphate/artesunate (3 180/60 mg tablets for <65 kg; 4 tablets for ≥ 65 kg) on days 8 – 10; sampling on day 10 Arm B: pyronaridine tetraphosphate/artesunate x 3 days; sampling on day	Arm A: 1.05 ^b Arm B: 0.75 ^b	Arm A 0.410 ^b (n=9) Arm B 0.433 ^b (n=13)
(65).	143 Cambodian adults with uncomplicated <i>falciparum</i> malaria	2, 4, or 6 mg/kg/day AS x 7 days	Day 0 2 mg/kg: 0.482 ^b 4 mg/kg: 0.518 ^b 6 mg/kg: 0.640 ^b	Day 0 2 mg/kg: 0.489 ^b 4 mg/kg: 0.499 ^b 6 mg/kg: 0.461 ^b
(67)	24 women in 2nd or 3 rd trimester or pregnancy and 23 paired non-pregnant women; all patients had uncomplicated <i>falciparum</i> malaria	3.6 mg/kg/day AS + mefloquine x 3 days; sampling on first day of treatment	Pregnant: 1.00 ^a Non-pregnant: 1.00 ^a	Pregnant 0.3 ^a Non-pregnant 0.4 ^a

a. Median b. Geometric mean

Table 1.6 Artesunate and DHA AUC and Cmax means following oral artesunate.

Ref.	Subjects	Oral AS regimen	AUC (ng*hr/mL)	C _{max} (ng/mL)
(44)	8 healthy male Thai adults	300 mg AS (Guilin and Arencu formulations)	AS Guilin: 406 Arencu: 190.8	AS Guilin: 397 Arencu: 194
			DHA Guilin: 1630 Arencu: 2600	DHA Guilin: 500 Arencu: 928
(45)	12 healthy male Malaysian adults	200 mg AS once	AS 119	AS 256.3
			DHA AUC _{0-t} : 1331	DHA 873.7
(50)	6 male Thai adults with uncomplicated <i>falciparum</i> malaria and 6 healthy male adults	100 mg AS once	AS AUC _{0-12hr} Healthy: 97 Patients: not determined	AS Healthy: 114 Patients: not determined
			DHA AUC _{0-12hr} Healthy: 501 Patients: 1144	DHA Healthy: 339 Patients: 554
(20)	8 healthy adults in Australia	150 mg once	AS AUC _{0-6hr} : 154 (n=6)	AS ^a 111 (n=6)
			DHA AUC _{0-6hr} : 824	DHA ^a 546

Table 1.6 Continued.

Ref.	Subjects	Oral AS regimen	AUC (ng*hr/mL)	C _{max} (ng/mL)
(48)	13 healthy adults in Africa	Mean dose: 4.26 mg/kg with (ACT) or without (AS only) amodiaquine single dose	AS AS only: 206.4 ACT: 183.3	AS AS only: 231.8 ACT: 141.6
			DHA AS only: 2044.4 ACT: 1410.5	DHA AS only: 844.5 ACT: 446.2
(41)	10 healthy male Vietnamese adults	200 mg once daily x 5 days	AS ^a Day 1: 67 Day 5: 60	AS ^a Day 1:67 Day 5: 58
			DHA ^a Day 1:1158 Day 5:1300	DHA Pooled:654
(49)	57 children (2-14 years) with uncomplicated <i>falciparum</i> malaria in Gabon	AS dose (mg/kg) Group A:2.1(1.4-2.4) Group B:3.3(2.4 – 3.9) Group C:4.8(3.0 – 6.1) Group D: 3.8(3.0-4.3)	AS Group A: 104 (n=12) Group B: 154 (n=12) Group C:232 (n=10) Group D: 179 (n=13)	AS Group A: 93 Group B:154 Group C: 287 Group D: 171
		Administered with pyronaridine	DHA Group A: 1055 Group B: 1989 Group C: 2961 Group D: 2245	DHA Group A:479 Group B: 940 Group C:1186 Group D:792

a. Median

Table 1.6 Continued.

Ref.	Subjects	Oral AS regimen	AUC (ng*hr/mL)	C _{max} (ng/mL)
(42)	40 children and adults with uncomplicated <i>falciparum</i> malaria in Pailin, Cambodia and 40 adults with uncomplicated <i>falciparum</i> malaria in Wang Pha, Thailand	At each site: Group 1: AS monotherapy: 2 mg/kg/day x 7 days Group 2: AS 4 mg/kg/day x 3 days + mefloquine	AS ^{†a} AUC _{0-24hr} Thailand Group 1: 128 Thailand Group 2: 237 Cambodia Group 1: 173 Cambodia Group 2: 338	AS ^{†a} Thailand Group 1: 171 Thailand Group 2: 200 Cambodia Group 1: 270 Cambodia Group 2: 316
			DHA ^{†a} AUC _{0-24hr} Thailand Group 1: 1308 Thailand Group 2: 2957 Cambodia Group 1: 1382 Cambodia Group 2: 4123	DHA ^{†a} Thailand Group 1: 859 Thailand Group 2: 1191 Cambodia Group 1: 802 Cambodia Group 2: 1590
(56)	86 acute uncomplicated <i>falciparum</i> malaria patients from Malawi and Gambia	1, 2, or 4 mg/kg AS with chlorproguanil and dapsone once daily x 3 days	AS ^b 1 mg/kg: 64.6 (n=16) 2 mg/kg: 151(n=19) 4 mg/kg: 400(n=23)	AS ^b 1 mg/kg: 48.9 2 mg/kg: 106 4 mg/kg: 224
			DHA ^b 1 mg/kg: 538 (n=24) 2 mg/kg: 1445(n=29) 4 mg/kg: 383(n=23)	DHA ^b 1 mg/kg: 228 2 mg/kg: 581 4 mg/kg: 1414

†Units converted to uniform scale a. Median b. Geometric mean

Table 1.6 Continued.

Ref.	Subjects	Oral AS regimen	AUC (ng*hr/mL)	C _{max} (ng/mL)
(47)	23 healthy Malaysian adults	200 mg once with amodiaquine as fixed or non-fixed product	AS† Fixed: 391.1 Non-fixed: 213.2	AS† Fixed: 333 Non-fixed: 444
			DHA† Fixed: 1468.9 Non-fixed: 1656.0	DHA† Fixed: 609.8 Non-fixed: 874.5
(46)	43 adults with uncomplicated <i>falciparum</i> malaria in Thailand	200 mg/day for fixed dose AS-mefloquine tablet (n=20) or 4 mg/kg/day as nonfixed (n=23) AS-mefloquine	AS AUC _{0-t} : Fixed: 310 (n=19) Nonfixed: 419 (n=21)	AS Fixed: 255 (n=19) Nonfixed: 451 (n=23)
			DHA AUC _{0-t} : Fixed: 3027 Non-fixed: 3633	DHA Fixed: 1234 Non-fixed: 2043
(57)	21 children (5 – 13 years) with uncomplicated malaria in Uganda	4 mg/kg once daily with amodiaquine x 3 days	AS 113 (data pooled from all subjects)	AS 51 (data pooled from all subjects)
			DHA ^a 1404	DHA ^a 473
(62)	26 health male Indian adults	100 mg once with amodiaquine as fixed or non-fixed product given per crossover design	AS Fixed: 66.6 Non-fixed: 89.0	AS Fixed: 67.0 Non-fixed: 154.8
			DHA Fixed: 433.2 Non-fixed: 521.5	DHA Fixed: 180.4 Non-fixed: 337.1

†Units converted to uniform scale a. Median

Table 1.6 Continued.

Ref.	Subjects	Oral AS regimen	AUC (ng*hr/mL)	C _{max} (ng/mL)
(61)	10 HIV-infected Nigerian adults receiving long term lamivudine/zidovudine/nevirapine therapy (ART Group)	200 mg AS with 600 mg amodiaquine daily x 3 days	AS Day 3 AUC ₀₋₉₆ ART Group: 105 Control Group: 69	AS Day 3 ART Group: 108 Control Group: 71
	11 HIV-infected Nigerian adults not receiving antiretroviral therapy (control Group)		DHA Day 3 AUC ₀₋₉₆ ART Group: 603 Control Group: 883	DHA Day 3 ART Group: 298 Control Group: 507
(29)	Thai women with uncomplicated <i>falciparum</i> malaria evaluated when pregnant (n=20) and again at 3 months postpartum (n=14)	4 mg/kg oral AS	AS Pregnant 217 ^a	AS Pregnant 212 ^a
			Postpartum 106 ^a	Postpartum 119 ^a
			DHA Pregnant 1940 ^a	DHA Pregnant 1040 ^a
			Postpartum 1550 ^a	Postpartum 915 ^a

†Units converted to uniform scale a. Median b. Geometric mean

Table 1.6 Continued

Ref.	Subjects	Oral AS regimen	AUC (ng*hr/mL)	C _{max} (ng/mL)
(63)	Healthy adults randomized to Arm A (n=17) or Arm B (n=16)	Arm A: 100 mg ritonavir twice daily x 17 days with pyronaridine tetraphosphate/artesunate (3 180/60 mg tablets for <65 kg; 4 tablets for ≥ 65 kg) on days 8 – 10; sampling on day 10	AS ^b AUC _{0-t} Arm A 120 Arm B 105	AS ^b Arm A 95.1 Arm B 95.5
		Arm B: pyronaridine tetraphosphate/artesunate x 3 days; sampling on day 3	DHA ^b AUC _{0-t} Arm A 1151 Arm B 1790	DHA ^b Arm A 539.5 Arm B 734.3
(65)	143 Cambodian adults with uncomplicated <i>falciparum</i> malaria	2, 4, or 6 mg/kg/day AS x 7 days	AS (Day 0) ^b AUC ₀₋₈ 91.2; 279; 453	AS (Day 0) ^b 83.1; 237; 374
			DHA (Day 0) ^b AUC ₀₋₈ 1331; 3854; 5989 Day 6 ^b 481; 1267; 2218	DHA (Day 0) ^b 554; 1515; 2129 Day 6 ^b 196; 497; 875
(67)	24 women in 2nd or 3 rd trimester of pregnancy and 23 paired non-pregnant women; all patients had uncomplicated <i>falciparum</i> malaria	3.6 mg/kg/day AS + mefloquine x 3 days; sampling on first day of treatment	AS Pregnant 89.0 ^a Non-pregnant 62.9 ^a	AS Pregnant 94.2 ^a Non-pregnant 62.9 ^a
			DHA Pregnant 1330 ^a Non-pregnant 1360 ^a	DHA Pregnant 756 ^a Non-pregnant 696 ^a

†Units converted to uniform scale a. Median b. Geometric mean

Table 1.7 DHA half-life means obtained following oral artesunate.

Ref.	Subjects	Artesunate regimen	DHA half-life (hours)
(52)	6 healthy adults in Geneva	200 mg AS once	0.65
(21)	12 Vietnamese adult male <i>vivax</i> malaria patients	100 mg single dose	0.67 (n=11)
(22)	26 Vietnamese adult patients with uncomplicated <i>falciparum</i> malaria	100 mg single dose	0.66 (n=16)
(43)	11 male Thai adults with uncomplicated <i>falciparum</i> malaria	200 mg AS once, followed by 100 mg 12 hours later, then 100mg once daily x 4 days	Acute: 0.64 ^a Convalescence: 0.66 ^a
(44)	8 healthy male Thai adults	300 mg AS (Guilin or Arencu formulation)	Guilin: 1.77 Arencu: 1.73
(45)	12 healthy male Malaysian adults	200 mg single dose	0.49
(23)	8 Vietnamese adults with uncomplicated <i>falciparum</i> malaria and 10 healthy Vietnamese adults	150 mg once	Healthy: 0.77 Patients: 0.88
(50)	6 male Thai adults with uncomplicated <i>falciparum</i> malaria and 6 healthy male adults	100 mg AS once	Healthy: 0.85 Patients: 1.06
(60)	10 healthy Vietnamese males	100 mg AS once	Half-life: 0.55 ^b
(51)	12 healthy adults	200 mg once	0.68
(58)	20 male and female healthy Thai adults	4 mg/kg once	0.74 ^a
(53)	15 healthy Cambodian male adults	4 mg/kg AS once with mefloquine	1.30 ^b
(55)	24 pregnant Karen women in the 2 nd and 3 rd trimesters with uncomplicated <i>falciparum</i> malaria	4 mg/kg once daily x 3 days with atovaquone plus proguanil	Half-life: 1.0 (n =13) ^a

a. Median b. Geometric mean

Table 1.7 Continued.

Ref.	Subjects	Artesunate regimen	DHA half-life (hours)
(54)	20 healthy adult males in Australia	200 mg/day x 3 days alone (Period 1); repeated with mefloquine after washout (Period 2)	Period 1/Day 1: 1.14 Period 1/Day 3: 1.14 Period 2/Day 1: 1.02 Period 2/Day 3: 1.09
(59)	24 children with uncomplicated <i>falciparum</i> malaria in Gabon	4 mg/kg once daily for 3 days in one of two formulations (blister pack and fixed dose) of AS/mefloquine	Fixed dose: 0.9(n=9) ^a Blister pack: 1.0 (n=11) ^a
(41)	10 healthy male Vietnamese adults	200 mg once daily x 5 days	0.87 (from pooled data)
(48)	13 healthy adults in Africa	Mean dose: 4.26 mg/kg with (ACT) or without (AS only) amodiaquine single dose	AS only: 1.46 ACT: 3.08
(49)	57 children (2-14 years) with uncomplicated <i>falciparum</i> malaria in Gabon	AS dose (mg/kg) Group A: 2.1(1.4-2.4) Group B: 3.3(2.4 – 3.9) Group C: 4.8(3.0 – 6.1) Group D: 3.8(3.0-4.3) Administered with pyronaridine	Group A: 1.0 Group B: 0.9 Group C: 1.2 Group D: 1.2
(42)	40 children and adults with uncomplicated <i>falciparum</i> malaria in Pailin, Cambodia and 40 adults with uncomplicated <i>falciparum</i> malaria in Wang Pha, Thailand	At each site: Group 1: AS monotherapy: 2 mg/kg/day x 7 days Group 2: AS 4 mg/kg/day x 3 days + mefloquine	Thailand Group 1: 0.71 ^a Thailand Group 2: 0.85 ^a Cambodia Group 1: 0.84 ^a Cambodia Group 2: 0.77 ^a
(56)	86 acute uncomplicated <i>falciparum</i> malaria patients from Malawi and Gambia	1, 2, or 4 mg/kg AS with chlorproguanil and dapsone once daily x 3 days	1 mg/kg: 0.779 ^b 2 mg/kg: 0.917 ^b 4 mg/kg: 1.09 ^b

a. Median b. Geometric mean

Table 1.7 Continued.

Ref.	Subjects	Artesunate regimen	DHA half-life (hours)
(47)	23 healthy Malaysian adults	200 mg once with amodiaquine as fixed or non-fixed product	Fixed: 1.68 Non-fixed: 1.42
(46)	43 adults with uncomplicated <i>falciparum</i> malaria in Thailand	200 mg/day for fixed dose AS-mefloquine tablet or 4 mg/kg/day as non-fixed AS-mefloquine	Fixed: 1.1 (n=14) Non-fixed: 0.8 (n=18)
(57)	21 children (5 – 13 years) with uncomplicated malaria in Uganda	4 mg/kg once daily with amodiaquine x 3 days	1.3 ^a
(62)	26 health male Indian adults	100 mg once with amodiaquine as fixed or non-fixed product given per crossover design	Fixed: 0.82 ^a Non-fixed: 0.75 ^a
(64)	26 2 nd and 3 rd trimester pregnant women with asymptomatic <i>falciparum</i> parasitemia, the same women postpartum, and 25 non-pregnant asymptomatic, parasitemic controls	200 mg once	Pregnant: 1.28 ^a Postpartum: 1.63 ^a Controls: 1.41 ^a
(61)	10 HIV-infected Nigerian adults receiving long term lamivudine/zidovudine/nevirapine therapy (ART Group) 11 HIV-infected Nigerian adults not receiving antiretroviral therapy (control group)	200 mg AS with 600 mg amodiaquine daily x 3 days	Day 3 ART Group: 1.6 Control Group: 3.2
(29)	Thai women with uncomplicated <i>falciparum</i> malaria evaluated when pregnant (n=20) and again at 3 months postpartum (n=14)	4 mg/kg oral AS	Pregnant 0.86 ^a Postpartum 1.02 ^a

a. Median b. Geometric mean

Table 1.7 Continued.

Ref.	Subjects	Artesunate regimen	DHA half-life (hours)
(63)	Healthy adults randomized to Arm A (n=17) or Arm B (n=16)	Arm A: 100 mg ritonavir twice daily x 17 days with pyronaridine tetrphosphate/artesunate (3 180/60 mg tablets for <65 kg; 4 tablets for ≥ 65 kg) on days 8 – 10; sampling on day 10 Arm B: pyronaridine tetrphosphate/artesunate x 3 days; sampling on day 3	Arm A 2.04 ^b (n=16) Arm B 2.18 ^b (n=14)
(65)	143 Cambodian adults with uncomplicated <i>falciparum</i> malaria	2, 4, or 6 mg/kg/day AS x 7 days	Day 0 ^b 0.838; 0.913; 1.13 Day 6 ^b 0.799; 0.851; 0.843
(67)	24 women in 2nd or 3 rd trimester of pregnancy and 23 paired non-pregnant women; all patients had uncomplicated <i>falciparum</i> malaria	3.6 mg/kg/day AS + mefloquine x 3 days; sampling on first day of treatment	Pregnant 1.2 ^a Non-pregnant 1.3 ^a

a. Median

b. Geometric mean

Table 1.8 Artesunate pharmacokinetic results following rectal artesunate.

Ref.	Subjects & Regimen	C _{max} (ng/mL)	T _{max} (hours)	Half-life (hours)	AUC (ng*hr/mL)
(73)	12 pediatric patients with uncomplicated <i>falciparum</i> malaria 50 mg AS as rectal suppository [0.86 – 2.55 mg/kg AS]	90†	0.58		
(45)	12 healthy Malaysian adults 200 mg AS as rectal suppository	448.5	1.43	0.95	796
(72)	16 pediatric patients with uncomplicated <i>falciparum</i> malaria 10 mg/kg (n=7) or 20 mg/kg (n=9) AS as rectal suppositories	507; 561† ^a	0.8; 1.0 ^a	0.9; 0.9 ^a	692; 1076† ^a

†Units converted to uniform scale a. Median

Table 1.9 DHA pharmacokinetic results following rectal artesunate.

Ref.	Subjects & Regimen	C _{max} (ng/mL)	T _{max} (hr)	CL/F (L/hr/kg)	V/F (L/kg)	Half-life (hr)	AUC (ng*hr/mL)
(73)	12 pediatric patients with uncomplicated <i>falciparum</i> malaria 50 mg AS rectal suppository [0.86 – 2.55 mg/kg AS]	180†	1.13				
(45)	12 healthy Malaysian adults 200 mg AS as rectal suppository	385.6†	1.80				AUC _{0-t} 965
(27)	34 Ghanaian children (8 months – 7 years) with moderate <i>falciparum</i> malaria Group 1: AS 10 mg/kg as rectal suppository, IV AS 2.4 mg/kg 12 hr later Group 2: AS 20 mg/kg AS as rectal suppository, IV AS 2.4 mg/kg 12 hr later Group 3: 2.4 mg/kg IV AS, 20 mg/kg AS as rectal suppository 12 hr later	Group 1: 682† ^a Group 2 & 3: 881† ^a	Group 1: 1.7 ^a Tlag: 0.63 ^a Group 2 & 3: 1.8 ^a Tlag: 0.37 ^a	Group 1: 2.6 Group 2 & 3: 3.9	Group 1: 4.4 ^a Group 2 & 3: 5.9 ^a	Group 1: 0.79 ^a Group 2 & 3: 0.85 ^a	Group 1: 2787 † ^a Group 2 & 3: 3753† ^a
(51)	12 healthy Sudanese adults 200 mg AS as rectal suppository	219.1†	1.95			1.21	1185.17
(72)	16 pediatric patients with uncomplicated <i>falciparum</i> malaria 10 mg/kg (n=7) or 20 mg/kg (n=9) AS as rectal suppositories	898; 1535† ^a	1.5; 2.0 ^a			1.3; 1.8 ^a	2403; 5633† ^a

†Units converted to uniform scale a. Median

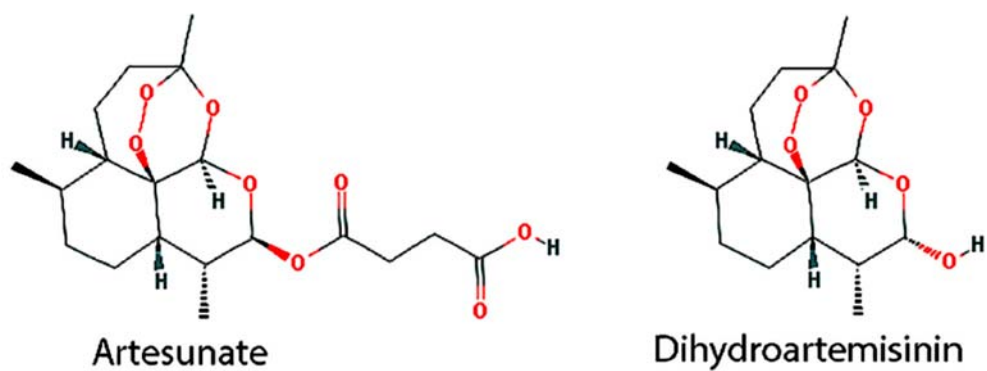


Figure 1.1 Structures of artesunate and dihydroartemisinin.

Source: Pubchem.

Artesunate structure:

(<http://pubchem.ncbi.nlm.nih.gov/summary/summary.cgi?cid=6917864>, accessed July 17, 2014);

Dihydroartemisinin structure:

(<http://pubchem.ncbi.nlm.nih.gov/summary/summary.cgi?cid=456410>, accessed July 17, 2014).

CHAPTER 2

EFFECT OF BODY SIZE AND GENDER ON ARTESUNATE PHARMACOKINETICS IN PEDIATRIC PATIENTS

Introduction

Given the therapeutic prominence of the artemisinin derivatives, and the particular vulnerability of the pediatric population to malaria-related mortality, any differences between children and adults in the disposition of artemisinins should be thoroughly characterized. However, as noted in two recent reviews, numerous gaps exist in our understanding of artemisinin derivative pharmacokinetics among pediatric patients (78, 79). A rather limited number of models are presently available in the literature which describe the population pharmacokinetics of artesunate and DHA following artesunate administration to pediatric patients. At the present time, one such model has been described for oral administration of artesunate, one for IM administration, and two for rectal administration.

The published model based on data from oral administration in pediatric patients was constructed by Stepniewska et al. (71), who performed a population pharmacokinetic analysis using sample concentrations from children 6 months to 5 years of age with uncomplicated *falciparum* malaria. All the children were administered oral artesunate in conjunction with the partner drug amodiaquine. Insufficient artesunate data were available to allow for utilization of artesunate concentrations in the modeling. However, DHA data were successfully fit using a one compartment model with first-order input. The authors identified age as a significant covariate on DHA apparent volume of distribution, although they noted that either weight or age, which were substantially

correlated in this population, could explain a substantial portion of the variability in DHA apparent volume of distribution. Additionally, an additive increase in DHA apparent clearance was modeled as occurring between the first and third days of treatment; the authors speculated that this apparent increase in clearance may reflect pharmacokinetic changes associated with the resolution of acute illness.

Hendriksen et al. (38) constructed a pediatric population pharmacokinetic model for IM administration of artesunate. Specifically, these investigators performed a population pharmacokinetic analysis of sample concentrations obtained following IM administration of artesunate to African children, ages 0.6 to 11 years, with severe malaria. Artesunate and DHA data were modeled using a fixed absorption rate for artesunate, a one compartment model for artesunate, and a one compartment model for DHA. Body weight was incorporated using standard allometric scaling (exponents of 0.75 for weight terms on clearances and 1 for weight terms on volumes). Covariate analysis revealed a significant relationship between hemoglobin levels and DHA apparent clearance, with a unit (g/dL) decrease in hemoglobin being associated with a 10.2% increase in DHA apparent clearance. Given that marked anemia and substantial hemolysis is common in young children with severe malaria, the authors posited that the release of heme associated with hemolysis could well result in iron-mediated degradation of the DHA endoperoxide bridge, thereby decreasing DHA concentrations. Although this represents an important finding with regard to artemisinin pharmacokinetics in severe malaria, the applicability of this hemoglobin/DHA apparent clearance relationship in patients with less severe illness is less clear.

Finally, the two population pharmacokinetic models built from concentrations obtained following rectal administration of artesunate were constructed by Simpson et al. (74) and Karunajeewa et al. (75). Simpson et al. modeled data from a mixed population of children and adults with moderately severe malaria. Although both artesunate and DHA concentrations were obtained, the artesunate concentrations failed to display a clear pharmacokinetic profile, and ultimately were not utilized in modeling. DHA data were modeled with a one compartment model with first-order appearance and elimination; DHA appearance rate and lag time for appearance were fixed. Allometric scaling with standard exponents, as described for the Hendriksen et al. model above, was applied to DHA apparent clearance and volume of distribution parameters in the model. DHA apparent volume of distribution was determined to increase, on a L/kg basis, with increasing patient weight. Additionally, gender was determined to be a significant covariate on DHA apparent clearance, with male gender being associated with a 1.14 L/hr/kg increase in DHA apparent clearance.

Karunajeewa et al. (75) modeled artesunate and DHA concentrations obtained following rectal artesunate administration to children with uncomplicated *falciparum* or *vivax* malaria in Papua New Guinea. The children received two doses, 12 hours apart. The authors utilized a one compartment model for artesunate, a one compartment model for DHA, and first-order artesunate absorption. Artesunate and DHA volumes of distribution were set equal to account for identifiability issues. The investigators determined that patient weight was an influential covariate on this volume term. Additionally, the authors incorporated a bioavailability term for the second dose relative to the first dose; the final model estimates indicated 28% lower bioavailability of the second as compared to the first dose. The authors speculated that the higher body temperatures of the patients when the initial dose was administered may have been associated with enhanced rectal blood flow, which in turn yielded increased bioavailability.

As is apparent from the limited number of population pharmacokinetic analyses performed using data obtained from pediatric patients administered artesunate, further work in this area is well warranted. The analysis that follows represents a description of the population pharmacokinetics of the artemisinin derivative artesunate, and its active metabolite DHA, in *falciparum* and *vivax* malaria patients participating in Phase II and III trials for the novel artemisinin-based combination therapy (ACT) pyronaridine tetraphosphate/artesunate (PA). The primary focus of this analysis was the description of artesunate and DHA pharmacokinetics in pediatric patients. As body size exerts a substantial influence on pediatric pharmacokinetics, and as the previously described population pharmacokinetic models in pediatric patients do identify varied, but substantial, effects of weight on DHA pharmacokinetics, a particular emphasis of this analysis was the evaluation of methods for describing the relationship between body size descriptors and clearance and volume parameters. The methods investigated included use of linear, estimated exponent, and allometric scaling models for body weight, as well as linear and estimated exponent models for body surface area (BSA) and lean body mass. A further purpose of this analysis was to estimate the magnitude of covariate effects of potential clinical interest using a full covariate model approach. The final aim was to assess the sensitivity of the estimated parameter-body size relationships and covariate-parameter relationships to inclusion or exclusion of adult data from the modeling dataset. It should be noted that much of content in the text, tables, and figures of this chapter has been previously published in *Antimicrobial Agents and Chemotherapy* in 2014 (80).

Methods

Data

Two datasets were utilized for modeling. The first, termed the full dataset, included data from both pediatric and adult participants in the five PA trials, which

included one Phase II and four Phase III studies. The second dataset, termed the pediatric dataset, was a subset of the full dataset. It contained data only from patients less than 12 years of age, the ICH age category cutoff between children and adolescents (81).

A summary of patient demographics for included clinical trials is given in Table 2.1. In all five trials, patients were administered PA once daily for three days without regard to food intake. In the Phase II study (Study 1), plasma samples were collected prior to the first dose of PA, and at 0.25, 0.5, 1, 1.5, 2.5, 4, 8, and 12 hours following that dose. In this study, patients were administered 2, 3, or 4 mg/kg/day artesunate (49). In the Phase III studies, two samples were drawn. The first sample was drawn during a 0.25 to 12 hour window following either the first or second PA dose, with a second sample being drawn during that same window following the third dose. During Phase III studies, patients received artesunate doses ranging from 2.3 to 4.6 mg/kg/day. A granule formulation of PA was administered to approximately one-fourth of the patients in the Phase II study and all of the patients in one of the Phase III studies (82). The same granule formulation was used throughout the Phase II and Phase III clinical trials from which artesunate and DHA concentration data were derived from this dataset. Similarly, the tablet formulation throughout Phase II and III clinical trials was held constant. All other patients were administered a tablet formulation. Written informed consent, in accordance with local practice, was obtained from participants in the studies, and approval for each study was granted by local Ethics Committees. With pediatric patients, written informed consent was provided by a parent or guardian, with patient assent sought where possible. Table 2.1 provides details regarding the number of subjects from each of the clinical trials in which artesunate and DHA pharmacokinetic data were

derived for use in the present analysis, as well as patient age, weight, gender, parasite count, infection type, and artesunate dose data for these patients.

Sample handling and analysis

Collected samples were processed as follows: blood was collected in tubes containing potassium oxalate/sodium fluoride for the separation of plasma drawn at times specified. The samples were centrifuged within 15 minutes of collection. Plasma was removed from cells and transferred into two approximately equal volume aliquots in screw cap cryovials immediately after the centrifugation. The plasma samples were immediately frozen at or below -80°C in a laboratory freezer. They were later shipped via air express on dry ice to the Clinical Pharmacokinetics Laboratory at the College of Pharmacy, the University of Iowa. All samples were stored at -80°C until drug analysis was performed.

Plasma concentrations of artesunate and DHA were quantified using the method described by Naik et al. (83). Briefly, plasma concentrations of artesunate and DHA were quantified by LC-MS. Chromatographic analysis was carried out on a Shimadzu Model 2010 liquid chromatograph and mass spectrometer (Shimadzu, Columbia, MD, USA) using a LC-10AD Solvent Delivery system. The injection was made with a Shimadzu SIL-10AD automatic injector. The analysis was carried out using Synergi Max-RP 80A HPLC column, $75\text{ mm} \times 4.6\text{ mm}$, $4\ \mu$ (Phenomenex, Torrance, CA, USA) using a guard column (Phenomenex) with C-12 max-RP cartridges. The lower limit of quantification was 1 ng/mL for both artesunate and DHA. The coefficients of variation for intra-day precision and inter-day precision were less than 15% for both analytes.

Base model

Prior to model building, artesunate and DHA data were converted from ng/mL to nmol/L values using the compounds' respective molecular weights. A visual exploratory data analysis was undertaken to examine the basic structure of the concentration-time data and to identify outliers. Due to the predominance of sparse sampling data, the more extensive full dataset was primarily used for base model development. However, all models which successfully converged with the full dataset were then implemented with the pediatric dataset to assess for reasonably similar model fit. Population pharmacokinetic modeling was performed using NONMEM 7.2 (84) implemented on a Windows XP operating system with a G95 Fortran compiler. Model development and evaluation was facilitated through use of Perl speaks NONMEM 3.5.3 (PsN) (85) and Pirana 2.6.0 (86).

For the models assessed in this analysis, inter-individual variability (IIV) was modeled as following a log-normal distribution for all parameters:

$$P_i = P_{\text{pop}} \cdot \exp(\eta_i)$$

where P_i is the estimated parameter value for individual i , P_{pop} represents the typical population estimate for the parameter, and η_i is the deviation of P_i from P_{pop} . The term η is assumed to be normally distributed with a mean of zero and a variance of ω^2 . For all models considered during base model development, both full and diagonal IIV variance-covariance matrices were evaluated. Models with some, but not all, covariance terms fixed to zero were assessed as deemed appropriate based on estimates from full matrix results.

Data were first modeled using a simultaneously implemented parent-metabolite model with first-order artesunate absorption, a one compartment model for artesunate, and a one-compartment model for DHA; complete conversion of artesunate to DHA was assumed. The concentration data were natural log transformed and an additive model for log-transformed data was applied:

$$\ln C_{ij} = \ln C_{\text{pred},ij} + \varepsilon_{ij}$$

where C_{ij} and $C_{\text{pred},ij}$ represent the j^{th} observed and model predicted analyte concentrations, respectively, for individual i . The term ε_{ij} denotes the residual random error for individual i and observation j , with ε assumed to be normally distributed with a mean of zero and a variance of σ^2 in the population. Models with single and distinct ε distributions for the two analytes were assessed during early model building; for distinct distributions, the covariance term was either estimated or fixed to zero. However, models with a single ε distribution for both analytes destabilized the model. That is, the parameter estimates obtained from converged model runs varied substantially in response to different sets of initial parameter estimates being specified. As such high responsiveness to initial parameter estimates casts substantial doubt on the accuracy of final model results, use of a single ε distribution model was rejected. Similar stability problems were encountered when a covariance term was estimated for residual variability of the two analytes; additionally, the estimated magnitude of the covariance term was near zero and was associated with very poor estimate precision (%relative standard error > 70%). Given the problems associated with modeling under the assumption of a single ε distribution or correlated ε values for the two analytes, for all but the earliest model

building, residual variability was modeled through estimation of distinct σ^2 values for the analytes with residual variability covariance for the analytes fixed to zero.

Estimation methods utilized during initial base model development included first-order conditional estimation (FOCE), importance sampling expectation maximization, and Laplacian estimation. Attempts were made to account for concentrations below the lower limit of quantification of the assay through implementation of the M2 and the M3 methods as described by Beal (87).

Alternative models were tested to improve upon the initial base model including the addition of a second DHA compartment, as well as evaluation of multiple alternative absorption models including zero-order absorption, transit compartment absorption, mixed zero-order/first-order absorption, and parallel first-order absorption. Mixed zero-order/first-order absorption and parallel first-order absorption models were of particular interest. Specifically, the reasonably high concentrations of artesunate commonly observed by 15 minutes post-dose suggest that a non-negligible degree of artesunate absorption from the stomach almost certainly occurs, with the remainder of absorption occurring following transit to the small intestine. Given the pH and surface area differences between the stomach and small intestine, potentially dissimilar patterns and/or rates of absorption at these two sites would not be unexpected. Therefore, models allowing for estimation of two distinct patterns and/or rates of absorption, such as the mixed zero-order/first-order and parallel first-order absorption, could presumably, given sufficient early post-dose data, offer a better fit for artesunate, and consequently possibly DHA data, than first-order absorption.

Additional base model variations assessed included a model with η on artesunate

bioavailability, with a diagonal ω matrix and population bioavailability (F1) set to 1. Bioavailability differences among patients presumably often account for a fair portion of the covariance observed between apparent clearance and volume parameters for an orally administered agent such as artesunate. Therefore, use of a diagonal ω matrix avoids modeling difficulties associated with essentially attempting to estimate F1 variability both directly as a distinct η distribution and indirectly in the apparent clearance and volume covariance terms of a full variance-covariance matrix. When implementing this model with a diagonal ω matrix and an η on F1, the typical (population average) value of F1 is still assumed to be 1, which aids interpretation of model-derived typical estimates for other pharmacokinetic parameters.

Finally, based on research suggesting differences in artemisinin derivative pharmacokinetics between the most acute phase of infection and the convalescence phase (29), a model with F1 fixed to 1 for the first day of treatment, and estimated for days 2 and 3, was also evaluated. In this model, F1 was not allowed to vary from patient to patient, but rather typical F1 estimates for bioavailability on the later days of treatment relative to the first day of treatment were obtained.

Model selection

Model selection was guided by the following factors: plausibility and precision of parameter estimates, goodness-of-fit plots, magnitude of residual variability, sensitivity of the model to initial estimates, minimum objective function value (MOFV), equal to minus twice the log likelihood function, and Akaike Information Criterion (AIC), equal to MOFV plus two times the number of parameters. Goodness-of-fit plots were stratified by age (<5 years, 5 through 11 years, 12 through 18 years, older than 18 years) to identify if

a given base model was associated with unique goodness-of-fit features in a particular age group. Additionally, given that DHA is considered principally responsible for antimalarial activity following oral artesunate administration, concerns regarding appropriate fit of DHA data took precedence over analogous concerns regarding artesunate data.

Regarding these model selection criteria, plausibility of parameter estimates was judged based principally on published non-compartmental and compartmental findings for artesunate and DHA. As derived parameters such as half-life are more readily available in the literature than apparent clearance and volume estimates for these agents, half-life values were derived from model parameter estimates in order to further gauge plausibility. Specifically, artesunate half-life estimates in excess of 1.5 hours and DHA half-life estimates in excess of 3 hours were deemed potentially problematic.

Goodness-of-fit plots included plots of conditional weighted residuals (CWRES) vs time after dose and CWRES vs. population predicted concentrations; these plots allow for identification of overestimation or underestimation by the model at particular time points or concentration ranges. Other plots include observed concentrations vs. population predicted concentrations and observed concentrations vs. individual predicted concentrations; these plots allow for assessment of how closely the model predictions are matching the observed data.

Regarding MOFV and AIC, consideration of MOFV values for models provides a simple and direct evaluation of how well the model predicts the observed data. However, giving undue weight to reductions, in particular small reductions, in MOFV values can enhance the risk of overfitting. For example, addition of a second artesunate

compartment could well result in a modest reduction in MOFV when modeling a given dataset; however, that closer fit of sample data may translate into poorer predictions for the population of interest. That is, inclusion of the peripheral artesunate compartment in the example could be improving fit for the sample data only by accounting for idiosyncrasies or noise in that specific dataset. Use of AIC helps mitigate these risk by including a penalty for increased model complexity. The penalty is sufficiently small to not lead to rejection of truly useful additions to model complexity, but does ward against acceptance of models where increased complexity yields minimal improvements in fit.

Covariate modeling: Body size descriptor

Following selection of the base model per the criteria describe above, relationships between various body size descriptors and the clearance and volume parameters of artesunate and DHA were modeled. These descriptors included total body weight (WT), body surface area (BSA), and two estimators of lean body mass (LBM1 and LBM2). The formulas for these descriptors are given in Table 2.2. The Haycock formula was selected in part because it was validated using a study sample with patients ranging in age from infancy to adulthood (88). However, multiple alternative formulas, as summarized Bonate (2011) (89), were also computed and compared to BSA estimates from the Haycock formula for all patients in the pediatric dataset. Overall, these alternative formulas provided reasonably similar estimates when compared to estimates generated from the Haycock formula. For both the Gehan and George (90) and the Mosteller (91) formulas, differences from the Haycock formula did not exceed a magnitude of more than 5% for any patient in the pediatric dataset. For the Dubois and Dubois (92) formula, the differences was less than 5% for 94% of the patients, with a

difference of less than 10% for all patients. Finally, for the Livingston and Lee formula (93), the magnitude of the difference was less than 5% in 79% of patients, less than 10% in 98% of patients, and less than 15% in all but one patient in the dataset.

Obtaining estimates of lean body mass was complicated by the lack of LBM formulas applicable across the entire age range in this dataset. Therefore, formulas were applied in a piecewise fashion according to age. To compute LBM1, formulas by Janmahasatian et al. (94), developed with adult subjects, were applied to patients at least 18 years of age, whereas formulas by Foster et al. (95), developed with children and adolescents, were applied to patients older than five but younger than eighteen years of age. This formula requires that each child's body mass index (BMI) z-score for age and gender be obtained. For purposes of this analysis, BMI z-scores corresponding to the CDC growth charts were computed using a SAS macro available from the CDC (<http://www.cdc.gov/nccdphp/dnpao/growthcharts/resources/sas.htm>; accessed July 15, 2014). As the Foster et al. formula was not developed with very young children, patients five years of age and younger had LBM1 set equal to total body weight.

The second lean body mass estimation approach followed the method proposed by Peters et al. (96). This method is based on the underlying assumption that the relationship between extracellular fluid volume (ECV) and lean body mass is similar between adults and children. Peters et al. apply a proportionality constant linking ECV and lean body mass in adults to a pediatric ECV estimation formula described by Bird et al. (97). This yields a lean body mass formula applied in the present analysis to patients less than 50 kg, a cutoff identified by Peters et al. For patients weighing 50 kg or more, a lean body mass formula derived by Boer (98), and utilized in the Peters et al. analysis,

was applied.

Artesunate and DHA clearance and volume parameters were modeled with the various body size parameters utilizing the following relationship (89):

$$P = \theta_1 \times \left(\frac{SIZE}{SIZE_{median}} \right)^{\theta_2}$$

where P is the typical value of a clearance or volume parameter, SIZE is the value of a given body size descriptor for an individual, $SIZE_{median}$ is the median value of the descriptor in the full dataset, and θ_1 is the typical value of that parameter for a person with SIZE equal to $SIZE_{median}$. The value of θ_2 was estimated as a free parameter or fixed to a set value. For all body size descriptors, θ_2 was estimated on all clearance and volume parameters for one model and set to a value of 1 for an alternative, linear model. For weight, an additional allometric scaling model was tested with the exponent on body size set to 0.75 for clearance terms and 1.0 for volume terms (89). For purposes of model harmony, a single type of body size descriptor was used on all clearance and volume parameters in any given model. All models were evaluated using both the full and pediatric datasets.

The models incorporating body size descriptors as described above were evaluated per multiple criteria in order to identify a model to be carried forward for subsequent analyses. These criteria included the following: developmental and physiologic plausibility of the estimated parameter/body size descriptor relationships, overall model goodness-of-fit and estimate precision, goodness-of-fit equivalency across age strata, model complexity, and sensitivity of parameter estimates to inclusion of adolescent and adult data.

The final criterion, namely sensitivity of parameter estimates to inclusion of data from patients 12 years of age and older, requires a brief explanation. Inclusion of this consideration was not intended as a claim that a body size model which does not display this characteristic is intrinsically flawed. Indeed, were one of the body size models to be associated with markedly superior goodness-of-fit for model results from implementation with the pediatric dataset, but displayed markedly different estimates when implemented with the full dataset, that model could, on balance, still be the most justifiable selection for the body size model to carry forward. However, under such circumstances, were the full dataset to be utilized in further analyses, the effect of age on body size-parameter relationships would need to be defined. This would necessitate estimation of additional parameters, which could destabilize the model or reduce estimate precision. Thus, giving a measure of preference to body size models yielding similar predictions for the two datasets essentially represented a means of avoiding unnecessary complications in modeling and potentially increasing the likelihood of developing a more parsimonious model.

Covariate modeling: Full covariate model

Once a model incorporating a body size descriptor was selected, additional covariate relationships of potential clinical interest were investigated in accordance with a full covariate model approach (99). These relationships included the effects of formulation on the absorption rate constant (K_a) and the effect of gender, after accounting for body size, on all artesunate and DHA clearance and volume parameters. The effects of the granule formulation on K_a were modeled as follows:

$$PopKa = \theta_1 \times \theta_2^{FORM}$$

where $\text{Pop}K_a$ is the typical value of K_a in the population, FORM is an indicator variable equal to 0 if patients were administered the tablet formulation and 1 if patients were administered the granule formulation, θ_1 is the typical value of K_a for patients administered the tablet formulation, and θ_2 is the multiplicative factor describing the increase or decrease in K_a associated with administration of the granule formulation.

The effects of gender on clearance and volume parameters were similarly modeled:

$$P = \theta_1 \times \left(\frac{SIZE}{SIZE_{median}} \right)^{\theta_2} \times (\theta_3)^{SEX}$$

where SEX is an indicator variable equal to 1 for males and 0 for females and θ_3 is a multiplicative factor describing the effect of male gender on the clearance or volume parameter.

In order to obtain estimates for the magnitude of the covariate effects in the population, PsN was used to generate 500 bootstrap datasets from the full dataset, with stratification by sampling type (extensive vs. sparse) and formulation specified. The final full covariate model was fitted to these datasets. This process was then repeated using the pediatric dataset. The distributions for the covariate effect estimates were then plotted using the *metrumrg* R package (100).

Predictive checks

After the full covariate models for both the full and pediatric datasets were obtained, PsN was used to perform numerical predictive checks (NPC) and visual predictive checks (VPC) for the analytes. For both NPCs and VPCs, one thousand virtual observations at each sampling time point were simulated using the final parameter

estimates. Due to the variability in administered dose, prediction-correction was employed for VPC. NPC and VPC results were stratified per the following age categories: five years and younger, six years through eleven years, twelve years through eighteen years, and greater than eighteen years. The latter two categories were not applicable to the pediatric dataset evaluation. VPC results were visualized using Xpose 4.4.0 (101). Categorical predictive checks for both artesunate and DHA were also implemented using PsN and Xpose. With a categorical predictive check, the 95% confidence interval for the proportion of concentrations below the lower limit of quantification for a given analyte is calculated from simulations and compared to the observed proportion of concentrations below the lower limit.

Covariate modeling: Exploring trends

After development of a full covariate model, CWRES for artesunate and DHA and individual η estimates for parameters were plotted against various remaining covariates in the datasets. These included the following: age, baseline parasite count, baseline clinical laboratory findings (hemoglobin, hematocrit, red blood cell count), baseline aspartate aminotransferases (AST) greater than $1.5 \times$ upper limit of normal (ULN), and baseline alanine aminotransferases (ALT) greater than $1.5 \times$ ULN. Covariates displaying potential and plausible relationships with parameters were tested for statistical significance using forward addition ($\alpha=0.05$) followed by backward elimination ($\alpha=0.01$).

Results

Data

Data arising from 631 uncomplicated *falciparum* or *vivax* malaria patients were included in the full dataset, with the 274 patients under 12 years of age also being included in the pediatric dataset. The full dataset contains data from 8 patients younger than two years, 266 patients 2 years through 11 years, 103 patients 12 years through 18 years, and 254 patients older than 18 years. A total of 1490 observations were available for artesunate and DHA in the full dataset, with 613 artesunate (41.2%) and 54 DHA (3.6%) concentrations below the lower limit of quantification. For the pediatric dataset, 786 observations were available, with 303 artesunate (38.6%) and 26 DHA (3.3%) concentrations below the lower limit of quantification.

Base model

The structural model ultimately selected included first-order artesunate absorption, a one compartment model for artesunate, and a one compartment model for DHA. Complete conversion of artesunate to DHA was assumed (34). The absorption rate constant for artesunate (K_a), as well as the apparent clearance and volume of distribution for artesunate (CL/F , $V2/F$) and DHA (CLM/F , $V3/F$), were estimated. An IIV structure with covariance terms between all clearance and volume parameters was selected. Such a structure acknowledges that non-negligible between subject differences in artesunate bioavailability likely exist within the population.

Models implemented with the first-order conditional estimation method or the Laplacian estimation method failed to successfully converge, despite numerous runs in which initial estimates, significant figure limits, and/or estimation algorithm settings were

varied. Since methods (M2, M3) (87) designed to better account for concentrations below the lower limit of quantification require Laplacian estimation, models intended to implement these methods were unsuccessful. Therefore, importance sampling expectation maximization was utilized for implementation of all models described in this chapter.

During model building, incorporation of a second DHA compartment not only introduced model convergence issues by increasing the rate of rounding errors, but even when successful convergence could be achieved by varying initial estimates, significant figure limits, and/or other estimation settings, the parameter estimates obtained yielded implausibly long estimates of DHA half-life (> 6 hours). Introduction of more complex absorption models was similarly unsuccessfully. Models including parallel first-order absorption failed to converge due to rounding errors. Although a model with a mixed zero-order, lagged first-order absorption process did converge, there was a lack of improvement in DHA goodness-of-fit when compared to a simple first-order absorption model. Therefore, the increase in model complexity was deemed to be unjustified. Models with transit compartment absorption yielded unreasonable estimates of artesunate apparent volume of distribution ($V2/F < 100$ L).

Models estimating IIV on F1 not only introduced substantial imprecision to the parameter estimates, but also markedly skewed the values of the apparent clearance, volume, and the absorption rate population averages themselves. Finally, a model constructed with F1 set to 1 for the first day of treatment and estimated for the second and third days was implemented, but imprecision in model estimates (%RSE for $CLM/F = 84\%$, $V3/F = 220\%$), precluded utilization of the model. For that model, the estimated

F1 values for days 2 and 3 were 0.711 (RSE: 48%) and 0.723 (RSE: 60%).

All of the models implemented during model building were associated with substantial residual variability. Inspection of the data suggested that patients displayed marked interoccasion variability (IOV). Specifically, hundreds of individual patient profiles were reviewed, and a pattern of seemingly random and often substantial differences (after accounting for sampling time differences) from the day 1 or 2 sample to day 3 sample were apparent. Although systematic disease effects may well be contributing to the variability, such an effect would be expected to display a directional pattern, likely producing higher concentrations on day 1 as compared to day 3. No such clear direction to the variability was apparent. Formally modeling IOV was not possible since, for all patients with samples taken on more than one occasion (Study 2 – 5), only a single sample of each analyte was available per occasion. With only a single sample per occasion, residual variability and IOV cannot be separately estimated. However, to assess the extent to which IOV was contributing to residual variability, the final base model was implemented with data from each occasion being considered as representing a distinct individual. This yielded marked declines in residual variability estimates, suggesting that IOV was a substantial contributor to the observed residual variability, albeit one that could not be characterized in the present analysis.

Covariate modeling: Body size descriptor

Since DHA is considered of greater clinical relevance than artesunate, the impact of incorporating various body size descriptors on DHA goodness-of-fit and DHA parameter estimates represented the principal focus of the body size descriptor modeling. Tables 2.3 and 2.4 contain the point estimates and NONMEM-derived relative standard

errors (%RSE) for CLM/F and V3/F related parameters, respectively. These point estimates were utilized to estimate the population predicted CLM/F and V3/F values for each individual in the dataset. As artemisinin derivative doses are typically expressed on a mg/kg basis, the population predicted apparent clearance and volume of distribution values were converted to L/hr/kg and L/kg units, respectively. Plots of weight-adjusted DHA CLM/F and V3/F population predicted values are given in Figure 2.1 and 2.2, respectively, for models including weight or BSA.

Goodness-of-fit plots did not suggest superiority of any particular body size model, regardless of whether or not stratification by age was applied; therefore, this criterion did not inform model selection. Examination of the results from the models with estimated exponents revealed that the predicted CLM/F vs. age and V3/F vs. age curves for the pediatric dataset models tended to differ, in some instances substantially, from their counterparts estimated with the full dataset. Any interpretation of these observed differences is complicated by the imprecision associated with the estimates for the parameters in the pediatric dataset-derived versions of these models. That is, due to the uncertainty in the parameter estimates, drawing conclusions based on the distinctions between the curves for the full and pediatric datasets would be inadvisable. Given this challenge, and the necessity of estimating four additional parameters, no models with estimated exponents were carried forward for use in further analyses.

The linear weight model was estimated with fairly good precision. However, the pediatric and full datasets yielded fairly different estimated parameter values across age. The linear LBM1 model displayed dramatic fluctuations across age, presumably due to the piecewise application of formulas used in LBM1 calculation. From a developmental

plausibility perspective, such abrupt fluctuations are clearly undesirable. In contrast, the linear LBM2 model did not display such fluctuations. Unfortunately, the parameter estimates for the full dataset version of this linear LBM2 model displayed extremely poor precision, which supported rejection of this model.

The allometric scaling model and the linear BSA model were both estimated with adequate precision and displayed a relative insensitivity to inclusion or exclusion of adolescent and adult data. In actuality, the predicted CLM/F values, as shown in Figure 2.1, were extremely similar between the two models, regardless of the dataset employed. Ultimately, the allometric scaling and linear BSA models were deemed to be the best body size descriptor models, as judged per the pre-specified criteria, from among the various models assessed. Given the similarities between the two models in the evaluation criteria, the most justifiable choice was to carry forward both models into further stages of modeling.

Full covariate model

The full covariate model included gender on all clearance and volume parameters and formulation on K_a . However, only unrealistically high estimates for the increase in K_a (> 30x increase) associated with the granule formulation could be obtained. Ultimately, the granule K_a was fixed to 10 h^{-1} to reflect the apparently quite rapid absorption of the formulation, with the tablet K_a left to be freely estimated.

The parameter estimates for the full covariate models with this modified K_a coding, and with the gender effects estimated on the clearance and volume parameters, are given in Table 2.5 for the pediatric dataset results for the allometric scaling and the linear BSA models, with analogous parameter estimates from the full population models

given in Table 2.6. The control streams and model output for the full covariate linear BSA and allometric scaling models are given in Appendices A - D. Covariance estimates are given in Table 2.7 for all pairs of these models and datasets. The 95% confidence intervals for the effects, determined through 500 bootstrap runs, are plotted for CLM/F and V3/F in Figures 2.3 and 2.4, respectively, with plots for the artesunate parameters provided in Figures 2.5 and 2.6. Plots of DHA CWRES vs. time after dose and population predicted DHA vs. observed DHA concentrations for the pediatric linear BSA model are given in Figure 2.7. The analogous plots for the allometric scaling model (not shown) were essentially identical. Goodness-of-fit was adequate given the inherent variability of the analyte.

To explore the issue of the apparent formulation effect, plots of observed artesunate and DHA concentrations vs. time (stratified by dose received) were examined. These plots revealed a relative lack of data describing the absorption phase for the granules due both to the sparse sampling nature of a majority of the granule data, as well as the apparent quite rapid absorption of this formulation. Once the apparent formulation effect on K_a were identified, attempts were also made to model a separate value for granule bioavailability relative to that of the tablet. Specifically, models were implemented in which a bioavailability (F1) was coded as equal to 1 for administration of the tablet formulation, with the relative bioavailability of the granule formulation being an estimated fixed effect. The NONMEM-derived 95% confidence intervals for granule F1 estimates were relatively broad. Specifically, granule F1 estimates for the linear BSA model were 1.05 (95% CI: 0.689 – 1.411) for the full data set implementation and 1.04 (95% CI: 0.820 – 1.260) for the pediatric dataset implementation. For the allometric

scaling model, estimates were 1.16 (95% CI: 0.95 – 1.37) for implementation with the full dataset, and 1.07 (95% CI: 0.856 0 1.284) for implementation with the pediatric dataset. Furthermore, the apparent DHA clearance from these models including F1 all varied from the models without F1 estimated by less than 4%. These granule F1 estimates are not indicative of any substantial formulation effect. Nonetheless, to further explore this concern, full covariate linear BSA and allometric scaling models were implemented using datasets from which artesunate and DHA concentrations of individuals administered granules were excluded. The apparent clearance and volume of distribution parameter estimates for artesunate and DHA obtained from these runs all fell within the corresponding bootstrap-derived 95% confidence intervals for the full covariate models. Had there been a strong formulation effect on bioavailability, the apparent clearance and volume of distribution estimates obtained when implementing the models with the tablet only dataset would diverge from those obtained with the datasets including patients administered granules. Given the apparent lack of evidence for a substantial, and thus potentially clinically relevant, formulation effect on bioavailability, the effects of the granule formulation were ultimately modeled as limited to K_a .

The full covariate models were used to conducted VPCs stratified by age. The DHA VPCs for the full population linear BSA model are given in Figure 2.8. DHA VPCs for remaining models were quite similar. The percentages of concentrations below the 5th percentile and above the 95th percentile of the simulated concentrations from the NPC are given in Table 2.8. Although these results do not indicate a clear difference in predictive ability for the two body size models, the stratification does indicate that predictive ability is superior for patients 18 years of age and younger. This is an

acceptable result given that the target population to be described by the analysis is pediatric patients.

Figures 2.9 and 2.10 display the categorical VPC results for artesunate and DHA, respectively, for the full population linear BSA model; alternative models yielded similar results. Per this evaluation, the proportion of artesunate concentrations below the lower limit of quantification is underpredicted by the model. However, for DHA, the simulated and actual proportions are well aligned, suggesting that failure to incorporate concentrations below the lower limit of quantification into the modeling did not bias predictions for DHA, the analyte of primary interest.

Covariate modeling: Exploring trends

The plots of DHA CWRES vs. age for patients 12 years of age and younger are given in Figure 2.11. There appears to be a slight trend towards underestimation of DHA concentrations for very young patients. For artesunate, this trend was also apparent (plots not shown). Plots of estimated η values vs. age indicated a trend towards negative η values for multiple parameters (CL/F, CLM/F, and V3/F) for patients four years of age and younger; that is, these plots suggested that the patients may have lower actual parameter values than predicted by the model. Given that this trend appears to be acting across multiple parameters, a likely explanation may be that the patients are displaying higher bioavailability than accounted for by the model. To investigate this possibility, F1 was set to 1 for patients older than four years, with relative bioavailability estimated for patients four years and younger. This did result in statistically significant differences ($p < 0.01$) in all models and datasets.

Major potential confounding factors related to this finding must be considered,

however. For example, among patients four years of age and younger, 77% of the patients were administered granules, as compared to 26% of patients ages 5 – 11. Considering only the pediatric dataset, for patients four years and younger, 91% of the artesunate and 86% of the DHA concentrations used in modeling were obtained on day 1, with the remainder obtained on day 3. In contrast, for patients between 5 – 11 years, 71% of the artesunate and 63 % of the DHA concentrations were obtained on day 1. Therefore, the modeled increase in bioavailability in this age group could reflect a bioavailability effect of acute illness or of the granule formulation. Unfortunately, neither of these effects was previously successfully modeled. To avoid spuriously ascribing an effect to age which in actuality likely might have stemmed from other causes, full evaluation of models including this effect was not pursued and the effect was not included in the final models

Discussion

The intent of this analysis was to describe the population pharmacokinetics of artesunate and DHA in pediatric patients utilizing data from 631 pediatric, adolescent, and adult uncomplicated malaria patients participating in Phase II and III clinical trials for the combination agent pyronaridine tetraphosphate/artesunate. To this end, a parent-metabolite base model with first-order artesunate absorption and a one-compartment model with first-order elimination for both artesunate and DHA was developed. Various methods for incorporating body size descriptors on clearance and volume parameters were assessed, and two highly similar models, a linear BSA model and an allometric scaling model, were ultimately selected as the optimal body size models. Building upon these two models, the effects of gender on the clearance and volume parameters were

evaluated using a full covariate model approach; although the covariate effect estimates were sufficiently imprecise to preclude drawing any definitive conclusions, the findings could be considered tentatively consistent with the lack of a clinically relevant effect of gender on DHA apparent clearance. Finally, in this analysis, it was found that modeling with a dataset including adolescent and adult data allowed for increased precision in estimation of parameters without introducing any meaningful bias in the point estimates for those parameters.

Physiologic basis for models

In this analysis, the clearances of artesunate and DHA were described using relationships with either weight or BSA, but not with patient age. The choice to not incorporate the covariate of age a priori with body size, as well as to not assess for an age effect in the full covariate model, essentially rested on two assumptions. The first assumption was that across the studied patient population, the hepatic clearances of artesunate and DHA would be dependent on the rate of hepatic blood flow rather than intrinsic clearance. The second assumption was that the developmental changes in hepatic blood flow could be satisfactorily accounted for using clearance-body size descriptor relationships. Additionally, it should be noted that no claim is being made that these assumptions would, or would not, be applicable to patients under two years of age. As there were only eight such patients in the dataset, all with sparse sampling data, no attempt was made in the analysis to derive and justify pharmacokinetic findings appropriate for this age group.

Evidence for the assumption that the analyte clearances will display hepatic blood flow-limited kinetics among patients as young as two years of age can be found in a study

by Nealon et al. (31). This study included assessment of artesunate and DHA pharmacokinetics following IV administration of artesunate to children with severe malaria. The two subgroups of children in the study had median ages of 36 and 21 months. Pooled pharmacokinetic findings from the two patient subgroups indicate median artesunate and DHA clearance values of 46 mL/min/kg and 25 mL/min/kg, respectively, with substantial individual variability being associated with both estimates. As a point of reference, the clearance of indocyanine green (102), a probe substrate for hepatic blood flow, had a mean clearance of 15.6 mL/kg/min (SD: 7.3 mL/kg/min) among patients younger than 10 years of age. Allowing for the observed variability in both the IV artesunate pharmacokinetic findings and hepatic blood flow estimates, it appears that artesunate and DHA clearances are not limited by intrinsic clearance even in children as young as 21 months.

Further evidence that intrinsic clearance does not limit artesunate and DHA clearances even in young children can be obtained from *in vivo* and *in vitro* findings for agents with analogous metabolic profiles. With regard to artesunate, pediatric pharmacokinetic findings for agents undergoing esterase mediated hydrolysis, such as oseltamivir and remifentanyl, are indicative of efficient esterase activity for patients at, and even prior to, one year of age (103, 104). With regard to DHA, various *in vivo* studies with morphine, a probe substrate for UGT2B7, have indicated achievement of adult UGT2B7 activity well prior to two years of age (105). Similar conclusions were reached following an *in vitro* investigation of epirubicin glucuronidation by UGT2B7 in pediatric and adult liver microsomes (106).

The pediatric IV artesunate results, coupled with the findings related to the ontogeny of the individual metabolizing enzymes, provide support for the assumption that artesunate and DHA hepatic clearance will be limited by hepatic blood flow among patients at least two years of age. Granting this assumption, then clearly a body size descriptor-clearance relationship appropriately modeling changes in hepatic blood flow would account for the developmental pattern of artesunate and DHA clearances. Hepatic blood flow is proportional to liver volume; liver volume, expressed per kg of total body weight, is higher in younger children than older children (107). Therefore, for agents with clearance dependent on hepatic blood flow, pediatric clearance values, expressed per kg of total body weight, decline as children mature. Liver volume, when normalized to BSA, but not to total body weight, is constant over the pediatric age range (107, 108). In actuality, a general nonlinear trend between age and per kg clearance in pediatric subjects is approximated by both the linear BSA model and the allometric scaling models, and both models have been extensively employed in pediatric pharmacokinetic analyses.

The potential clinical implications of this nonlinear trend in per kg clearance do merit attention. For example, with the allometric scaling model, given patients administered equivalent mg/kg doses, a typical 10 kg patient's expected DHA exposure (AUC) would be approximately one-quarter and one-third lower, respectively, than that of a 35 kg or a 60 kg patient. Put another way, given a 60 kg patient administered 3 mg/kg/day artesunate, a 10 kg patient would need to receive, on average, 4.5 mg/kg/day to attain similar exposure. Of course, such estimates of exposure differences reflect expected population values; for a given pair of individuals, exposure differences are far less predictable.

Covariate Model: Gender Effects

For the full covariate model, the effect intervals for all of the gender-parameter relationships crossed 1.0, indicating a lack of statistically significant effects. No interval, regardless of parameter, model, or dataset employed, had a bootstrap 95% confidence interval contained entirely within the 0.75 – 1.25 interval for a clinically irrelevant effect. Essentially, the results indicated that insufficient information was available to conclusively judge any effect as clinically relevant or irrelevant. It is worth noting, however, that for CLM/F, the large bulk of the effect estimate distribution for each model fell within the 0.75 – 1.25 no effect region. This would appear to offer some evidence for the lack of a clinically relevant gender effect on CLM/F. For strictly predictive purposes, more parsimonious models without the gender effects would be justifiable.

The standard interval of 0.75 – 1.25 was used to indicate a clinically irrelevant effect of a covariate on a parameter. This interval was adopted because, at the time of this analysis, a clear relationship between concentrations and clinical efficacy remains largely undefined for the artemisinin derivatives (65). However, were such a relationship to be determined, the full covariate modeling in the present analysis could be reinterpreted. For example, if a threshold DHA AUC for efficacy were known, the CLM/F gender effect results could be used to estimate the probability that being male would result in failure to meet that target. More generally, additional pharmacodynamic information could be used to adjust the 0.75 – 1.25 default limits to artesunate-specific, and more importantly DHA-specific, values.

Pharmacokinetic Comparisons

One of the studies (Study 1) included in the present analysis was previously analyzed using non-compartmental methods (49). The mean apparent DHA clearance from the non-compartmental analysis, approximated from subgroup means, was 2.4 L/hr/kg. For the average weight of 18.5 kg, the full population and pediatric allometric scaling models yield a prediction of 2.1 L/hr/kg. Given that this value reflects a population prediction for an average weight, this model predicted value is adequately similar to the non-compartmental findings.

As previously described, the population pharmacokinetics of oral artesunate in pediatric patients were examined by Stepniewska et al., who studied artesunate pharmacokinetics following oral artesunate administration to uncomplicated *falciparum* malaria patients in Burkina Faso between six months and five years of age (71). The authors estimated a DHA apparent clearance of 0.636 L/hr/kg for the first dosing period with a substantial increase of 0.760 L/hr/kg associated with the third dosing period, yielding a day 3 apparent clearance of approximately 1.4 L/hr/kg.

Considering a patient with a weight of 13 kg, an approximate average weight for patients in the Stepniewska et al. study, the population predicted CLM/F would be 2.2 L/hr/kg for a female per the allometric scaling model (pediatric or full dataset) and 2.4 L/hr/kg for a male. Clearly, the estimated apparent clearance in the Stepniewska et al. study, particularly for day 1, is substantially lower than the model estimated apparent clearance from the present analysis. The difference is unlikely to be due in any large part to the failure of the model to account for a simple effect of acute infection on day 1 pharmacokinetics. After all, as previously described, Study 1 non-compartmental results, which were derived entirely from day 1 samples, are consistent with model estimated

clearance predictions. However, a more complex disease effect, dependent on the severity of infection and the age of the patients, could perhaps be operating. The median parasite count for patients in the pediatric dataset in the present analysis was 10,341, whereas the median parasite counts for the two cohorts of the Stepniewski et al. study were 29,000 and 30,000. In a recent analysis of artesunate pharmacokinetics in pregnant women, it was observed that women who were moderately unwell displayed significantly higher combined exposure to artesunate and DHA than women who were mildly unwell (29). This dynamic could account for some of the discrepancy observed for day 1 clearance estimates. Furthermore, the median age in the two cohorts of the Stepniewski et al. study was 3.1 and 2.7 years, compared to 7 years in the pediatric dataset of the present analysis. It is not inconceivable that very young patients might experience a more dramatic physiologic response to acute illness than older patients, resulting in a more pronounced disease effect on artesunate and DHA pharmacokinetics. Further investigation would be required to characterize such a potential interaction effect between age and acute illness.

Inclusion of adult data

Throughout this analysis, models were evaluated using two datasets, one with the full age range of patients, and another including patients only younger than 12 years of age. The intention of this parallel modeling approach was to allow for utilization of additional data, which could bolster model stability and estimate precision, while simultaneously checking for possible estimate bias in covariate-parameter relationships introduced through inclusion of data from non-pediatric patients. Indeed, the full dataset models did allow for more precise estimation of gender effects, as well as multiple other

parameters, than their pediatric counterparts. However, the point estimates of the final models for essentially all of the parameters were quite similar, suggesting that bias was not introduced through inclusion of the adolescent and adult data.

A major factor to be considered, however, with regard to the insensitivity of the two final models to the presence or absence of data from older patients is the nature of the data in the pediatric and full datasets. In the present analysis, the only extensive sampling data available is from Study 1, a pediatric Phase II study. All adult data included in the full dataset were derived from Study 2, 3, and 4, in which only sparse sampling was conducted. The richer data available for pediatric patients may well have served to reinforce the apparent insensitivity of the selected body size models to the inclusion of adult data. Given this imbalance between the datasets with regard to extensive sampling data, it would be extremely inadvisable to draw any definitive conclusions regarding the sensitivity of the linear BSA and allometric scaling models to inclusion of artesunate and DHA concentrations obtained from sampling of adolescents and adults.

Conclusions

Overall, the results of the present analysis indicate that the pharmacokinetics of artesunate and DHA following oral artesunate administration can be described for pediatric patients using either an allometric scaling or linear BSA model, a finding consistent with the likely tight relationship between hepatic blood flow and artesunate/DHA clearance. Limitations of the dataset used in this analysis include the relatively mild infection experienced by a majority of the patients and the minimal number of patients below two years of age. Both the allometric scaling and linear BSA

models predict that, for the same mg/kg artesunate dose, younger children are expected to have lower DHA exposure than older children or adults. The extent to which this pattern can be extrapolated to children younger than two years of age is dependent on the relative influences of hepatic blood flow and metabolizing enzyme maturation, as well as any interaction between age and an acute disease effect. Further investigation clearly is required, and should be undertaken, to elucidate these various dynamics. Given the high risk of malaria-related morbidity mortality experienced by young children, there is clearly a significant need for such investigation.

Table 2.1 Summary of covariate data for patients in the five clinical trials from which the full and pediatric datasets were derived.

	Study 1 (Phase II)	Study 2 (Phase III)	Study 3 (Phase III)	Study 4 (Phase III)	Study 5 (Phase III)	All studies
Subjects with pharmacokinetic data	57 African children with <i>falciparum</i> malaria	268 African and Asian children and adults with <i>falciparum</i> malaria	196 African children and adults with <i>falciparum</i> malaria	23 Asian children and adults with <i>vivax</i> malaria	87 African children with <i>falciparum</i> malaria	631
Artesunate mg/kg dose	3.4 (2.8, 3.9)	3.3 (3.0, 3.6)	3.3 (2.9, 3.9)	3.4 (3.0, 3.7)	3.0 (2.6, 3.3)	3.3 (2.9, 3.6)
Age (years)	5 (4, 6)	24 (19, 35)	11 (8, 17)	19 (14, 34)	5 (3, 7)	14 (7, 25)
Weight (kg)	16 (14, 20)	50 (44, 56)	30 (25, 48)	47 (35, 53)	17 (14, 20)	38 (22, 52)
Gender (% Male)	51	77	46	61	48	61
Parasite count (per μ L)	6,304 (2,051, 14,926)	12,838 (5,843, 31,168)	12,607 (3,363, 29,408)	10,275 (3,757, 15,692)	10,074 (1,994, 44,068)	11,462 (3,569, 29,060)
Patients administered granules (N)	15	0	0	0	87	102
Patients <12 years (N)	56	23	104	4	87	274

Note: Values given as median (interquartile range) unless otherwise specified

Table 2.2 Formulas for body size descriptors used in modeling (94).

Body size descriptor	Age range	Formula
BSA: Body surface area (m ²)	All ages	$(\text{Weight}^{0.5378}) * (\text{Height}^{0.3964}) * 0.024265$
LBM1: Lean body mass method 1 (kg) ^a	Age ≤ 5	Total body weight
	5 < Age < 18	<u>Males^b</u> $\ln(\text{LBM}) = -2.8990 + 0.8064 * \ln(\text{Height}) + 0.5674 * \ln(\text{Weight}) + 0.0000185 * \text{Weight}^2 - 0.0153 * (\text{BMIz})^2 + 0.0132 * \text{Age}$ <u>Females^b</u> $\ln(\text{LBM}) = -3.8345 + 0.954 * \ln(\text{Height}) + 0.6515 * \ln(\text{Weight}) - 0.0102 * (\text{BMIz})^2$
	Age ≥ 18	<u>Males</u> $(9.27 \times 10^3 \times \text{Weight}) / (6.68 \times 10^3 + 216 * \text{BMI})$ <u>Females</u> $(9.27 \times 10^3 \times \text{Weight}) / (8.78 \times 10^3 + 244 * \text{BMI})$
LBM2: Lean body mass method 2 (kg) ^a	Weight < 50 kg	$3.8 * (0.0215 \times \text{Weight}^{0.6469} \times \text{Height}^{0.7236})$
	Weight ≥ 50 kg	<u>Male</u> $0.407 * \text{Weight} + 0.267 * \text{Height} - 19.2$ <u>Females</u> $0.252 * \text{Weight} + 0.473 * \text{Height} - 48.3$

Note: In all formulas, weight is in kg, height in cm, and age is in years.

a. LBM1 and LBM2 were constrained to not exceed total body weight.

b. BMIz represents the z-score for the subject's body mass index.

Table 2.3 NONMEM estimates and relative standard errors (%RSE) for DHA apparent clearance (CLM/F) in various body size models implemented with the full and pediatric datasets.

		Full dataset		Pediatric dataset	
	CLM/F	θ_1 (%RSE)	θ_2 (%RSE)	θ_1 (%RSE)	θ_2 (%RSE)
Linear Weight	$\theta_1 \times \left(\frac{WT}{38}\right)$	70.1 (4.0%)		79.4 (5.6%)	
Allometric Scaling	$\theta_1 \times \left(\frac{WT}{38}\right)^{0.75}$	67.0 (4.1%)		67.2 (4.4%)	
Estimated Weight	$\theta_1 \times \left(\frac{WT}{38}\right)^{\theta_2}$	67.6 (5.2%)	0.820 (9.3%)	88. (13.7%)	1.18 (15.8%)
Linear BSA	$\theta_1 \times \left(\frac{BSA}{1.23}\right)$	65.5 (8.8%)		64.1 (5.6%)	
Estimated BSA	$\theta_1 \times \left(\frac{BSA}{1.23}\right)^{\theta_2}$	67.0 (4.5%)	1.19 (9.7%)	84.8(42.9%)	1.62 (48.4%)
Linear LBM1	$\theta_1 \times \left(\frac{LBM1}{28}\right)$	64.7 (9.1%)		71.6 (9.4%)	
Estimated LBM1	$\theta_1 \times \left(\frac{LBM1}{28}\right)^{\theta_2}$	63.6 (5.6%)	0.854 (14.3%)	91.0 (18%)	1.42 (19.9%)
Linear LBM2	$\theta_1 \times \left(\frac{LBM2}{31}\right)$	67.3 (48%)		73.9 (5.9%)	
Estimated LBM2	$\theta_1 \times \left(\frac{LBM2}{31}\right)^{\theta_2}$	66.0 (12.7%)	0.883 (29.4%)	82.2 (14.8%)	1.18 (20.4%)

Table 2.4 NONMEM estimates and relative standard errors (%RSE) for DHA apparent volume of distribution (V3/F) in various body size models implemented with the full and pediatric datasets.

		Full dataset		Pediatric dataset	
	Model: V3/F	θ_3 (%RSE)	θ_4 (%RSE)	θ_3 (%RSE)	θ_4 (%RSE)
Linear Weight	$\theta_3 \times \left(\frac{WT}{38}\right)$	66.6 (8.8%)		75.5 (15.5%)	
Allometric Scaling	$\theta_3 \times \left(\frac{WT}{38}\right)$	64.2 (4.1%)		74.6 (8.8%)	
Estimated Weight	$\theta_3 \times \left(\frac{WT}{38}\right)^{\theta_4}$	64.8 (10.5%)	0.883 (19.6%)	99.3 (28%)	1.42 (33.7%)
Linear BSA	$\theta_3 \times \left(\frac{BSA}{1.23}\right)$	62.3 (5.1%)		61.0 (9.7%)	
Estimated BSA	$\theta_3 \times \left(\frac{BSA}{1.23}\right)^{\theta_4}$	64.1 (9.1%)	1.29 (11.8%)	95.7 (22.5%)	2.02 (15.7%)
Linear LBM1	$\theta_3 \times \left(\frac{LBM1}{28}\right)$	61.6 (10.7%)		67.7 (5.2%)	
Estimated LBM1	$\theta_3 \times \left(\frac{LBM1}{28}\right)^{\theta_4}$	60.7 (27.8%)	0.887 (34.2%)	106 (21.2%)	1.79 (20.6%)
Linear LBM2	$\theta_3 \times \left(\frac{LBM2}{31}\right)$	64.2 (162%)		70.7 (8.2%)	
Estimated LBM2	$\theta_3 \times \left(\frac{LBM2}{31}\right)^{\theta_4}$	63.5 (7.8%)	0.940 (48.3%)	89.7 (22.4%)	1.41 (29.6%)

Table 2.5 A summary of the results from the final allometric scaling and linear BSA models implemented using the pediatric dataset.

Parameter	Allometric Scaling		Linear BSA	
	Model estimate (Bootstrap %RSE)	Bootstrap 95% CI	Model estimate (Bootstrap %RSE)	Bootstrap 95% CI
CL/F (L/h)	923 (9.41%)	765, 1101	884 (9.40%)	732, 1052
V2/F (L)	1130 (16.6%)	794, 1538	884 (16.6%)	617, 1208
CLM/F (L/h)	65.1 (8.54%)	55.2, 77.5	62.3 (8.56%)	52.8, 74.3
V3F (L/hr)	79.1 (12.1%)	61.6, 101	63.9 (12.0%)	49.6, 80.9
K _a (hr ⁻¹)	2.46 (20.7%)	1.92, 3.92	2.27 (19.8%)	1.78, 3.54
Gender on CL/F	1.07 (12.0%)	0.826, 1.34	1.08 (11.9%)	0.829, 1.35
Gender on V2/F	1.06 (22.9%)	0.738, 1.72	1.06 (23.3%)	0.745, 1.70
Gender on CLM/F	1.05 (10.6%)	0.861, 1.29	1.05 (10.7%)	0.858, 1.30
Gender on V3/F	0.891 (17.6%)	0.600, 1.21	0.927 (17.2%)	0.612, 1.26
IIV-CL/F	0.279 (22.4%)	0.165, 0.412	0.278 (22.5%)	0.160, 0.407
IIV-V2/F	0.830 (21.1%)	0.499, 1.19	0.827 (22.6%)	0.498, 1.22
IIV - CLM/F	0.248 (25.7%)	0.147, 0.408	0.258 (25.8%)	0.154, 0.428
IIV-V3/F	0.414 (29.7%)	0.192, 0.643	0.424 (29.3%)	0.201, 0.642
IIV- K _a	0.987 (50.8%)	0.548, 2.55	0.975 (50.0%)	0.547, 2.46
Residual variability (σ^2) for AS	0.586 (29.2%)	0.510, 1.19	0.583 (29.5%)	0.509, 1.19
Residual variability (σ^2) for DHA	0.876 (15.5%)	0.575, 1.13	0.872 (15.6%)	0.574, 1.13

Note: CL/F, V2/F, and K_a are artesunate apparent clearance, apparent volume of distribution, and absorption rate constant, respectively. CLM/F and V3/F are DHA apparent clearance and apparent volume of distribution, respectively

Table 2.6 A summary of the results obtained from the allometric scaling model and linear BSA model as implemented with the full population dataset.

Parameter	Allometric Scaling		Linear BSA	
	Model estimate (Bootstrap %RSE)	Bootstrap 95% CI	Model estimate (Bootstrap %RSE)	Bootstrap 95% CI
CL/F (L/h)	900 (7.11%)	765, 1003	905 (7.71%)	762, 1030
V2/F (L)	1030 (13.1%)	797, 1314	906 (13.3%)	662, 1170
CLM/F (L/h)	63.5 (6.05%)	56.8, 71.3	62.6 (6.47%)	55.5, 71.4
V3/F (L/hr)	72.9 (10.4%)	58.3, 87.7	66.9 (9.75%)	54.3, 79.5
K _a (hr ⁻¹)	3.88 (24.1%)	2.85, 6.51	2.99 (22.0%)	2.39, 5.12
Gender on CL/F	1.09 (7.96%)	0.933, 1.29	1.09 (88.0%)	0.921, 1.29
Gender on V2/F	1.07 (13.8%)	0.808, 1.39	1.11 (15.3%)	0.85, 1.49
Gender on CLM/F	1.10 (7.43%)	0.962, 1.28	1.10 (7.66%)	0.954, 1.28
Gender on V3/F	0.828 (13.5%)	0.647, 1.08	0.925 (12.4%)	0.734, 1.18
IIV-CL/F	0.186 (23.3%)	0.120, 0.291	0.207 (21.5%)	0.135, 0.305
IIV-V2/F	0.568 (23.8%)	0.296, 0.845	0.544 (25.4%)	0.284, 0.822
IIV - CLM/F	0.255 (22.8%)	0.149, 0.382	0.277 (22.1%)	0.158, 0.398
IIV-V3/F	0.427 (26.0%)	0.217, 0.650	0.436 (24.1%)	0.227, 0.659
IIV- K _a	2.28 (40.5%)	1.07, 4.84	1.96 (43.9%)	1.03, 4.54
Sigma ² AS	0.623 (28.9%)	0.566, 1.32	0.623 (26.7%)	0.592, 1.25
Sigma ² DHA	0.967 (10.9%)	0.768, 1.19	0.943 (12.0%)	0.736, 1.18

Note: CL/F, V2/F, and K_a are artesunate apparent clearance, apparent volume of distribution, and absorption rate constant, respectively. CLM/F and V3/F are DHA apparent clearance and apparent volume of distribution, respectively. RSE is relative standard error.

Table 2.7 Covariance estimates, with bootstrap relative standard errors and confidence intervals, for the final linear BSA and allometric scaling models

	Allometric: Full Pop.	Linear BSA: Full pop.	Allometric: Ped. only	Linear BSA: Ped. only
CL, V2	0.217 (27.5%); [0.110, 0.340]	0.233 (26.5%); [0.118, 0.370]	0.348 (25.1%); [0.193, 0.545]	0.346 (26.4%); [0.184, 0.560]
CLM, CL	0.179 (23.3%); [0.108, 0.276]	0.189 (22.0%); [0.119, 0.284]	0.210 (23.2%); [0.123, 0.322]	0.214 (23.1%); [0.126, 0.325]
CLM, V2	0.315 (25.2%); [0.161, 0.471]	0.328 (25.1%); [0.165, 0.499]	0.336 (24.8%); [0.190, 0.520]	0.346 (25.2%); [0.195, 0.540]
V3, CL	0.242 (25.4%); [0.139, 0.379]	0.260 (23.0%); [0.151, 0.396]	0.259 (27.7%); [0.125, 0.397]	0.267 (27.5%); [0.126, 0.406]
V3, V2	0.229 (36.6%); [0.0855, 0.414]	0.279 (29.9%); [0.117, 0.451]	0.178 (49.6%); [0.0121, 0.367]	0.208 (44.7%); [0.0317, 0.418]
V3, CLM	0.276 (26.9%); [0.146, 0.432]	0.304 (23.9%); [0.159, 0.456]	0.250 (32.3%); [0.117, 0.435]	0.268 (31.0%); [0.126, 0.448]

Note: Presented values represent: Model estimate (Bootstrap Relative Error); [Bootstrap 95% confidence interval].

Table 2.8 Results of stratified numerical predictive checks for DHA.

	≤ 5 years	6 - 11 years	12 - 18 years	>18 years
Allometric Scaling: Full dataset	4.1%/3.8%	5.4%/1.8%	6.3%/2.6%	8.0%/1.8%
Allometric Scaling: Pediatric	3.8%/4.4%	6.1%/3.4%		
Linear BSA: Full dataset	2.4%/3.2%	5.2%/2.9%	5.3%/2.1%	7.2%/1.8%
Linear BSA: Pediatric	3.8%/4.1%	5.9%/2.9%		

Note: Cells contain percentages of observations falling below the 5th percentile/above the 95th percentile for each model and dataset.

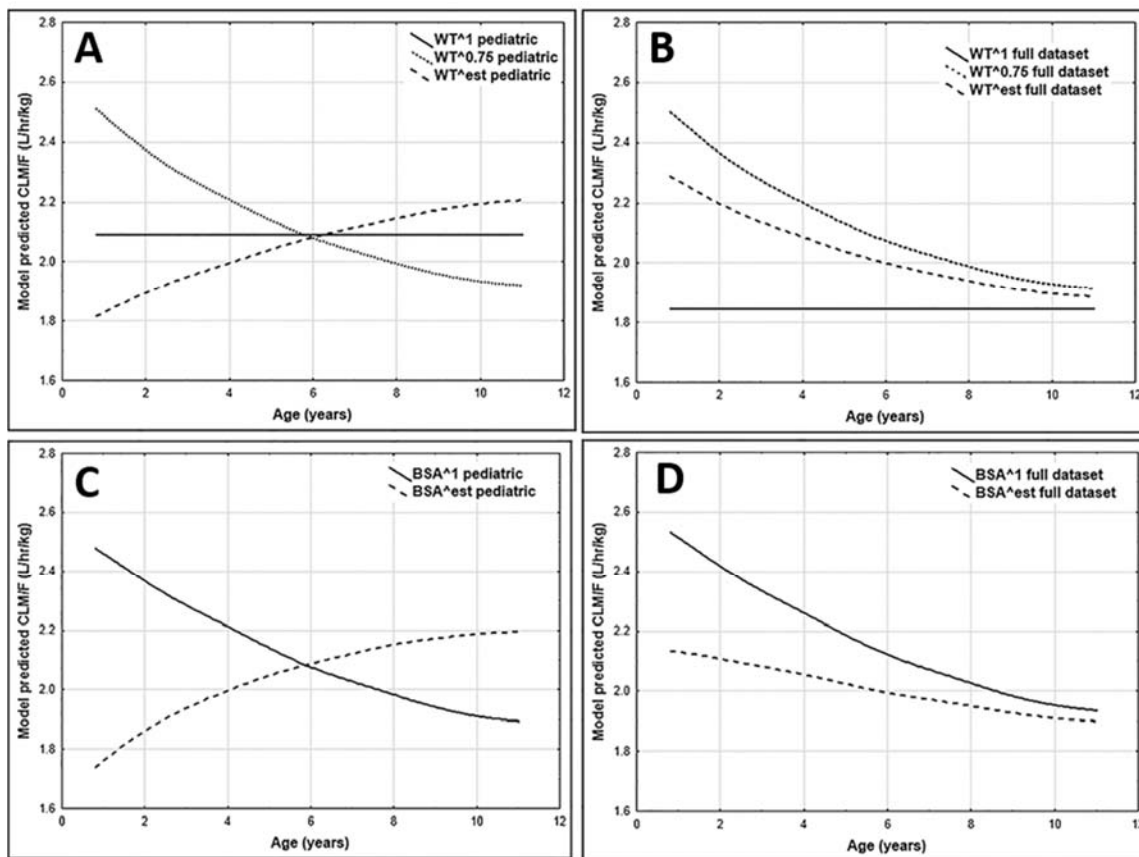


Figure 2.1 Plots of patient age vs. best-fit lines for population-predicted DHA apparent clearance (L/hr/kg) obtained from implementation of the weight and BSA body size models. Plots A and B correspond to weight-based body size models implemented with the pediatric and full datasets, respectively; Plot C and D correspond to the BSA-based body size model implemented with the pediatric and full datasets, respectively.

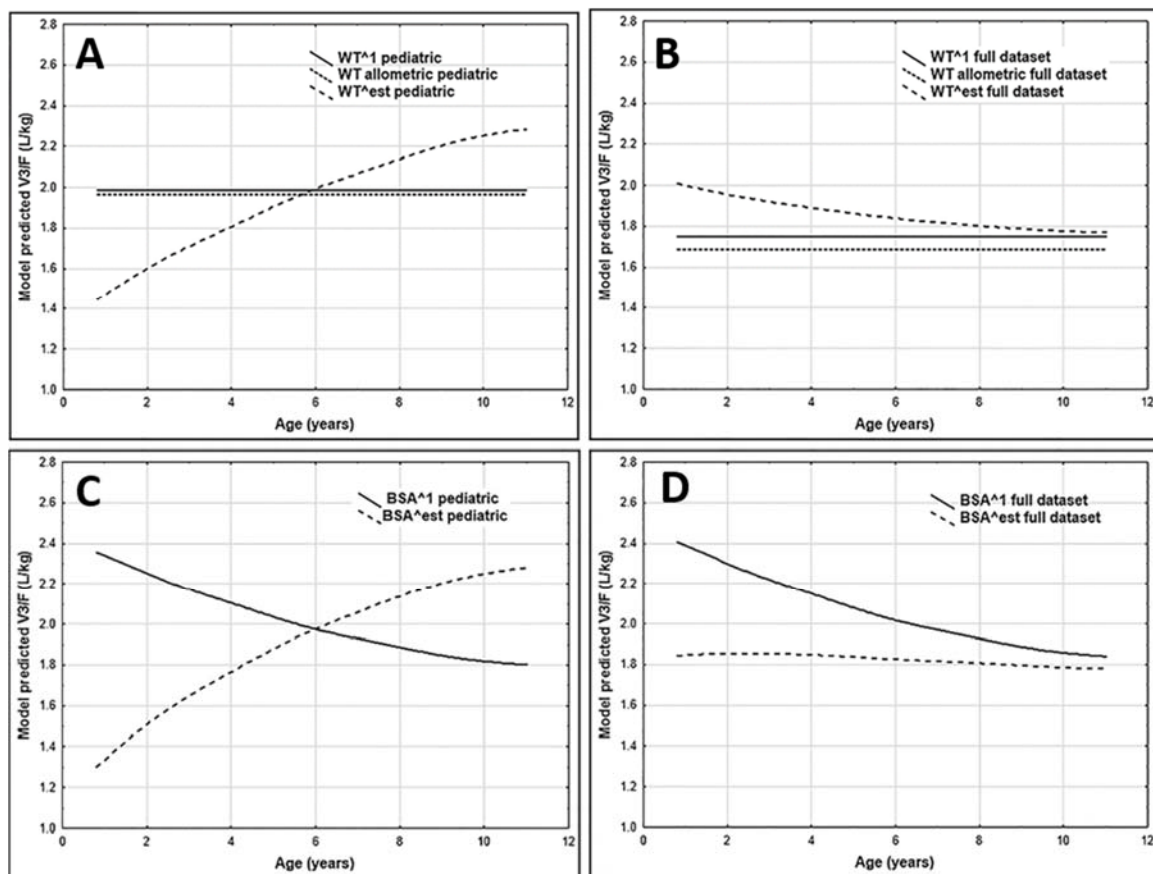


Figure 2.2 Plot of patient age vs. best-fit lines for population-predicted DHA apparent volume of distribution (L/kg) obtained from implementation of the weight and BSA body size models. Plots A and B correspond to weight-based body size models implemented with the pediatric and full datasets, respectively; Plot C and D correspond to the BSA-based body size model implemented with the pediatric and full datasets, respectively.

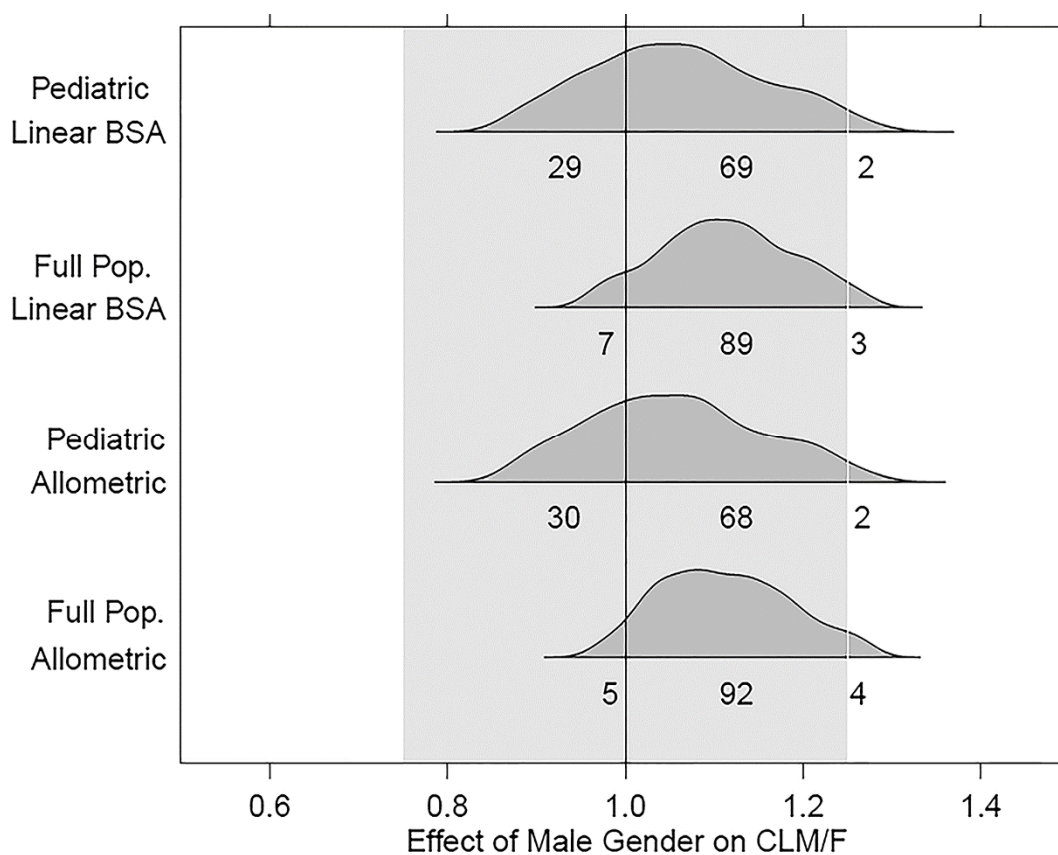


Figure 2.3 Covariate effect plots for the effect of male gender on DHA apparent clearance for the linear BSA and allometric scaling models as implemented with the pediatric or full dataset. The shaded region spanning from 0.75 to 1.25 represents the predefined no relevant clinical effect interval.

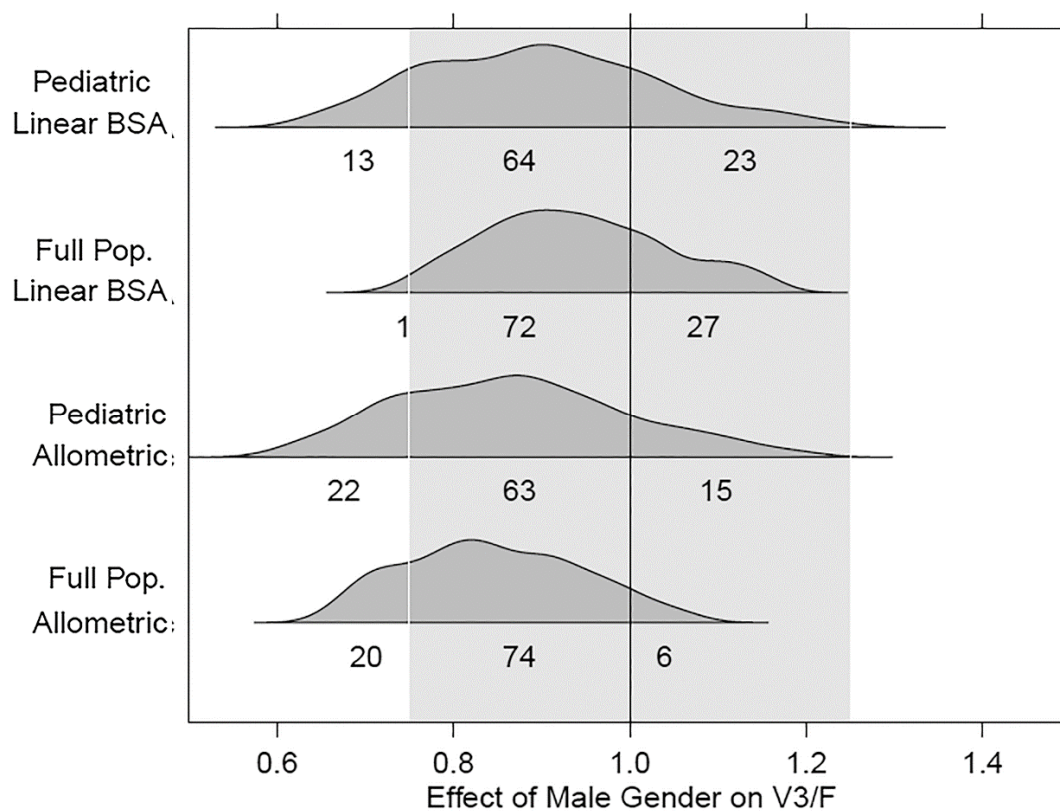


Figure 2.4 Covariate effect plots for the effect of male gender on DHA apparent volume of distribution for the linear BSA and allometric scaling models as implemented with the pediatric or full dataset. The shaded region spanning from 0.75 to 1.25 represents the predefined no relevant clinical effect interval.

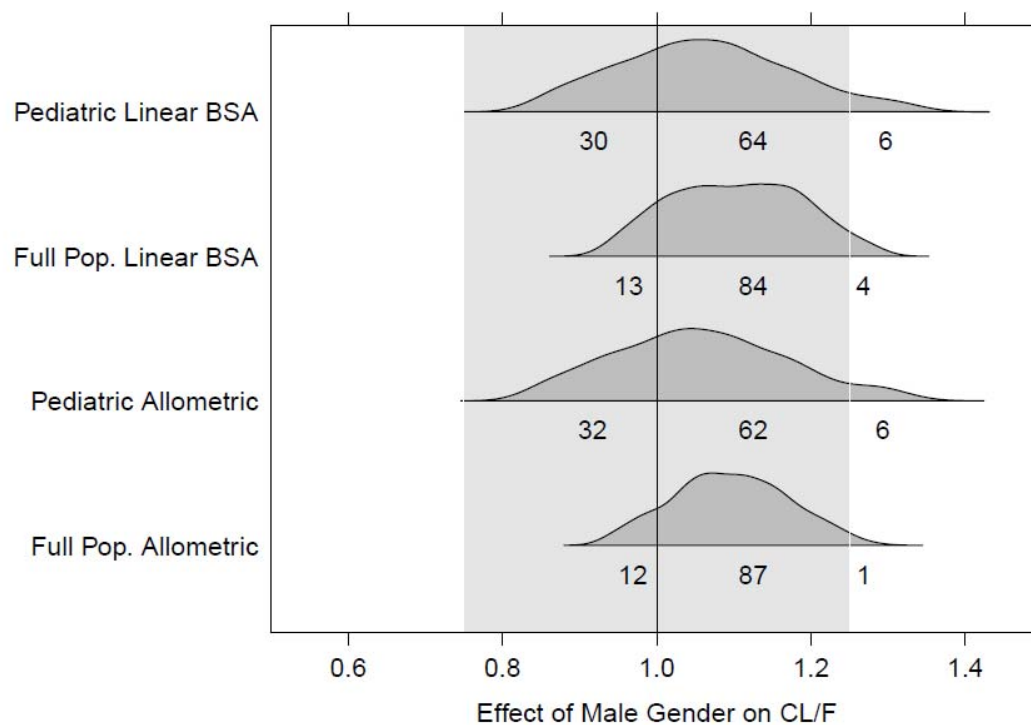


Figure 2.5 Covariate effect plots for the effect of male gender artesunate apparent clearance for the linear BSA and allometric scaling models as implemented with the pediatric or full dataset. The shaded region spanning from 0.75 to 1.25 represents the predefined no relevant clinical effect interval.

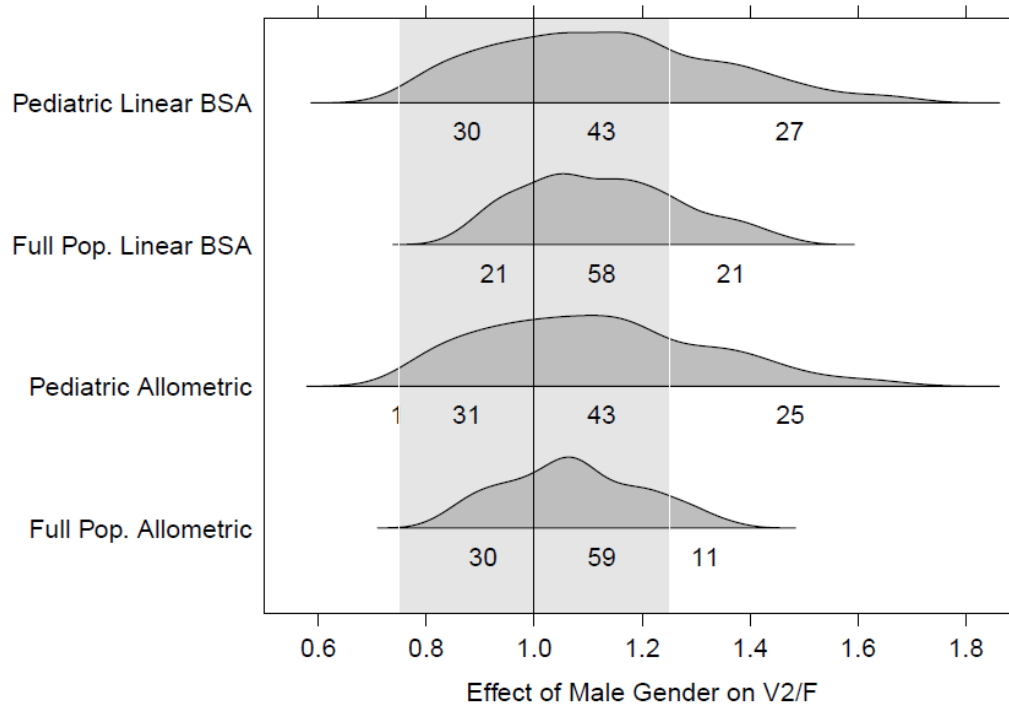


Figure 2.6 Covariate effect plots for the effect of male gender on artesunate apparent volume of distribution for the linear BSA and allometric scaling models as implemented with the pediatric or full dataset. The shaded region spanning from 0.75 to 1.25 represents the predefined no relevant clinical effect interval.

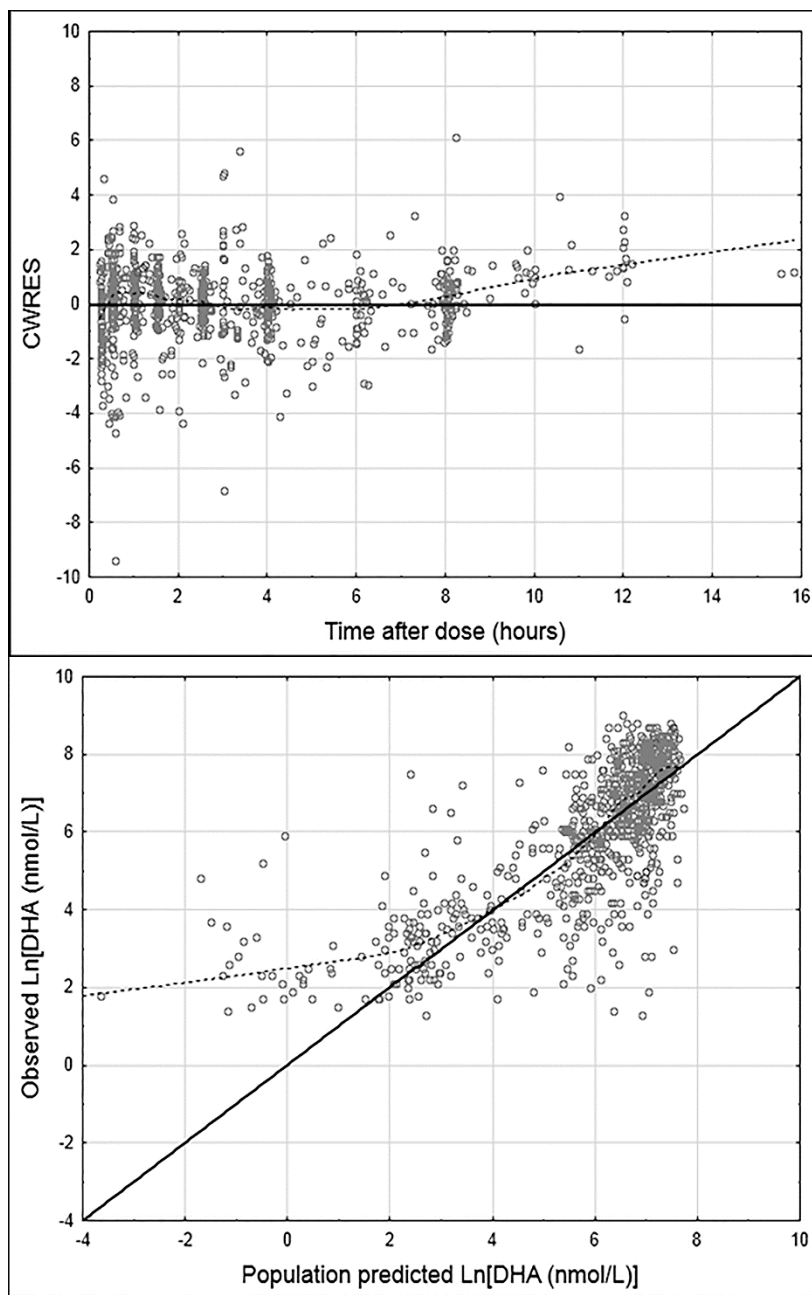


Figure 2.7 Goodness-of-fit plots for DHA for the final linear BSA model as implemented with the pediatric dataset. The solid lines are lines of identity. The broken lines are smoothing lines. The top plot displays conditional weighted residuals (CWRES) vs. time after dose in hours. The bottom plot displays observed DHA concentrations vs. population predicted DHA concentrations.

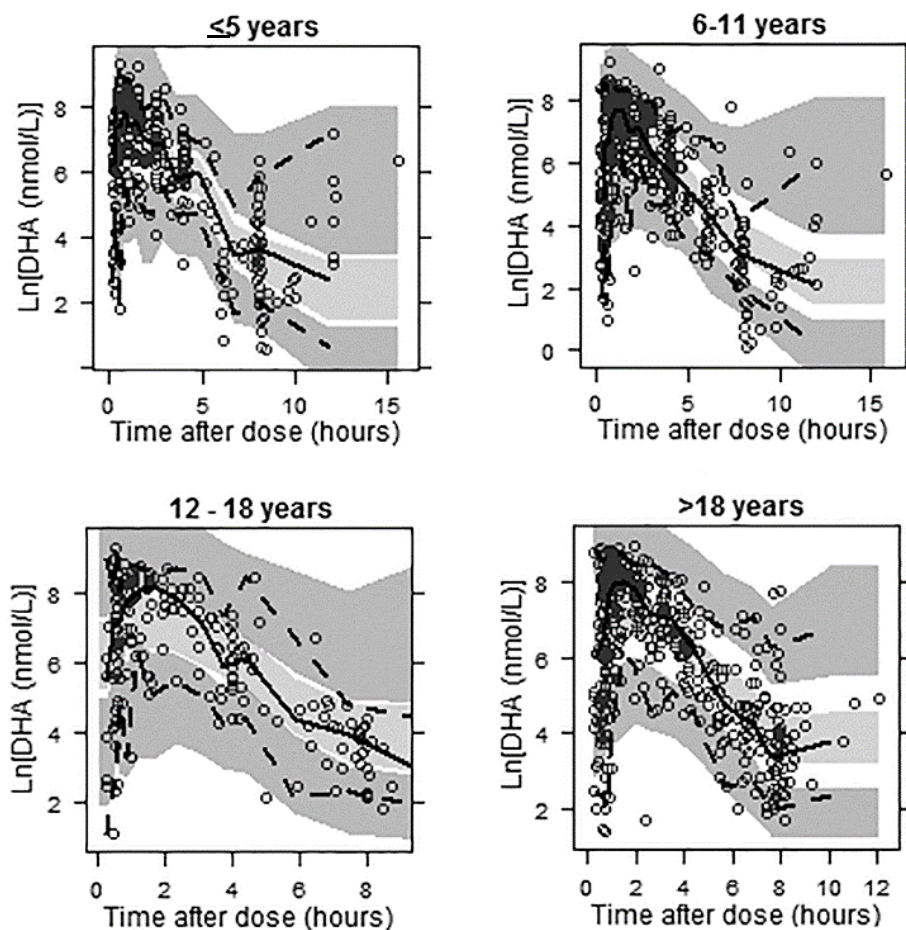


Figure 2.8 Visual predictive check plots for DHA stratified by age for the final linear BSA model implemented with the full dataset. The open circles represent the observed concentrations, the solid line represents the median of the observed data, the dashed lines represent the 5th and 95th percentiles for the observed data, and the shaded areas represent the 95% confidence intervals surrounding the prediction intervals (5th, 50th, and 95th percentiles) obtained from the simulations.

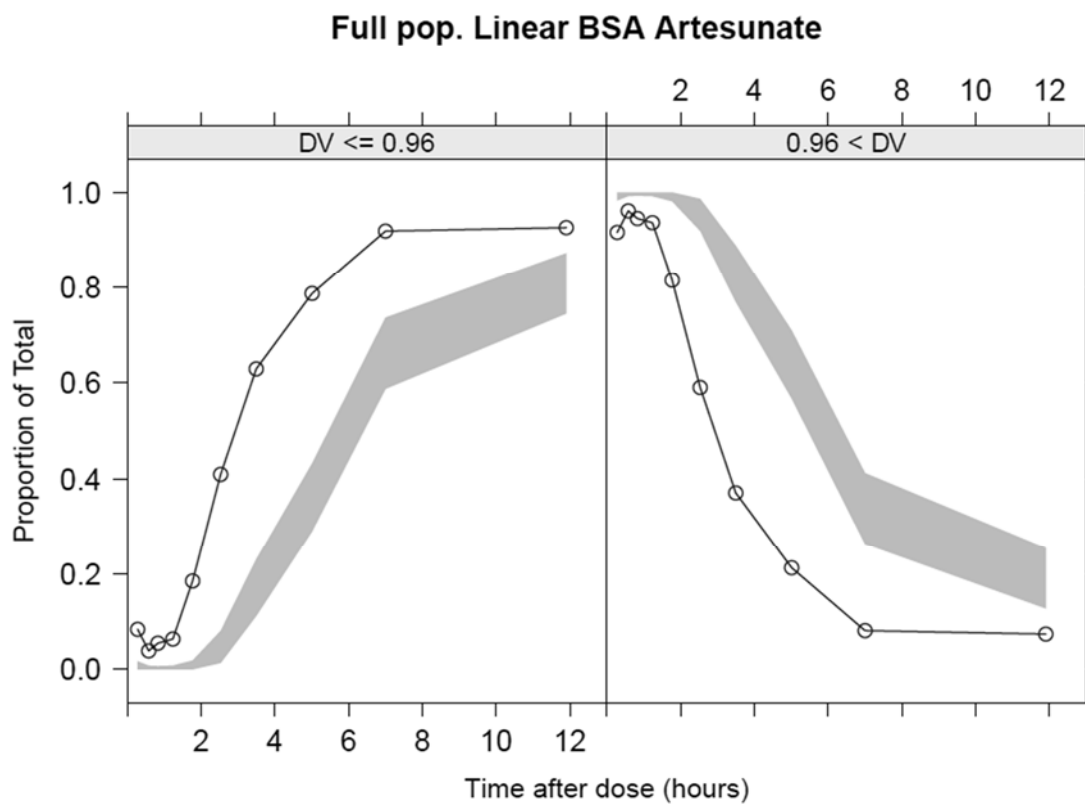


Figure 2.9 Categorical visual predictive check for proportion of artesunate concentrations below the lower limit of quantification for the linear BSA model implemented with the full dataset. The line represents the observed data; the shaded area represents the 95% confidence interval for the simulated data. The value 0.96 is lower limit of quantification of artesunate expressed as the natural log of the artesunate lower limit of quantification (1 ng/mL) in nmol/L.

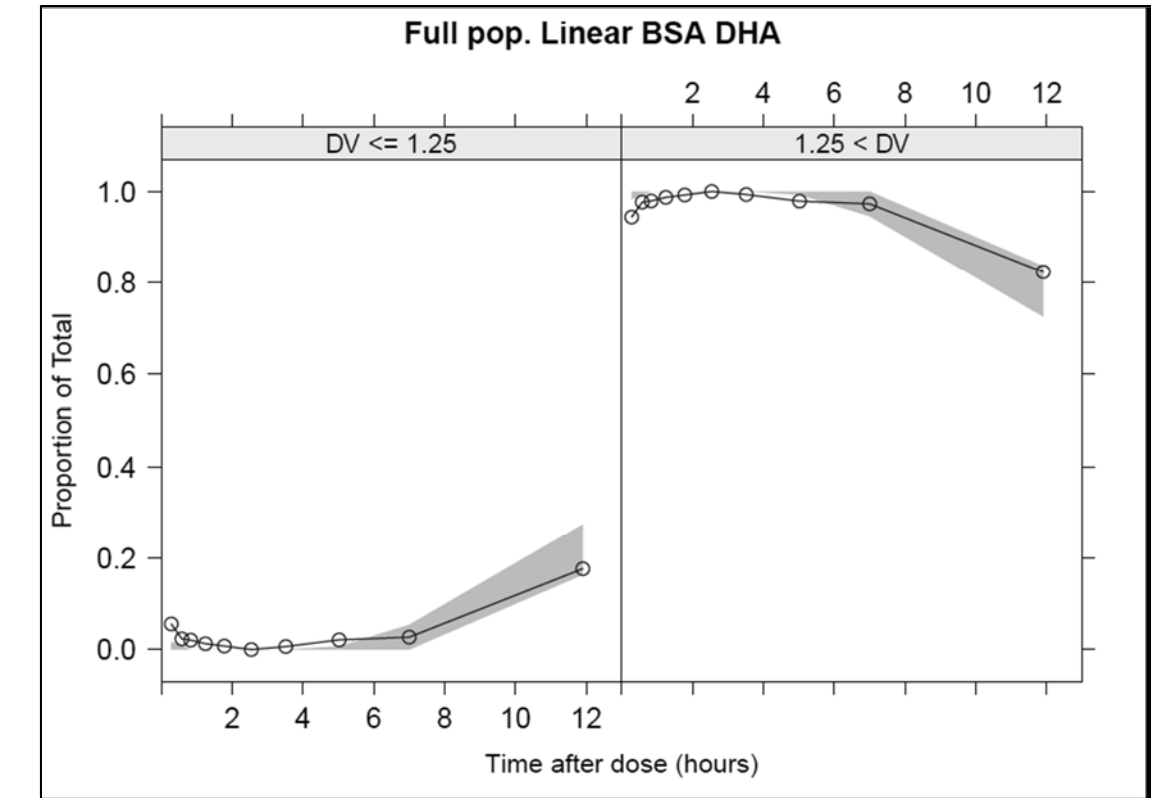


Figure 2.10 Categorical visual predictive check for proportion of DHA concentrations below the lower limit of quantification for the linear BSA model implemented with the full dataset. The line represents the observed data; the shaded area represents the 95% confidence interval for the simulated data. The value 1.25 is lower limit of quantification of DHA expressed as the natural log of the DHA lower limit of quantification (1 ng/mL) in nmol/L.

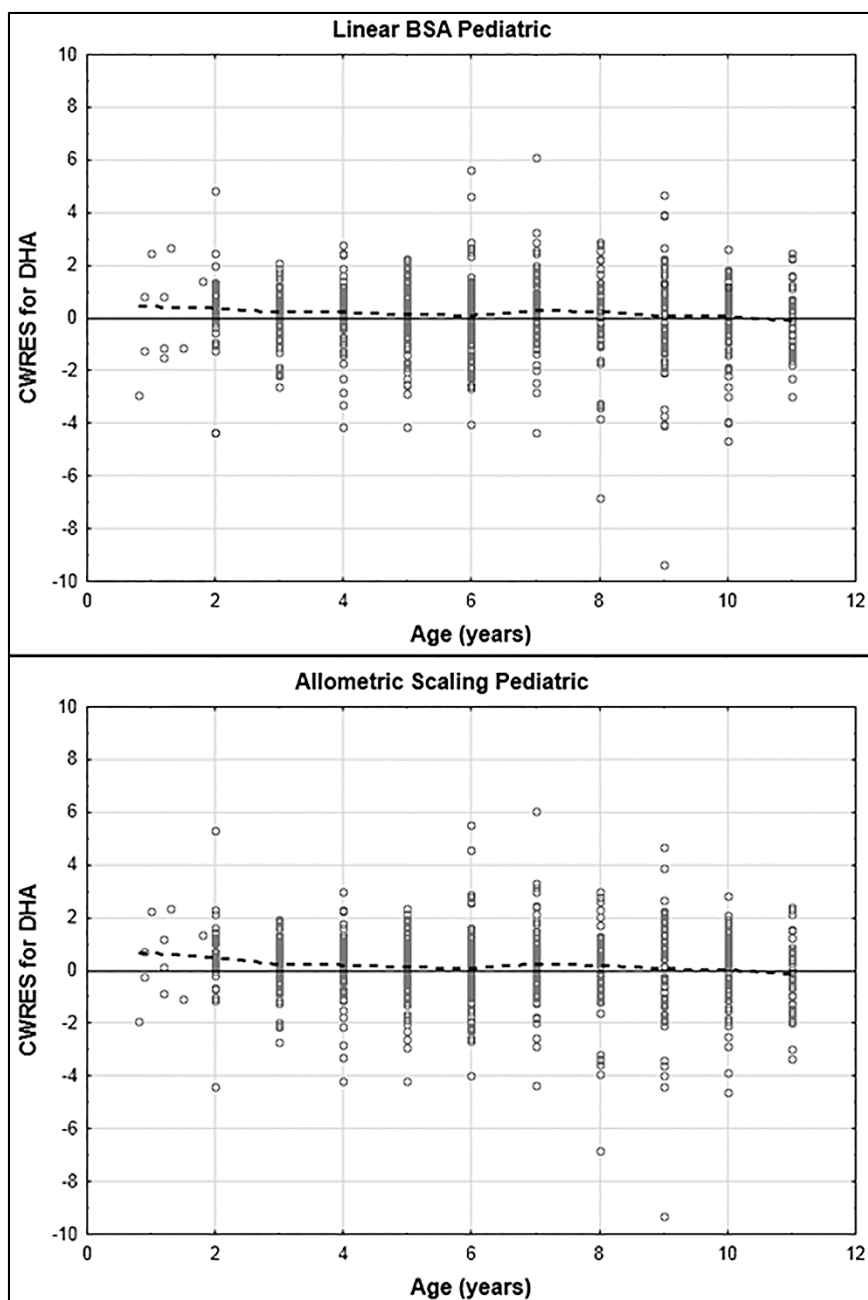


Figure 2.11 Plots of DHA Conditional Weighted Residuals (CWRES) vs. age for the final linear BSA and allometric scaling models implemented with the pediatric dataset

CHAPTER 3

POPULATION PHARMACOKINETICS OF ARTESUNATE AND
DIHYDROARTEMISININ IN PREGNANCYBackground

Malaria infection during pregnancy can have substantial health consequences for both the pregnant woman and the developing child. In regions of unstable or low malaria transmission, pregnant women are more likely than non-pregnant adults to develop severe malaria. In high transmission regions, including much of sub-Saharan Africa, pregnant women are more likely to carry *falciparum* parasites in their blood and to develop marked anemia due to malaria infection. Furthermore, women in such regions are at substantial risk of displaying placental malaria infection, in which *P. falciparum* sequesters within placental tissue. Such sequestration, particularly when occurring with malaria-related anemia, can result in impaired fetal nutrition, low birth weights, and preterm birth. In sub-Saharan Africa, malaria infection in pregnancy is responsible for an estimated 20% of low birth weight deliveries and a consequent 100,000 infant deaths every year (7).

WHO recommends artemisinin-based combination therapy (ACT) as a first-line treatment for acute, uncomplicated *falciparum* malaria in the second and third trimesters of pregnancy (3). Additionally, the inclusion of artemisinin derivatives in novel intermittent preventative treatment regimens for pregnant women has been proposed as a means to combat the effects of increasing resistance to the currently used agent, sulphadoxine-pyrimethamine (SP) (109). However, despite the current and potential applications of artemisinin derivatives to the treatment and prevention of malaria in pregnant women, understanding of how the physiologic changes of pregnancy may alter

the pharmacokinetics, and therefore potentially the efficacy, of artemisinin derivatives is relatively limited. Furthermore, as described in Chapter 1, the findings of those studies which have been conducted have proven somewhat discordant. Therefore, the intent of the analysis in this chapter was to utilize a population pharmacokinetic approach to model the pharmacokinetics of oral artesunate in parasitemic pregnant women and non-pregnant controls and to identify clinically relevant covariates associated with inter-individual variability in artesunate and DHA pharmacokinetics in this population. It should be noted that much of the content of this chapter was previously published in *Malaria Journal* in 2011 (110).

Methods

Study design

Data for this analysis were obtained from a single center, open label study (Clinicaltrials.gov: NCT00538382), the clinical aspects of which were conducted at the Kingasani Maternity Clinic in Kinshasa, Democratic Republic of Congo (DRC). Women presenting for prenatal care at the clinic were screened for study eligibility if they were between 18 and 40 years of age and at less than 22 weeks gestation, determined by last menstrual period. Women confirmed by ultrasound to be between 8 to 21 weeks gestation (inclusive) were invited to be participants in the study. Women were asked to return between 22 to 26 weeks gestation for screening and enrollment; women not enrolled at 22 to 26 weeks were screened again at 32 to 36 weeks gestation. A cohort of non-pregnant female controls was also enrolled. At the time of enrollment, both the pregnant and non-pregnant subjects had asymptomatic *Plasmodium falciparum* parasitemia, with a parasite density between 200 and 300,000 parasite/ μ L, were HIV

seronegative, and were without anemia (hematocrit >30%) or other major medical problems (e.g. chronic hypertension, diabetes, etc.). *Plasmodium falciparum* parasite density was assessed through Giemsa staining of thick and thin blood films; infection was later PCR-confirmed using DNA extracted from dried blood spots (111). The study protocol was approved by the ethical committees of the University of North Carolina at Chapel Hill, the Kinshasa School of Public Health, and the Research Triangle Institute. The study was carried out in accordance with the Helsinki Declaration. Only women able to understand the study protocol and who gave informed consent were enrolled in the study. Further details of the clinical and safety aspects of this trial, including additional biochemical assessments, are described by Onyamboko et al. (64).

For pregnant subjects, pharmacokinetic studies were conducted both at the time of enrollment, as well as at three months postpartum. All subjects received 200 mg oral artesunate, administered as four 50 mg tablets (Guilin Pharmaceutical Co. Ltd) at the beginning of an inpatient stay at the clinic. Blood samples (5 mL) for pharmacokinetic analysis were drawn at pre-dose and at 0.25, 0.5, 0.75, 1, 1.5, 2, 3, 4, 6, and 8 hours after artesunate administration. Twenty-four hours following artesunate administration, malaria-infected women received 1725 mg SP to complete treatment. Blood sampling schedule and sample handling were uniformly applied for pregnant, postpartum, and control subjects. Blood samples were collected in pre-chilled tubes containing potassium oxalate/sodium fluoride. Following collection, tubes were placed on wet ice; within 5 minutes of collection, samples were centrifuged. Immediately following centrifugation, plasma was removed from the cells and transferred into cryovials. The plasma samples were transferred to liquid nitrogen until they could be frozen at or below -80°C in a

laboratory freezer; samples were later shipped on dry ice to the Clinical Pharmacokinetics Laboratory at the College of Pharmacy, University of Iowa, where they were stored at -80°C until drug analysis was performed.

Sample analysis

Determination of artesunate and DHA plasma concentrations was performed using a validated liquid chromatography-mass spectrometric method described by Naik et al. (83) with minor modifications to allow for extraction from a smaller plasma volume. Briefly, solid phase extraction was used to extract artesunate, DHA and the internal standard artemisinin from 0.25 mL of human plasma. The reconstituted extracts were chromatographed isocratically. Mass spectroscopy in positive ion mode was used to detect and quantify the compounds. The lower limit of quantification (LLQ) for both artesunate and DHA was 1 ng/mL. Assay validation indicated that assay precision was 5.8 – 8.6% (coefficient of variation) for artesunate and 6.5 – 8.2% for DHA.

Population pharmacokinetic analysis

Nonlinear mixed effect model building was conducted using NONMEM software version 7 (ICON Development Solutions, Ellicott City, MD) implemented on a Windows XP operating system (Microsoft Corporation, Seattle, WA) with a G95 Fortran compiler (Free Software Foundation, Boston, MA). Monte Carlo importance sampling expectation maximization with interaction (IMP INTER) estimation method was used to fit models. Pdx-Pop 4.0 (ICON Development Solutions, Ellicott City, MD) and Xpose version 4.1.0 (Uppsala University, Uppsala, Sweden) (101) were used in processing NONMEM 7 output. Plots were generated with TIBCO Spotfire S+ version 8.1 (TIBCO Software Inc., Palo Alto, CA) and R version 2.10.0 (Free Software Foundation, Boston, MA).

Model selection was guided by the following criteria: plausibility and precision of parameter estimates, minimum objective function value (MOFV), equal to minus twice the log likelihood function, Akaike Information Criterion, equal to MOFV plus two times the number of parameters, condition number, equal to the ratio of the largest eigenvalue to the smallest eigenvalue, and inspection of diagnostic plots.

Prior to modeling, artesunate and DHA concentrations were converted from ng/mL to nmol/L values using the compounds' respective molecular weights; the concentrations were then natural log-transformed. The 200 mg artesunate dose was similarly converted to the appropriate value in nmols. Modeling was initially conducted with an aggregate data set of pregnancy, postpartum, and control observations. A structural model adequately describing data from all three groups could not be identified. As this difficulty appeared to stem from the erratic and unpredictable artesunate and DHA observations from the postpartum subjects, the data were subsequently divided into pregnancy/control and postpartum data sets for structural model identification. Since an adequate structural model could only be identified for the pregnancy/control data set, the Base model development and Covariate model building sections that follow describe model building using the pregnancy/control data set, with details regarding attempts to model postpartum data provided in Results.

Base model development

Modeling was first performed with artesunate data only; first-order absorption with one compartment and two compartment models were fitted to these data. DHA data were also initially modeled independently in order to determine if a one or two compartment model better characterized observed concentrations. Alternative

absorption processes were also assessed utilizing artesunate data only, including first-order absorption, zero-order absorption with lagged first-order absorption, first-order absorption with lagged zero-order absorption, parallel dual first-order absorption, transit compartment absorption, and single Weibull absorption. Use of a Weibull function to describe absorption allows for flexibility to characterize absorption profiles not amenable to description with first-order or other simple absorption functions. The Weibull function includes absorption rate constants for both a rapid and slower phase of absorption and contains shaping factors which further allow for characterization of atypical absorption profiles (112).

Multiple simultaneous parent-metabolite models consisting of a one compartment model for artesunate and a one compartment model for DHA with various artesunate absorption types were assessed. Complete, irreversible conversion of artesunate to DHA was assumed for all models (34). Simultaneous models were implemented using ADVAN 5. These simultaneous models included the absorption processes assessed with artesunate data only, as well as parallel dual first-order absorption of both artesunate and DHA from a gut compartment. This particular model represents an attempt to describe absorption of DHA present in the gut due to acid-catalyzed degradation of artesunate to DHA which may occur in the acidic environment of the stomach (40).

Inter-individual variability (IIV) was modeled on pharmacokinetic parameters using a log-normal distribution:

$$P_i = P_{\text{pop}} \cdot \exp(\eta_i)$$

where P_i represents the parameter estimate for individual i , P_{pop} represents the population estimate for the parameter, and η_i represents the deviation of P_i from P_{pop} .

Residual variability (RV) was modeled with an additive model for log-transformed data:

$$\ln C_{ij} = \ln C_{\text{pred}, ij} + \varepsilon_{ij}$$

where C_{ij} represents the j th observation for individual i , $C_{\text{pred}, ij}$ represents the predicted artesunate or DHA concentration for individual i , and ε_{ij} represents the residual random error for the j th observation of individual i .

Covariate model building

Once the optimal base model was determined, covariate analysis was undertaken to identify any covariates explaining a significant portion of the observed IIV. Covariates examined included age, weight, BMI, baseline alpha-2 acid glycoprotein, baseline albumin, pregnancy status, and window of pregnancy. Examined covariates represented available demographic and clinical variables which could plausibly alter artesunate or DHA pharmacokinetics. Potential covariate-parameter relationships were identified by examining plots of covariates versus parameter estimates and covariates versus IIV. Covariate screening was also conducted using generalized additive modeling in Xpose software. Physiologically plausible covariate-parameter relationships suggested by evaluation of covariate plots and/or by generalized additive modeling were evaluated for statistical significance using the process of forward addition followed by backward elimination (113). The statistical criteria for a covariate to be retained in the model during the forward addition stage was $p < 0.05$; for the backward elimination stage, the criteria was $p < 0.001$.

Categorical covariates were modeled using a proportional function:

$$P = \theta_1 \cdot (1 + \theta_2 \cdot \text{COV})$$

where θ_1 represents the parameter estimate in subjects with the covariate coded as 0 and θ_2 representing the change in the parameter associated with the categorical covariate being tested.

Continuous covariates were centered on their median and modeled using a linear function:

$$P = \theta_1 + \theta_2 \cdot (\text{COV} - \text{COV}_{\text{median}})$$

where θ_1 represents the parameter estimates for an individual with COV equal to $\text{COV}_{\text{median}}$, and θ_2 represents the change in the parameter estimate associated with the difference between COV from $\text{COV}_{\text{median}}$.

Model evaluation

Diagnostic plots used to assess model goodness-of-fit included observed concentrations versus population predictions, observed concentrations versus individual predictions, conditional weighted residuals (CWRES) versus population predictions, and CWRES versus time. Population predictions were obtained using the EPRED option in NONMEM 7.

One thousand bootstrap runs were conducted using Perl-Speaks-NONMEM version 3.1.0 (114) in order to assess the precision of the parameter estimates. Model stability was assessed by condition number, with a condition number less than 1000 considered indicative of model stability. The predictive ability of the model was evaluated by simulating 1000 virtual observations for each sampling time point at which artesunate or DHA concentrations had been above LLQ in the original data set. The

observed concentrations were plotted with the 5th, 50th, and 95th percentiles of the simulated data.

Results

Subject data

Demographic and clinical data for the pregnant women and controls enrolled in this study are provided in Table 3.1. Thirteen pregnant women were enrolled in each of the two windows of pregnancy. All pregnant (n=26) and control subjects (n=25) were assessed as slide positive and PCR-positive for *falciparum* parasitemia at enrollment, although at the time of artesunate administration, typically occurring one day following enrollment, two pregnant and 11 control subjects were assessed as slide negative for parasitemia. All infections were *P. falciparum* mono-infections with the exception of one pregnant woman with *P. falciparum* - *Plasmodium malariae* co-infection. All previously pregnant subjects were lactating at the time of postpartum evaluation. All postpartum subjects were PCR-positive for infection, but only two postpartum subjects were slide positive for parasitemia, including one subject with a mixed infection.

Of the collected samples for pregnancy and control group patients, 41% of artesunate (40% pregnancy, 41% control) and 2% of DHA observations (<1% pregnancy, 2% control) fell below the lower limit of quantification and were excluded prior to model building. One artesunate observation and one DHA observation were identified as outliers and excluded from the analysis. Modeling was conducted using 300 artesunate and 498 DHA concentrations.

Model development

When artesunate data were modeled independently using first-order absorption, a two compartment model did not improve model fit as compared to a one-compartment model. A two compartment model was also not preferable to a one compartment model for DHA data. A simultaneous parent-metabolite model with a one compartment model for artesunate, a one compartment model for DHA, and mixed zero-order, lagged first-order absorption was associated with lower bias in goodness-of-fit plots, particularly in the initial two hours post-dose, than simultaneous models with alternative artesunate absorption processes. Use of mixed zero-order, lagged first-order absorption was associated with a decrease in MOFV of 665 as compared to a simple first-order absorption model.

The final base model, illustrated in Figure 3.1, was parameterized in terms of the duration of the zero-order absorption process ($D2$), the rate constant of the lagged first-order absorption process ($K12$), the fraction of the dose absorbed by the first-order absorption process ($F1$), the lag time for the first-order absorption process ($ALAG1$), the apparent clearance of artesunate (CL/F), the apparent clearance of DHA (CLM/F), the apparent volume of distribution of artesunate ($V2/F$), and the apparent volume of distribution of DHA ($V3/F$).

The following covariate relationships were assessed during the forward addition step of covariate modeling: pregnancy status on CLM/F , CL/F , $D2$, and $V3/F$ and weight on $V2/F$, CLM/F , and $V3/F$. Only one covariate, pregnancy status on clearance of DHA, was retained as significant at the $p < 0.001$ level in the final model. Although not statistically significant in the full covariate analysis, the effect of pregnancy status on DHA volume of distribution was the only tested covariate relationship, apart from

pregnancy status on CLM/F, that was significant ($p < 0.05$) in the initial forward addition step of covariate modeling. Pregnancy was associated with a trend towards increased DHA volumes of distribution of approximately 37%.

The IIV values associated with CL/F and F1 were fixed after conclusion of covariate model building due to poor precision in omega estimates. NONMEM parameter estimates and relative standard errors are given in Table 3.2. The final parameter estimates for the model were used to generate the typical DHA concentration-time profiles, plotted in Figure 3.2, for the pregnant and non-pregnant women. The control stream and model output results for the final model are given in Appendix E and F, respectively.

For postpartum data, the following absorption models, with a one-compartment model for artesunate and a one-compartment model for DHA, were assessed: first-order absorption, zero-order absorption, zero-order absorption with lagged first-order absorption, first-order absorption with lagged zero-order absorption, parallel dual first order absorption, single Weibull absorption, transit compartment absorption, and absorption of both artesunate and DHA from the gut. None of the structural models assessed provided adequate predictive power for DHA observations. Specifically, more than 20% of the DHA concentrations fell outside the visual predictive check 90% prediction interval. Attempts to model only DHA observations using various absorption processes were similarly unsuccessful.

Model evaluation

Goodness-of-fit plots for artesunate and DHA are given in Figures 3.3 and 3.4, respectively. Mean parameter estimates and percentile-based bootstrap 95% confidence

intervals obtained from 1000 bootstrap runs are given in Table 3.2. Minimization was successful in 99.9% of bootstrap runs. All parameter estimates from the final model fall within the bootstrap confidence intervals. The condition number for the final model is 7.2, indicating good model stability. The visual predictive check plots for artesunate and DHA are in Figure 3.5. In the VPC for artesunate, the lines representing the 5th, 50th, and 95th percentiles of the observed data fell within the 95% confidence intervals for the 5th, 50th, and 95th percentiles of the simulated data; this suggests adequate predictive ability. For DHA, the 50th and 95th percentile line do lie within their respective simulated confidence interval throughout the sampling period. However, the 5th percentile of the observed data falls outside the simulated confidence interval for the 6 and 8 hour time points, suggests potential underprediction of DHA in the later post-dose period. Given that the 50th and 95th percentiles of observed data do not display this pattern, the precise nature and cause of this apparent underprediction is difficult to elucidate given available data.

Discussion

In the present analysis, a population pharmacokinetic model was developed for artesunate and its active metabolite DHA using extensive sampling data from 26 pregnant and 25 non-pregnant women in the DRC. The model consists of a one-compartment model for artesunate and a one-compartment model for DHA, with artesunate absorption occurring through a mixed zero-order, lagged first-order absorption process. Upon absorption, artesunate is rapidly converted to DHA, with an approximate artesunate elimination half-life of 9.1 minutes. The model indicates that DHA apparent clearance is

approximately 42% higher in pregnant than non-pregnant subjects, with resultant DHA elimination half-life estimates of 45 minutes and 59 minutes for pregnant and non-pregnant subjects, respectively.

The rapid elimination of artesunate found in this analysis is consistent with findings of pharmacokinetic analyses with IV artesunate, with an artesunate half-life estimate of 13.2 minutes obtained by Newton et al. (32) and estimates of less than ten minutes found by Binh et al. (23) and Batty et al. (22). Given this rapid conversion of artesunate to DHA, the rate of DHA formation may be limited by the rate of artesunate absorption. The multiple samples collected in this study during the early period following artesunate administration allowed for artesunate absorption to be characterized using a mixed zero-order, lagged first-order absorption process that offered marked improvement in model fit over simpler absorption models. Given that artesunate is a weak acid with a pKa of 4.6 (14), absorption through this mixed-order process may reflect artesunate solubility and permeability changes occurring in the differing pH environments encountered in gastrointestinal transit. Gastric absorption of artesunate may be limited by the solubility of the free acid form of artesunate (168.2 $\mu\text{g/mL}$) (115); such solubility-limited absorption would plausibly correspond to a zero-order process (112) such as the process characterizing the initial phase of artesunate absorption in the mixed-order absorption model utilized in the present analysis.

Erratic artesunate absorption in the postpartum women appears to have contributed substantially to the difficulty in identifying a satisfactorily predictive structural model for describing data from the postpartum subjects. Given the rapid conversion of artesunate to DHA upon artesunate absorption, unpredictable artesunate

absorption would be expected to produce a pattern of DHA appearance inconsistent with standard compartmental modeling. The source of this atypical absorption may relate to breastfeeding; the women in the study were encouraged to bring their infants to the study site and to feed the children prior to artesunate administration. The effects of lactation on maternal kinetics have not been extensively studied. However, some studies have been performed evaluating the effects of lactation on ethanol kinetics. These studies report changes in ethanol pharmacokinetics, which may represent altered patterns of ethanol absorption, associated with the lactational state in general, as well as more acute effects induced by breast pumping or, presumably, infant suckling (116-118). Suckling appears to trigger the release of various hormones responsible for regulation of digestion; these hormones can alter rates of processes such as gastric emptying (116). Therefore, it is plausible that the erratic artesunate absorption patterns observed for the postpartum subjects in this study may have resulted from the effects of lactation and recent infant suckling on artesunate absorption.

The only significant covariate identified in the present analysis was the effect of pregnancy on the clearance of DHA; this effect was estimated to produce a 42.3% (95% CI: 19.7% - 72.3%) proportional increase in DHA clearance in pregnant women as compared to non-pregnant controls. Clearance did not appear to differ substantially between the two windows of pregnancy, but more subjects in each trimester would likely be required for a difference between trimesters to be reliably detected. The disparate DHA clearance values of the pregnant and control subjects identified were highly similar to those obtained by non-compartmental analysis of the data. Non-compartmental analysis also indicates an increase in DHA volume of distribution associated with

pregnancy. Apparent DHA clearance values for pregnancy and control subjects in the present analysis are similar to those obtained by non-compartmental methods, although apparent DHA volume of distribution was somewhat lower in the population, as compared to the non-compartmental, analysis (64). In the present analysis, the apparent volume of distribution of DHA trended higher for pregnant subjects, but the association between pregnancy status and increased volume of distribution did not meet the statistical significance criteria ($p < 0.001$) for the forward addition/backward elimination covariate analysis methods. However, given that this association was associated with a clear trend in the post hoc individual parameter estimates, the effect of pregnancy on DHA apparent volume of distribution could likely be precisely defined with data from a larger pool of subjects.

The source of the pregnancy-related accelerated DHA clearance identified in this analysis is difficult to determine, as pharmacokinetic changes resulting from the physiological changes of pregnancy are not presently well understood. As DHA is metabolized through hepatic glucuronidation by UGT1A9 and UGT2B7 (34), induction of these enzymes could result in accelerated DHA clearance. Induction of hepatic glucuronidation, potentially by elevated sex hormone levels in pregnancy, may be responsible for the substantial pregnancy-related increases in glucuronidation observed for various drugs, including lamotrigine (119, 120), oxcarbazepine (121), and lorazepam (122). However, given that DHA is a high extraction ratio drug, alterations in hepatic blood flow are more likely to be responsible for changes in DHA clearance. Although such alterations in blood flow during pregnancy have been investigated, the results of these investigations are not in agreement (12). Additionally, blood flow changes may not

be consistent across trimesters (123). Therefore, the manner in which hepatic blood flow alterations would be expected to contribute to pregnancy-associated DHA pharmacokinetic changes is difficult to predict.

A limited number of pharmacokinetic trials have been conducted to characterize artesunate/DHA pharmacokinetic changes that may be associated with the physiologic changes of pregnancy. McGready et al. (2006) (55) modeled the pharmacokinetics of DHA following oral administration of artesunate to second and third trimester pregnant women with acute uncomplicated malaria. Non-compartmental analysis of their data yielded estimates of 4.0 L/hr/kg for CL/F and 3.4 L/kg for V/F. Using population pharmacokinetic analysis methods, these authors modeled DHA data using a one-compartment model with a first-order rate of formation modeled. The parameter estimates obtained, adjusted for the median weight of the subjects (50 kg), were 88.5 L/hr [95% CI 60 – 117 L/h] for oral DHA clearance and 231.5 L [95% CI 57 – 406 L] for DHA volume of distribution. The estimate for DHA apparent clearance in pregnant patients is similar to the estimate in the present analysis (91 L/h). The volume of distribution estimate from the present analysis (91.4 L) is lower than found by these investigators. However, both the 91.4 L estimate and the 95% bootstrap confidence interval for that estimate (78.5-109 L), fall within their 95% confidence interval.

McGready et al. (29) conducted a subsequent study in 20 second and third trimester pregnant women with uncomplicated *falciparum* malaria in Thailand. One cohort of women received IV artesunate at 4 mg/kg on day 0 followed by oral artesunate at 4 mg/kg/day for six additional days; the second cohort received 4 mg/kg oral artesunate on day 0, 4 mg/kg IV artesunate on day 1, and then 4 mg/kg/day oral

artesunate for five days. Extensive sampling for artesunate and DHA concentrations were obtained on days 0 and 1, with limited samples taken on day 6. At three months postpartum the women returned and were administered the regimen they had been administered while pregnant. The authors did not identify statistically significant differences in artesunate or DHA pharmacokinetics between pregnant and postpartum women when examining parameters derived from concentrations observed following IV artesunate administration. However, following oral artesunate administration, median AUC values for artesunate and DHA were both significantly higher in pregnant women as compared to the same women postpartum. Additionally, estimated bioavailability was significantly higher in pregnancy for artesunate and DHA. Following oral dosing, DHA exposure was significantly higher on days 0 and 1 as compared to day 6. This effect was observed with pregnant but not postpartum women; the authors speculated that this pattern reflects the effects of acute illness on days 0 and 1. Although these results would seem to clearly support a disease effect on artesunate/DHA pharmacokinetics, this disease effect would seem to render any pregnancy-related changes far more difficult to interpret.

Valea et al. (67) examined the pharmacokinetics of artesunate and DHA following oral artesunate/mefloquine administration to 24 pregnant and 24 matched non-pregnant women with uncomplicated *falciparum* malaria in Burkina Faso. Based on non-compartmental analyses, the authors described median artesunate CL/F estimates of 39.5 L/hr/kg and 60.0 L/hr/kg ($p < 0.05$), for pregnant and non-pregnant women, respectively. artesunate V/F estimates were not significantly different, with median values of 19.3 L/kg in pregnant and 26.0 L/kg in non-pregnant women. Furthermore, neither DHA CL/F or

DHA V/F significantly differed between the pregnant and non-pregnant groups. The authors indicate that further investigation would be required to elucidate the artesunate findings. Additionally, the authors speculate that the seeming lack of any marked pregnancy-related effect on DHA apparent clearance could stem from the higher parasite density observed in the pregnant as compared to the non-pregnant women in the study. That is, the authors conjectured that a greater disease effect in the pregnant women, as supported by higher levels of parasitemia, could have masked a pregnancy-related increase in DHA clearance.

Limitations and Summary

The pregnant women included in the present study were asymptomatic, displayed low-grade parasitemia, and were otherwise generally healthy. Therefore, the results from this study can be generalized to populations for which intermittent preventative treatment regimens are indicated. Given that the model was not constructed using data from pregnant women with acute symptomatic malaria, it is not known if the model would optimally describe artesunate and DHA pharmacokinetics in such patients. In these patients, lower DHA blood levels resulting from accelerated DHA clearance could translate into reduced efficacy of artesunate and related compounds. Lower levels could also select for survival of parasites more tolerant to these compounds, increasing the risk of resistance development.

In summary, this analysis describes a stable and adequately precise population pharmacokinetic model for artesunate and DHA in pregnant and non-pregnant women in the DRC. A central finding of this analysis is that an increase in DHA oral clearance is associated with pregnancy. The model indicates that pregnant patients would need to

receive a higher dose of artesunate in order to achieve equivalent DHA blood levels as obtained by non-pregnant patients receiving the standard adult dose. Although a larger study would be required to comprehensively characterize the artesunate dose adjustments needed for pregnant patients to achieve the same antimalarial exposure as non-pregnant patients, the substantial pregnancy-associated increase in DHA clearance described in the present analysis underscores the need for such a study.

Table 3.1 Demographic and clinical data for study participants.

	Pregnancy	Postpartum	Controls
Age (years)	23 (19 - 35)	24 (20 - 36)	24 (18 - 38)
Weight (kg)	63 (40 - 71)	55 (39 - 67)	52 (42 - 84)
BMI (kg/m ²)	23.2 (17.7 - 26.9)	55 (39 - 67)	20.7 (17.2 - 28)
Parasite density at enrollment ^a	528 (372 - 842)	NA ^b	807 (325 - 2215)
Baseline ALT (Units/L)	14.5 (8 - 31)	21 (12 - 71)	18 (11 - 67)
Baseline AST (Units/L)	26 (19 - 43)	29 (17 - 64)	32 (19 - 46)
Baseline Albumin (g/dL)	2.6 (2.1 - 3.4)	3.3 (1.8 - 5.7)	3.3 (2.8 - 4)
Baseline AGP (mg/dL)	69.5 (43 - 123)	80 (32 - 162)	99 (62 - 177)

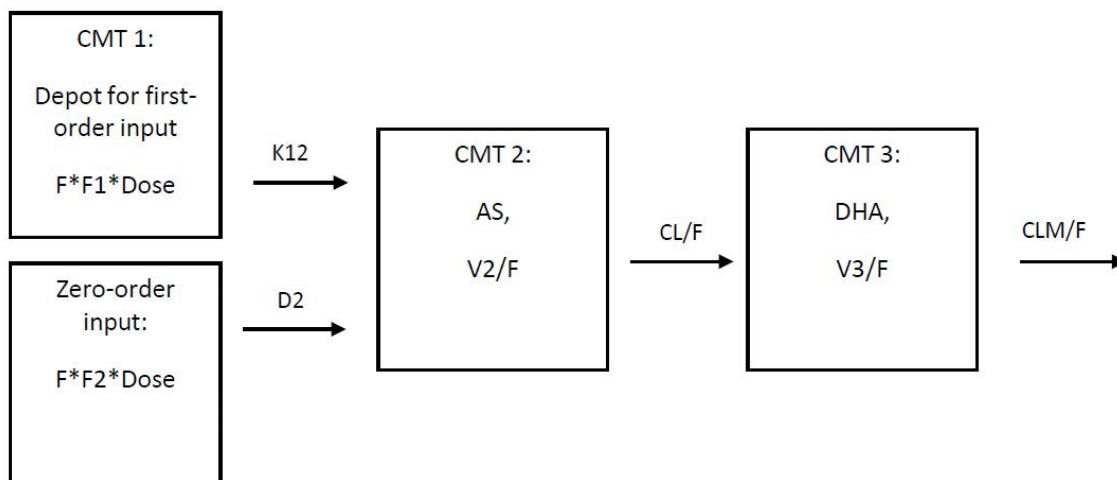
a. Values given as median (interquartile range). All other values given as median (range)

b. Only two women in the postpartum group were slide positive for malaria.

Table 3.2 Final model parameter estimates for model describing the pharmacokinetics of artesunate and DHA in pregnant and non-pregnant women.

Parameter	Estimate	%RSE	Bootstrap mean (95% CI)
K12(h ⁻¹)	4.28	23.6	4.43 (2.73-7.16)
D2 (h)	4.04	19.5	3.99 (2.37-6.27)
ALAG1 (h)	0.627	10.9	0.63 (0.494-0.771)
F1	0.864	1.56	0.867 (0.839-0.887)
CL/F (L/h)	895	5.9	904 (788-1045)
V2/F (L)	195	16.4	201 (139-285)
CLM/F (L/h)	64.0	6.53	64.2 (55.1-75.2)
V3/F (L)	91.4	6.15	92.1 (78.5-109)
PREG on CLM/F	0.423	30.3	0.427 (0.197-0.723)
Between subject variability Variances (%CV)			
IIV – K12	1.84 (136)	25.3	1.76 (0.986-2.77)
IIV – D2	1.33 (115)	22.9	1.33 (0.64-2.15)
IIV – ALAG	0.573 (75.7)	20.8	0.581 (0.333-0.91)
IIV – V2/F	0.604 (77.7)	30.1	0.568 (0.253-0.942)
IIV – CLM/F	0.0802 (28.3)	24.9	0.0711 (0.031-0.113)
IIV – V3/F	0.0790 (28.1)	34.7	0.00661 (0.00591-0.139)
Residual Variability - Variances			
AS	0.696	11.6	0.721 (0.515-0.971)
DHA	0.174	9.94	0.174 (0.129-0.226)

Note: K12 is the rate constant for the first-order absorption process; D2 is the duration of the zero-order absorption process; ALAG1 is the lag time for initiation of first-order absorption; F1 is the fraction of the absorbed dose which was absorbed by the first-order process; CL/F and V/F are the apparent clearance and volume of distribution for artesunate, respectively; CLM/F and V3/F are the apparent clearance and volume of DHA, respectively; PREG on CLM/F is the proportional increase in DHA apparent clearance associated with pregnancy.



CMT: Compartment

F: Oral Bioavailability

F1: Fraction of dose absorbed by first-order process

F2: Fraction of dose absorbed by zero-order process, equal to $1 - F_1$

K_{12} : Absorption rate constant for first-order process

D_2 : Duration of zero-order absorption process

CL/F : Apparent AS clearance

V_2/F : Apparent volume of distribution of AS

CLM/F : Apparent DHA clearance

V_3/F : Apparent volume of distribution of DHA

Figure 3.1 Diagram of final structural model for artesunate and DHA pharmacokinetics as developed to model artesunate and DHA pharmacokinetics in pregnant and non-pregnant women with asymptomatic parasitemia.

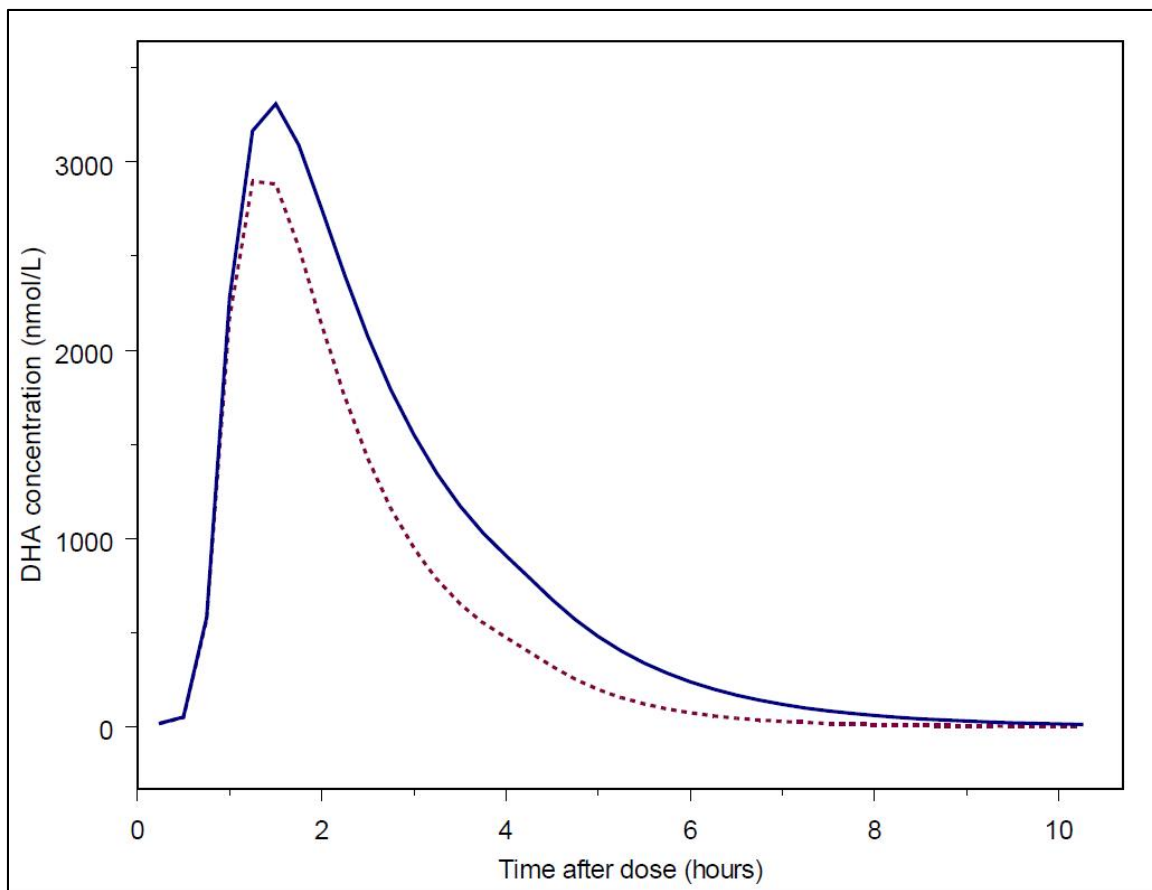


Figure 3.2 Typical DHA concentration-time profiles for pregnant and non-pregnant women based on final model parameter estimates. The dashed line represents the typical profile for pregnant women. The solid line represents the typical profile for non-pregnant women. A 200 mg dose of artesunate was specified in generating the typical profiles.

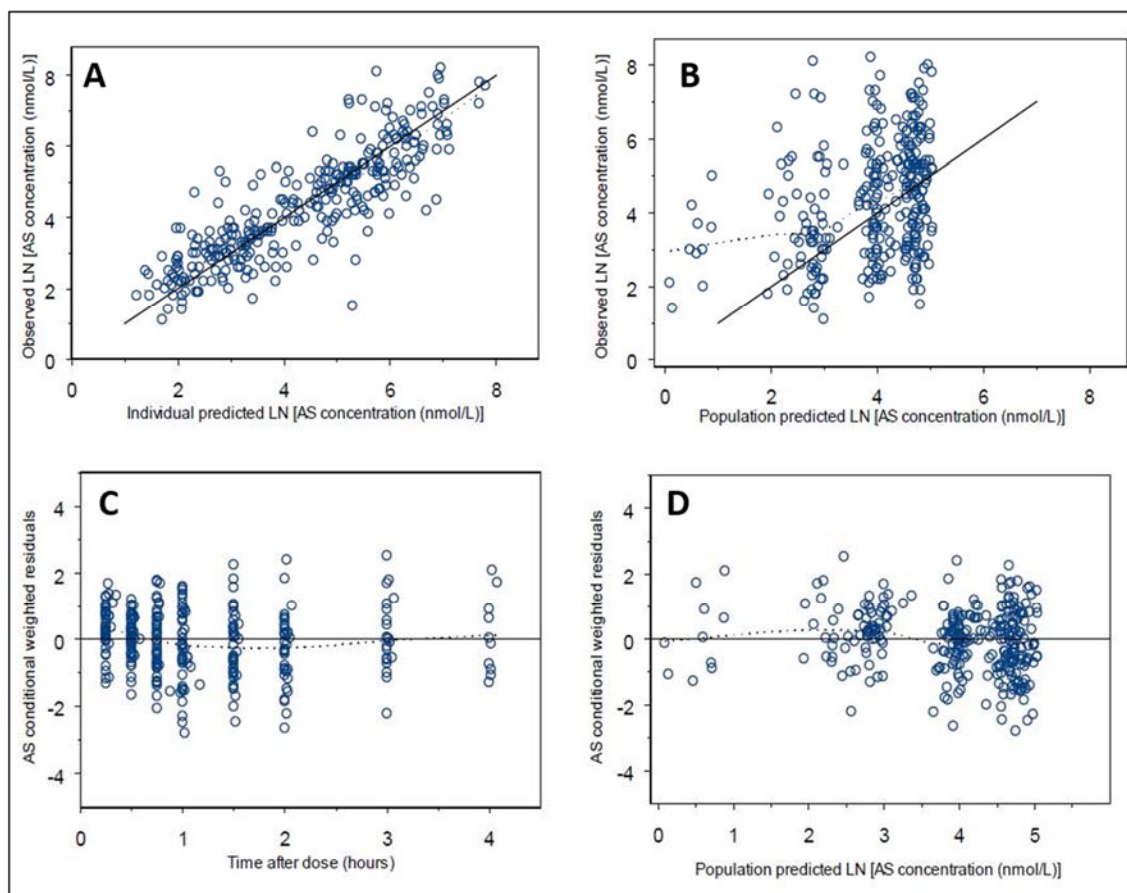


Figure 3.3 Goodness-of-fit plots for artesunate for final model. Open circles are observed data. Dotted lines are smoothing lines. Solid lines are lines of identity. Plot A displays observed artesunate vs. individual predicted artesunate. Plot B displays observed artesunate vs. population predicted artesunate. Plot C displays conditional weighted residuals (CWRES) for artesunate vs. time after dose. Plot D displays CWRES for artesunate vs. population predicted.

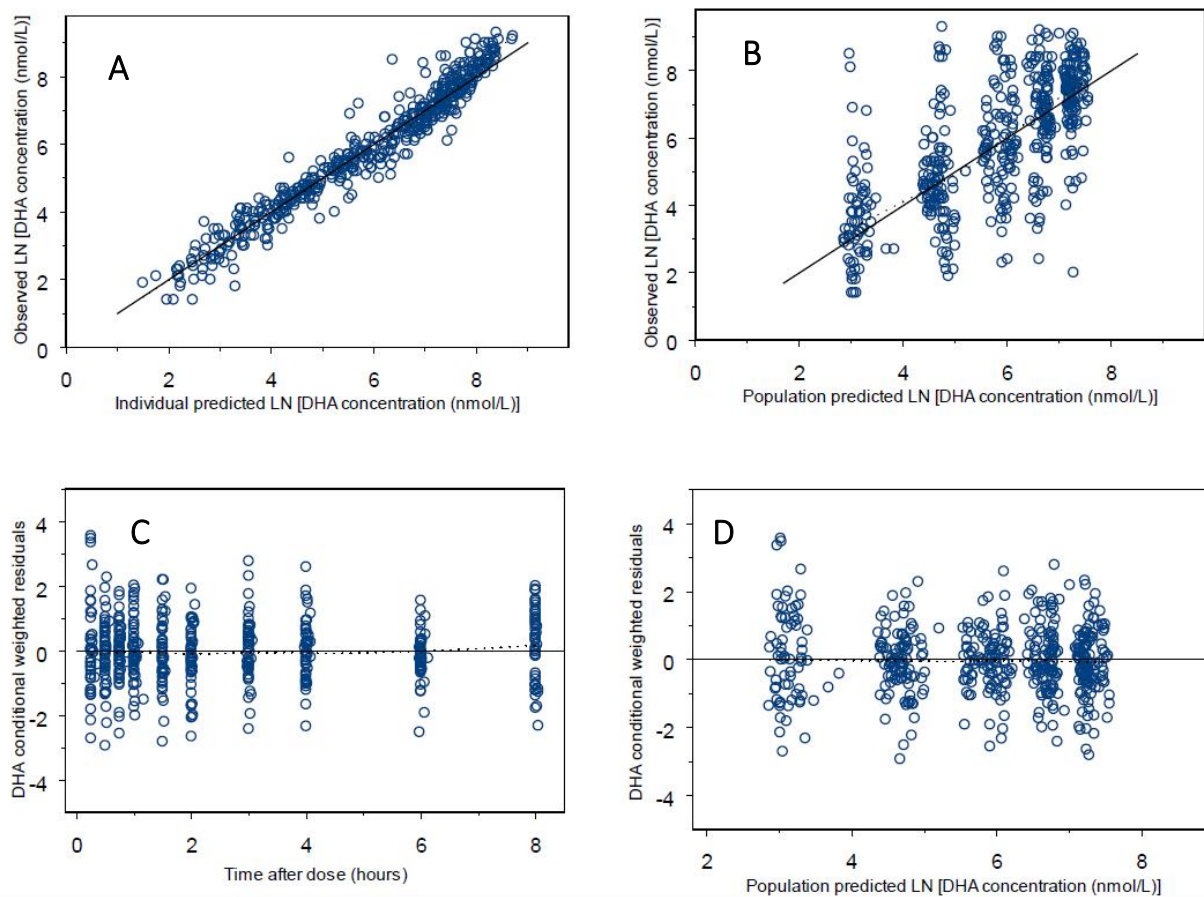


Figure 3.4 Goodness-of-fit plots for DHA for final model. Open circles are observed data. Dotted lines are smoothing lines. Solid lines are lines of identity. Plot A displays observed DHA vs. individual predicted artesunate. Plot B displays observed DHA vs. population predicted artesunate. Plot C displays conditional weighted residuals (CWRES) for DHA vs. time after dose. Plot D displays CWRES for DHA vs. population predicted artesunate.

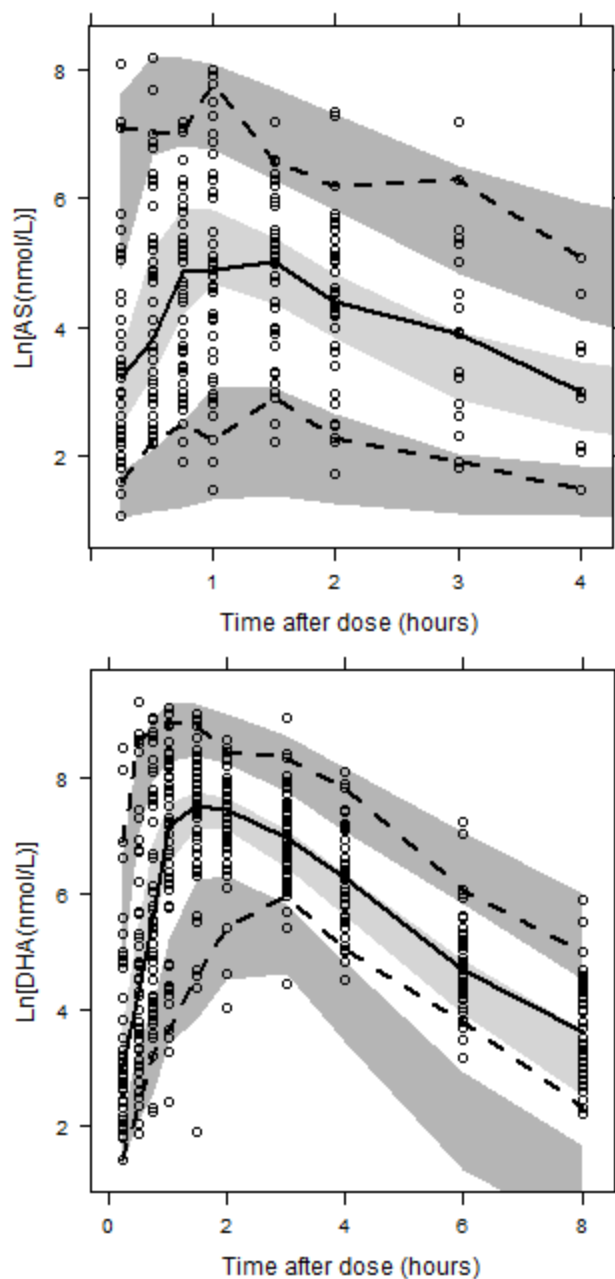


Figure 3.5 Visual predictive check plots for artesunate and DHA for the final model. The open circles represent the observed concentrations, the solid line represents the median of the observed data, the dashed lines represent the 5th and 95th percentiles for the observed data, and the shaded areas represent the 95% confidence intervals surrounding the prediction intervals (5th, 50th, and 95th percentiles) obtained from the simulations.

CHAPTER 4

CLINICAL IMPLICATIONS AND CONCLUSIONS

The principal objectives of the research in the preceding chapters of this thesis were to develop population pharmacokinetic models describing the concentrations of artesunate and DHA in children and pregnant women with malaria. Individuals in these two special populations are not only exceptionally vulnerable to malaria infection, but are also quite likely to display discrepant artesunate pharmacokinetics as compared to the non-pregnant adults upon whom most artesunate pharmacokinetic knowledge is based. The population pharmacokinetic analyses described above reveal differences in the pharmacokinetics of individuals in these populations. Specifically, the models indicate that for a given mg/kg artesunate dose, pregnant women and young children would be expected to display lower DHA concentrations than achieved by a non-pregnant adult given the same dose.

Optimizing dose selection

Current WHO treatment guidelines specify a target artesunate dose for treatment of uncomplicated malaria of 4 mg/kg/day for three days, to be given in combination with a long acting partner drug, with a therapeutic dosing range of 2 – 10 mg/kg/day (3). The high upper limit of this range reflects the relative safety of artesunate, which is generally well tolerated, with minimal symptomatic adverse effects. The dose-limiting toxicity of artesunate would appear to be reversible neutropenia, a dose-dependent effect identified as occurring to a clinically relevant extent following oral doses of 6 mg/kg/day for 7 days (124). It is difficult to predict the likelihood of neutropenia resulting from the standard three days of dosing; regardless, clinically, use of doses near 6 mg/kg/day would be highly unusual.

The lower limit and target doses for the WHO recommendations are supported by the findings of a 2002 dose-response study in which Angus et al. evaluated the artesunate dose-response relationship using parasite clearance data from 47 non-pregnant Thai adults with uncomplicated *falciparum* malaria. These patients were randomized to groups receiving 0, 25, 50, 75, 100, 150, 200, or 250 mg artesunate, equivalent to 0 – 6 mg/kg; all patients received mefloquine one hour following artesunate administration. Using a sigmoid inhibitory effect model with mg/kg dose as the independent variable and shortening parasite clearance times as the effect, the investigators determined that for a typical individual, an artesunate dose of 2 mg/kg/day would provide for maximally effective concentrations (125). Ultimately, given the concentration variability observed with artesunate and DHA, the authors considered 4 mg/kg/day as part of combination therapy to be likely to yield maximally effective antimalarial concentrations in most patients.

Antimalarial dosing regimens determined using dose response data solely from non-pregnant adults may not yield appropriate concentrations in young children and pregnant women. Barnes et al. state that overall antimalarial treatment failure rates are higher in young children and pregnant women than non-pregnant adults and conjecture that the lower concentrations which have been observed for many antimalarial drugs in these patients may, in conjunction with comparatively lower immunity, contribute to this higher failure rate (126). Although sufficient data are not available at present to evaluate this argument in its entirety with regard to artesunate, the population pharmacokinetic models presented in this thesis do predict that non-pregnant adults given 2 mg/kg artesunate will, on average, have higher DHA concentrations than children or pregnant women administered the same dose. Therefore, it is reasonable to assume that while 2 mg/kg artesunate was the lowest dose displaying maximum efficacy, on average, in non-pregnant Thai adults, a higher mg/kg dose may be needed to achieve maximal efficacy in

a typical young child or pregnant woman for both pharmacokinetic and physiological and immunological reasons.

Employing mg/kg dose as the independent variable to model treatment response may be practical in relatively homogenous groups, such as non-pregnant adults from the same region, who are expected to display somewhat similar drug concentrations following a given mg/kg dose; however, for modeling artesunate therapeutic response across a more clinically and demographically diverse group of patients, direct concentration-effect modeling may inform a more comprehensive understanding of the pharmacokinetic-pharmacodynamic relationship for artesunate. Were a model for this relationship established, a pharmacokinetic therapeutic target, such as a given DHA C_{max} or AUC, could be determined. Using such a target, population pharmacokinetic models, including those described in the preceding chapters of this thesis, could be utilized in rational dose selection for patients with various sets of covariates. Furthermore, using simulations, the proportion of patients with a given set of covariates displaying concentrations meeting the target could be predicted. Extensive work is presently being undertaken in research groups worldwide to establish such targets for various patient populations. For example, the Worldwide Antimalarial Resistance Network is working to compile drug concentrations, patient demographic and clinical characteristics, and treatment outcomes data for antimalarial drugs from researchers and clinicians across numerous countries (127).

Partner drugs in children and pregnant women

The efficacy of artemisinin-based pharmacologic treatment of uncomplicated malaria is not only potentially influenced by concentrations of the artemisinin derivative, but also presumably by concentrations of the partner drug. Three days of treatment with an artemisinin derivative alone would result in a poor success rate; the short duration of treatment utilized with artemisinin-based combination therapies is built on the

assumption that the long-acting partner drug will eliminate the parasites remaining after the third day of treatment. Therefore, the pharmacokinetics of these partner drugs in children and pregnant women merit attention. There is some evidence that young children display higher weight-adjusted clearance than adults of the antimalarials lumefantrine, sulfadoxine, pyrimethamine, and piperaquine (79). Studies regarding partner drug pharmacokinetics in pregnancy are somewhat limited. However, available studies suggest that pregnancy may be associated with lower peak concentrations of mefloquine and lower exposure to sulfadoxine and pyrimethamine; there is also somewhat tenuous evidence for lower day 7 lumefantrine concentrations in pregnant women (128).

Overall, this research suggests that exposure to various partner drugs may be lower in young children and pregnant women given the same mg/kg dose as a non-pregnant adult. As one role of the partner drug is to eliminate any parasites displaying reduced susceptibility to artesunate, thereby reducing the risk of resistance development, these findings are particularly concerning. Furthermore, considering the findings presented in the preceding chapters of this thesis, a young child or pregnant women administered artesunate, as well as a partner drug with altered pharmacokinetics using standard dosing, would likely display lower concentrations of both DHA and the partner drug than would be observed in a non-pregnant adult patient. Such a circumstance could lead to treatment failure. This scenario underscores the need to fully optimize artesunate dosing in children and pregnant women given that, clearly, relying on the activity of the partner drug to ensure successful treatment in these populations would be unwise.

Pharmacokinetics and resistance

When evaluating the implications of individuals displaying abnormally low concentrations of an antimalarial agent, consideration must be given not only to the potential for suboptimal efficacy, but also the potential for encouragement of resistance

development. The initial step in emergence of resistance to an antimalarial can occur when *Plasmodium* parasites are exposed to antimalarial concentrations that suppress growth of fully sensitive parasites, but which are inadequate to suppress growth of parasites displaying decreased sensitivity to the antimalarial due to spontaneous mutations (129). Low antimalarial drug concentrations, such as might be displayed in patients with atypical pharmacokinetics, increase the probability of survival for these less sensitive parasites (129). However, given how rapidly artemisinin derivatives are eliminated, the period during which concentrations would allow for selection of less susceptible parasites would be quite short; for this reason, spontaneous emergence of resistance to the artemisinin derivatives was, for many years, considered extremely unlikely to occur. Unfortunately, following extensive use of artemisinin monotherapies in parts of Southeast Asia, patients on the Cambodia-Thailand border and, to a lesser extent, on the Myanmar-Thailand border began displaying infections with *falciparum* parasites having sufficiently decreased sensitivity to the artemisinin derivatives so as to discernibly influence parasite clearance times. The resistance has reached a level at which increasing the artesunate dose to 8 mg/kg/day or splitting the daily dose did not yield improvements in parasite clearance time. However, previously, an improvement in parasite clearance half-life for patients on the Myanmar-Thailand border, but not the Cambodia-Thailand border, had been demonstrated for 4 mg/kg dosing as compared to 2 mg/kg dosing (42). This suggests that, at least for parasites on the Myanmar-Thailand border, some degree of dose-response was still intact as of 2009. It is clear, then, that even with artemisinin antimalarials, reductions in susceptibility are possible. This possibility further reinforces the need for further investigation of the pharmacokinetics of artemisinin derivatives in groups, such as children and pregnant women, who may well have suboptimal concentrations. Barnes et al. posit that, for antimalarial drugs in general, underdosing of pregnant women and young children may be a potential cause of decreasing parasite susceptibility (126).

Needed future research

The efforts of the Worldwide Antimalarial Resistance Network may well yield highly useful findings in time. The developers of the database and data collection process have taken great care to request information regarding differences in drug concentration assays and parasite count evaluations. However, even armed with such information, adjusting for these differences is an imperfect process. Therefore, large scale clinical studies in which all data collected reflect the same drug assay and treatment response evaluation methods still have substantial merit. An ideal study for optimizing dosing pregnant women or young children would employ sparse sampling for artesunate and DHA concentrations in order to obtain concentrations from a large numbers of pregnant women or infants and young children receiving artesunate based combination therapies for uncomplicated malaria; additionally, demographic and clinical covariate data would be collected, as would parasite counts from as many time points as possible. Furthermore, whenever possible, samples would also be obtained to assay the concentrations of the partner drugs. Such a study would ideally also have less stringent inclusion criteria regarding co-morbidities and concomitant drugs than typically employed; this would enable development of a model potentially more applicable to the full clinical population of interest. Armed with all of the data from such a study, a population pharmacokinetic-pharmacodynamic model, incorporating important explanatory covariates, could be developed. In developing the pharmacodynamic model, various metrics associated with parasite clearance could be assessed as the outcome measure. Once the optimal full model was established, it could be utilized to identify the minimum dose expected to display maximum efficacy for very nearly all of the patients displaying specific combinations of clinical and demographic covariates included in the model.

APPENDIX A

CONTROL STREAM FOR LINEAR BSA MODEL IN CHAPTER 2

```

;PROJECT NAME: FINAL ANALYSIS
;PROJECT ID: NO PROJECT DESCRIPTION
$PROB RUN# RUN503
$INPUT ID TIME TAD DV AMT EVID CMT WT HT SEX GEO PARA LOGPA OCC HCT HGB RBC ALT AST
FORM AGE BSA DAY BMI LBM RBC1 HCT1 HGB1 FFM TRAD AGEGRP LBM2 AGEFLG
$DATA PEDONLY.CSV IGNORE=C
$SUBROUTINE ADVAN6 TRANS=1 TOL=6

$MODEL
NCOMPS=3
COMP= (DEPOT,DEFDOSE)
COMP= (CENTRAL,DEF OBS)
COMP= (METABOL,NODOSE)

$PK
TVCL=(THETA(1)*(BSA/1.23))*(THETA(6)**SEX)
MU_1 = LOG(TVCL)
CL = EXP(MU_1+ETA(1))
TVV2=(THETA(2)*(BSA/1.23))*(THETA(7)**SEX)
MU_2 = LOG(TVV2)
V2 = EXP(MU_2+ETA(2))
TVCLM=(THETA(3)*(BSA/1.23))*(THETA(8)**SEX)
MU_3 = LOG(TVCLM)
CLM = EXP(MU_3+ETA(3))
TVV3=(THETA(4)*(BSA/1.23))*(THETA(9)**SEX)
MU_4 = LOG(TVV3)
V3 = EXP(MU_4+ETA(4))
TVKA=THETA(5)*(1-FORM) + FORM*(10)
MU_5=LOG(TVKA)
KA=EXP(MU_5 + ETA(5))
K23=CL/V2
K30=CLM/V3
TAS=LOG(2)/K23
TDHA=LOG(2)/K30
S2=V2
S3=V3

$DES
DADT(1)=-KA*A(1)
DADT(2)=KA*A(1)-K23*A(2)
DADT(3)=K23*A(2)-K30*A(3)

$ERROR
PROP=0
IF(CMT.EQ.2)PROP=EPS(1)
IF(CMT.EQ.3)PROP=EPS(2)
IPRE=LOG(1)
IF(F.GT.0)IPRE=LOG(F)
Y=IPRE+PROP

$OMEGA BLOCK(4)
0.5 ;IIV CL
0.1 ;COV CL-V2
0.5 ;IIV V2
0.1 ;COV CLM-CL
0.1 ;COV CLM-V2
0.5 ; IIV CLM
0.1 ;COV V3-CL
0.1 ; COV V3-V2
0.1 ;COV V3-CLM
0.5 ;IIV V3

```

\$OMEGA
0.5 ;IIV KA

\$THETA
(0.1, 900) ;[CL]
(0.1,900) ;[V2]
(10,60) ;[CLM]
(10,80) ;[V3]
(0.1,4.5) ;[KA]
(1) ;[GENDER ON CL]
(1) ;[GENDER ON V2]
(1) ;[GENDER ON CLM]
(1) ;[GENDER ON V3]

\$SIGMA
0.8 ;[A] SIGMA(1,1)
0.8 ;[A] SIGMA(2,2)

\$EST METHOD=IMP SEED=54321 NITER=1000 CTYPE=3 NOABORT PRINT=1 SIGL=6

\$COV UNCONDITIONAL PRINT=E SIGL=9

\$TABLE ID TIME TAD DV CMT PRED EVID DV IPRE CWRES CL V2 V3 CLM KA WT AGE BMI BSA LBM
FFM TRAD SEX GEO ALT AST OCC DAY FORM ONEHEADER NOPRINT FILE=503.TAB
\$TABLE ID TIME CL V2 V3 CLM KA ONEHEADER NOAPPEND NOPRINT FILE=503.PAR
\$TABLE ID ETA1 ETA2 ETA3 ETA4 ETA5 FIRSONLY NOAPPEND NOPRINT ONEHEADER FILE=503.ETA
\$TABLE ID CL V2 V3 CLM KA ETA1 ETA2 ETA3 ETA4 ETA5 ONEHEADER NOAPPEND NOPRINT
FILE=PATAB503
\$TABLE ID IPRE ONEHEADER NOPRINT FILE=SDTAB503

APPENDIX B

CONTROL STREAM FOR ALLOMETRIC SCALING MODEL IN CHAPTER 2

```

;PROJECT NAME: FINAL ANALYSIS
;PROJECT ID: NO PROJECT DESCRIPTION
$PROB RUN# RUN504
$INPUT C ID TIME TAD DV AMT EVID CMT WT HT SEX GEO PARA LOGPA OCC HCT HGB RBC ALT
AST FORM AGE BSA DAY BMI LBM RBC1 HCT1 HGB1 FFM TRAD
$DATA PEDONLY.CSV IGNORE=C
$SUBROUTINE ADVAN6 TRANS=1 TOL=6

$MODEL
NCOMPS=3
COMP= (DEPOT,DEFDOSE)
COMP= (CENTRAL,DEF OBS)
COMP= (METABOL,NODOSE)

$PK
TVCL=(THETA(1)*(WT/38)**0.75)*(THETA(6)**SEX)
MU_1 = LOG(TVCL)
CL = EXP(MU_1+ETA(1))
TVV2=(THETA(2)*(WT/38))*(THETA(7)**SEX)
MU_2 = LOG(TVV2)
V2 = EXP(MU_2+ETA(2))
TVCLM=(THETA(3)*(WT/38)**0.75)*(THETA(8)**SEX)
MU_3 = LOG(TVCLM)
CLM = EXP(MU_3+ETA(3))
TVV3=(THETA(4)*(WT/38))*(THETA(9)**SEX)
MU_4 = LOG(TVV3)
V3 = EXP(MU_4+ETA(4))
TVKA=THETA(5)*(1-FORM) + FORM*(10)
MU_5=LOG(TVKA)
KA=EXP(MU_5 + ETA(5))
K23=CL/V2
K30=CLM/V3
TAS=LOG(2)/K23
TDHA=LOG(2)/K30
S2=V2
S3=V3

$DES
DADT(1)=-KA*A(1)
DADT(2)=KA*A(1)-K23*A(2)
DADT(3)=K23*A(2)-K30*A(3)

$ERROR
PROP=0
IF(CMT.EQ.2)PROP=EPS(1)
IF(CMT.EQ.3)PROP=EPS(2)
IPRE=LOG(1)
IF(F.GT.0)IPRE=LOG(F)
Y=IPRE+PROP

$OMEGA BLOCK(4)
0.5 ;IIV CL
0.1 ;COV CL-V2
0.5 ;IIV V2
0.1 ;COV CLM-CL
0.1 ;COV CLM-V2
0.5 ; IIV CLM
0.1 ;COV V3-CL
0.1 ; COV V3-V2
0.1 ;COV V3-CLM
0.5 ;IIV V3

```

\$OMEGA
0.5 ;IIV KA

\$THETA
(0.1, 900) ;[CL]
(0.1,900) ;[V2]
(10,60) ;[CLM]
(10,80) ;[V3]
(0.1,4.5) ;[KA]
(1) ; [GENDER ON CL]
(1) ; [GENDER ON V2]
(1) ; [GENDER ON CLM]
(1) ; [GENDER ON V3]

\$SIGMA
0.8 ;[A] SIGMA(1,1)
0.8 ;[A] SIGMA(2,2)

\$EST METHOD=IMP SEED=54321 NITER=1000 CTYPE=3 NOABORT PRINT=1 SIGL=6

\$COV UNCONDITIONAL PRINT=E SIGL=9

\$TABLE ID TIME TAD DV CMT PRED EVID DV IPRE CWRES CL V2 V3 CLM KA WT AGE BMI BSA LBM
FFM TRAD SEX GEO ALT AST OCC DAY FORM ONEHEADER NOPRINT FILE=504.TAB
\$TABLE ID TIME CL V2 V3 CLM KA ONEHEADER NOAPPEND NOPRINT FILE=504.PAR
\$TABLE ID ETA1 ETA2 ETA3 ETA4 ETA5 FIRSONLY NOAPPEND NOPRINT ONEHEADER FILE=504.ETA
\$TABLE ID CL V2 V3 CLM KA ETA1 ETA2 ETA3 ETA4 ETA5 ONEHEADER NOAPPEND NOPRINT
FILE=PATAB504
\$TABLE ID IPRE ONEHEADER NOPRINT FILE=SDTAB504

APPENDIX C

OUTPUT SUMMARY FOR LINEAR BSA MODEL IN CHAPTER 2

Estimation results

#1 Importance Sampling

Objective function value:	1505.895
Termination message:	optimization completed
Estimation time:	31m:29s
Covariance step time:	37s
Checks:	No boundary problems reported by NONMEM

Parameter estimates

Theta	Description	Estimate	FIX	SE	RSE	95%CI	[lower, upper]	init	upper
1	[CL]	884	-	91.3	10.3%	705.052- 1062.948	0.1	900	+Inf
2	[V2]	884	-	129	14.6%	631.16- 1136.84	0.1	900	+Inf
3	[CLM]	62.3	-	4.94	7.9%	52.618- 71.982	10	60	+Inf
4	[V3]	63.9	-	8.92	14%	46.417- 81.383	10	80	+Inf
5	[KA]	2.27	-	0.373	16.4%	1.539- 3.001	0.1	4.5	+Inf
6	[GENDER ON CL]	1.08	-	0.138	12.8%	0.81- 1.35	-Inf	1	+Inf
7	[GENDER ON V2]	1.06	-	0.201	19%	0.666- 1.454	-Inf	1	+Inf
8	[GENDER ON CLM]	1.05	-	0.111	10.6%	0.832- 1.268	-Inf	1	+Inf
9	[GENDER ON V3]	0.927	-	0.168	18.1%	0.598- 1.256	-Inf	1	+Inf

Omega	Description	Estimate	SE	RSE	Etabar	p val	Shrinkage
1,1	IIV CL	0.278	0.0645	23.2%	-0.002 (0.019)	0.9151	40.9%
2,1	.	0.346	0.0891	25.8%	.	.	.
2,2	IIV V2	0.827	0.159	19.2%	0.001 (0.033)	0.9845	39.9%
3,1	.	0.214	0.0473	22.1%	.	.	.
3,2	.	0.346	0.102	29.5%	.	.	.
3,3	IIV CLM	0.258	0.0746	28.9%	-0.002 (0.019)	0.9211	37.7%
4,1	.	0.267	0.0722	27%	.	.	.
4,2	.	0.208	0.106	51%	.	.	.
4,3	.	0.268	0.0905	33.8%	.	.	.
4,4	IIV V3	0.424	0.166	39.2%	-0.004 (0.022)	0.8627	43.9%
5,5	IIV KA	0.975	0.304	31.2%	0.043 (0.029)	0.137	51.5%

Sigma	Description	Estimate	SE	RSE	Shrinkage
1,1	[A] sigma(1,1)	0.583	0.101	(17.3%)	13.2%
2,2	[A] sigma(2,2)	0.872	0.0894	(10.3%)	5.1%

* Correlations in omega are shown as the off-diagonal elements. SAME blocks are not shown.
Output summary generated by Pirana 2.9.0

APPENDIX D

OUTPUT SUMMARY FOR ALLOMETRIC SCALING MODEL IN CHAPTER 2

Estimation results

#1 Importance Sampling

Objective function value:	1509.826
Termination message:	optimization completed
Estimation time:	32m:15s
Covariance step time:	37s
Checks:	No boundary problems reported by NONMEM

Parameter estimates

Theta	Description	Estimate	FIX	SE	RSE	95%CI	[lower, init, upper]
1	[CL]	923	-	95.6	10.4%	735.624- 1110.376	0.1 900 +Inf
2	[V2]	1130	-	157	13.9%	822.28- 1437.72	0.1 900 +Inf
3	[CLM]	65.1	-	5.12	7.9%	55.065- 75.135	10 60 +Inf
4	[V3]	79.1	-	11.5	14.5%	56.56- 101.64	10 80 +Inf
5	[KA]	2.46	-	0.383	15.6%	1.709- 3.211	0.1 4.5 +Inf
6	[GENDER ON CL]	1.07	-	0.14	13.1%	0.796- 1.344	-Inf 1 +Inf
7	[GENDER ON V2]	1.06	-	0.178	16.8%	0.711- 1.409	-Inf 1 +Inf
8	[GENDER ON CLM]	1.05	-	0.108	10.3%	0.838- 1.262	-Inf 1 +Inf
9	[GENDER ON V3]	0.891	-	0.157	17.6%	0.583- 1.199	-Inf 1 +Inf

Omega	Description	Estimate	SE	RSE	Etabar	p val	Shrinkage
1,1	IIV CL	0.279	0.0607	21.8%	-0.002 (0.019)	0.8989	41.1%
2,1	.	0.348	0.0861	24.7%	.	.	.
2,2	IIV V2	0.83	0.156	18.8%	0.003 (0.033)	0.9371	39.4%
3,1	.	0.21	0.0431	20.5%	.	.	.
3,2	.	0.336	0.0856	25.5%	.	.	.
3,3	IIV CLM	0.248	0.0655	26.4%	-0.002 (0.019)	0.9274	38%
4,1	.	0.259	0.0746	28.8%	.	.	.
4,2	.	0.178	0.1	56.2%	.	.	.
4,3	.	0.25	0.0912	36.5%	.	.	.
4,4	IIV V3	0.414	0.189	45.7%	-0.005 (0.021)	0.8152	44.7%
5,5	IIV KA	0.987	0.318	32.2%	0.042 (0.029)	0.1469	51.9%

Sigma	Description	Estimate	SE	RSE	Shrinkage
1,1	[A] sigma(1,1)	0.586	0.0982	(16.8%)	12.9%
2,2	[A] sigma(2,2)	0.876	0.0884	(10.1%)	6.9%

* Correlations in omega are shown as the off-diagonal elements. SAME blocks are not shown.
Output summary generated by Pirana 2.9.0

APPENDIX E

CONTROL STREAM FOR MODEL IN CHAPTER 3

```
;Model Desc: WITHOUT OUTLIER PREG ON CLM
;Project Name: final
;Project ID: NO PROJECT DESCRIPTIO
$PROB RUN# 600
$INPUT C ID AMT TIME DV CMT RATE EVID AGE WT BMI PREG HCT ALB AGP
$DATA GAM4.CSV IGNORE=C
$SUBROUTINE ADVAN5
```

```
$MODEL
```

```
  NCOMPS=3
  COMP=(DEPOT,DEFDOSE)
  COMP=(CENTRAL,DEFOBS)
  COMP=(METAB)
```

```
$PK
```

```
  TVK12=THETA(1)
  K12=THETA(1)*EXP(ETA(1))
  TVD2=THETA(2)
  D2=TVD2*EXP(ETA(2))
  TVALAG1=THETA(3)
  ALAG1=TVALAG1*EXP(ETA(3))
  TVCL=THETA(4)
  CL=TVCL*EXP(ETA(4))
  TVV2=THETA(5)
  V2=TVV2*EXP(ETA(5))
  TVCLM=THETA(6)*(1+THETA(9))*PRE
  G) CLM=TVCLM*EXP(ETA(6))
  TVV3=THETA(7)
  V3=TVV3*EXP(ETA(7))
  TVF1=THETA(8)
  F1=TVF1*EXP(ETA(8))
  MU_1=LOG(TVK12)
  MU_2=LOG(TVD2)
  MU_3=LOG(TVALAG)
  MU_4=LOG(TVCL)
  MU_5=LOG(TVV2)
  MU_6=LOG(TVCLM)
  MU_7=LOG(TVV3)
  MU_8=LOG(TVF1)
  IF(ALAG1<0)ALAG1=0
  IF(F1.LE.0)F1=0.001
  IF(F1.GE.1)F1=0.999
  F2=1-F1
  K23=(CL/V2)
  K30=(CLM/V3)
  DEL=0
  IF(TIME.NE.0)DEL=1
  S2=V2
  S3=V3
  SID=ID
  OBS=DV
```

```

$ERROR
PROP=0
IF(CMT.EQ.2)PROP=EPS(1)
IF(CMT.EQ.3)PROP=EPS(2)
IPRE=LOG(1)
IF(F.GT.0)IPRE=DEL*LOG(F)
Y=IPRE+PROP

$THETA
(0, 4.4, 10) ;[K12]
(0, 2.9) ; [D2]
(0, 0.6) ; [ALAG1]
(0, 966);[CL]
(0, 221) ; [V2]
(0, 80) ; [CLM]
(0, 104) ; [V3]
(0, 0.85, 1) ;[F1]
(-9999, 0.3) ;[PREG ON CLM]

$OMEGA
0.6 ;[P] omega K12
0.6 ;[P] omega D2
0.5 ;[P] omega ALAG1
0
FIXED0.
5 ;[P]
omega
V2
0.1 ;[P] omega CLM
0.05 ;[P] omega V3
0 FIXED

$SIGMA
0.5 ;[A] SIGMA(CMT2)
0.5 ;[A] SIGMA(CMT3)

$EST METHOD=IMP INTERACTION NOABORT NITER=100 PRINT=1 ISAMPLE=500

$COV MATRIX=R PRINT=E UNCONDITIONAL

$TABLE ID SID TIME CMT IPRE DV CWRES PRED EWRES ECWRES EPRED CPRED AGE WT BMI PREG HCT ALB AGP
K12 D2 ALAG1 CL V2 CLM V3 F1 NOPRINT ONEHEADER FILE=600.TAB
$TABLE ID CL V2 F1 K12 CLM V3 ALAG1 D2 NOPRINT ONEHEADER FILE=600.PAR
$TABLE ID SID TIME IPRE CMT ONEHEADER NOPRINT FILE=SDTAB600
$TABLE ID PREG ONEHEADER NOPRINT FILE=CATAB600
$TABLE ID AGE WT BMI HCT ALB AGP NOPRINT NOAPPEND FILE=COTAB600
$TABLE ID ETA1 ETA2 ETA3 ETA4 ETA5 ETA6 ETA7 ETA8 FIRSTONLY NOPRINT FILE=600.ETA
$TABLE ID CL V2 F1 K12 CLM V3 ALAG1 D2 ETA1 ETA2 ETA3 ETA4 ETA5
ETA6 ETA7 ETA8 ONEHEADER NOPRINT FILE=PATAB600

```


APPENDIX F

OUTPUT SUMMARY FOR MODEL IN CHAPTER 3

Estimation Methods:

1 Importance Sampling

Results for Importance Sampling

TERMINATION STATUS:

OPTIMIZATION NOT TESTED

FINAL VALUE OF OBJECTIVE FUNCTION: 525.370

COVARIANCE STEP SUCCESSFUL

MODEL DEFINITION:

ROUTINE ADVAN5

NCOMPS=3

COMP=(DEPOT,DEFDOSE)

COMP=(CENTRAL,DEFOBS)

COMP=(METAB)

TVK12=THETA(1)

K12=THETA(1)*EXP(ETA(1))

TVD2=THETA(2)

D2=TVD2*EXP(ETA(2))

TVALAG1=THETA(3)

ALAG1=TVALAG1*EXP(ETA(3))

TVCL=THETA(4)

CL=TVCL*EXP(ETA(4))

TVV2=THETA(5)

V2=TVV2*EXP(ETA(5))

TVCLM=THETA(6)*(1+THETA(9)*PREG)

CLM=TVCLM*EXP(ETA(6))

TVV3=THETA(7)

V3=TVV3*EXP(ETA(7))

TVF1=THETA(8)

F1=TVF1*EXP(ETA(8))

MU_1=LOG(TVK12)

MU_2=LOG(TVD2)

MU_3=LOG(TVALAG1)

MU_4=LOG(TVCL)

MU_5=LOG(TVV2)

MU_6=LOG(TVCLM)

MU_7=LOG(TVV3)

MU_8=LOG(TVF1)

IF(ALAG1<0)ALAG1=0

IF(F1.LE.0)F1=0.001

IF(F1.GE.1)F1=0.999

F2=1-F1

K23=(CL/V2)

K30=(CLM/V3)

DEL=0

IF(TIME.NE.0)DEL=1

S2=V2

S3=V3

SID=ID

OBS=DV

PROP=0

IF(CMT.EQ.2)PROP=EPS(1)

IF(CMT.EQ.3)PROP=EPS(2)

IPRE=LOG(1)

IF(F.GT.0)IPRE=DEL*
 LOG(F) Y=IPRE+PROP

TABLES CREATED: 600.TAB
 600.PAR SDTAB600 CATAB600
 COTAB600 600.ETA PATAB600

	FINAL ESTIMATE	%RSE	95% CONFIDENCE INTERVAL		DESCRIPTOR/ VARIABILITY
			LBOUND	UBOUND	
THETA					
1	4.28	23.6%	2.30	6.26	K12
2	4.04	19.5%	2.50	5.58	D2
3	0.627	10.9%	0.493	0.761	ALAG1
4	895	5.90%	792	998	CL
5	195	16.4%	132	258	V2
6	64.0	6.53%	55.8	72.2	CLM
7	91.4	6.15%	80.4	102	V3
8	0.864	1.56%	0.838	0.890	F1
9	0.423	30.3%	0.172	0.674	PREG ON CLM
INTERINDIVIDUAL VARIABILITY					
OMEGA					
1,1	1.84	25.3%	0.927	2.75	CV = 136%
2,2	1.33	22.9%	0.732	1.93	CV = 115%
3,3	0.573	20.8%	0.340	0.806	CV = 75.7%
4,4	0.00	?????????????
5,5	0.604	30.1%	0.247	0.961	CV = 77.7%
6,6	0.0802	24.9%	0.0410	0.119	CV = 28.3%
7,7	0.0790	34.7%	0.0253	0.133	CV = 28.1%
8,8	0.00	?????????????
RESIDUAL VARIABILITY					
SIGMA					
1,1	0.696	11.6%	0.537	0.855	SD = 0.834
2,2	0.174	9.94%	0.140	0.208	SD = 0.417

*Indicates 95% confidence interval that includes zero
 %RSE is percent relative standard error (100% x SE/EST)

Akaike Information
 Criterion: 563.37 Schwarz
 Bayesian Criterion: 652.33
 CONDITION NUMBER = 7.2 (DOES NOT EXCEED 1000)

APPENDIX G

LIST OF PUBLICATIONS

Morris C.A., Pokorny R., Lopez-Lazaro L., Miller R.M., Arbe-Barnes S., Duparc S., Borghini-Fuhrer I., Shin J-S., Fleckenstein L. Pharmacokinetic interaction between pyronaridine/artesunate and metoprolol. Accepted for publication by *Antimicrob. Agents Chemother.*

Morris, C.A.; Dueker, S. R.; Lohstroh, P. N.; Wang, L.-Q.; Fang, X.-P.; Jung, D.; Lopez-Lazaro, L.; Baker, M.; Duparc, S.; Borghini-Fuhrer, I., Mass balance and metabolism of the antimalarial pyronaridine in healthy volunteers. *Eur. J. Drug Metab. Pharmacokinet.* **2014**, 1-12.

Morris, C.A.; Tan, B.; Duparc, S.; Borghini-Fuhrer, I.; Jung, D.; Shin, C. S.; Fleckenstein, L., Effects of body size and gender on the population pharmacokinetics of artesunate and its active metabolite dihydroartemisinin in pediatric malaria patients. *Antimicrob. Agents Chemother.* **2013**, 57 (12), 5889-5900.

Morris, C. A.; Lopez-Lazaro, L.; Jung, D.; Methaneethorn, J.; Duparc, S.; Borghini-Fuhrer, I.; Pokorny, R.; Shin, C.-S.; Fleckenstein, L., Drug-drug interaction analysis of pyronaridine/artesunate and ritonavir in healthy volunteers. *Am. J. Trop. Med. Hyg.* **2012**, 86 (3), 489.

Morris, C.A.; Duparc, S.; Borghini-Fuhrer, I.; Jung, D.; Shin, C. S.; Fleckenstein, L., Review of the clinical pharmacokinetics of artesunate and its active metabolite dihydroartemisinin following intravenous, intramuscular, oral or rectal administration. *Malar. J.* **2011**, 10, 263.

Morris, C. A.; Onyamboko, M. A.; Capparelli, E.; Koch, M. A.; Atibu, J.; Lokomba, V.; Douoguih, M.; Hemingway-Foday, J.; Wesche, D.; Ryder, R. W.; Bose, C.; Wright, L.; Tshetu, A. K.; Meshnick, S.; Fleckenstein, L., Population pharmacokinetics of artesunate and dihydroartemisinin in pregnant and non-pregnant women with malaria. *Malar. J.* **2011**, 10, 114.

REFERENCES

1. World Health Organization, World Malaria Report 2013. Geneva, Switzerland: WHO, 2014.
2. White, N. J.; Pukrittayakamee, S.; Hien, T. T.; Faiz, M. A.; Mokuolu, O. A.; Dondorp, A. M., Malaria. *Lancet* **2014**, 383 (9918), 723-35.
3. World Health Organization., *Guidelines for the Treatment of Malaria -- 2nd Edition, Rev. 1*. World Health Organization: Geneva, Switzerland, 2011.
4. Malaguarnera, L.; Musumeci, S., The Immune Response to Plasmodium Falciparum Malaria. *Lancet Infect. Dis.* **2002**, 2 (8), 472-8.
5. Crawley, J.; Chu, C.; Mtove, G.; Nosten, F., Malaria in Children. *Lancet* **2010**, 375 (9724), 1468-1481.
6. Schantz-Dunn, J.; Nour, N. M., Malaria and Pregnancy: A Global Health Perspective. *Rev. Obstet. Gynecol.* **2009**, 2 (3), 186 – 192.
7. Desai, M.; ter Kuile, F. O.; Nosten, F.; McGready, R.; Asamo, K.; Brabin, B.; Newman, R. D., Epidemiology and Burden of Malaria in Pregnancy. *Lancet Infect. Dis.* **2007**, 7 (2), 93-104.
8. Shulman, C. E.; Dorman, E. K.; Bulmer, J. N., Malaria as a Cause of Severe Anaemia in Pregnancy. *Lancet* **2002**, 360 (9331), 494.
9. Steketee, R. W.; Nahlen, B. L.; Parise, M. E.; Menendez, C., The Burden of Malaria in Pregnancy in Malaria-Endemic Areas. *Am. J. Trop. Med. Hyg.* **2001**, 64 (1-2 Suppl), 28-35.
10. World Health Organization. *WHO Policy Recommendation on Intermittent Preventative Treatment During Infancy with Sulfadoxine-Pyrimethamine (SP-IPTi) for Plasmodium Falciparum Malaria Control in Africa*; World Health Organization: Geneva, Switzerland, 2010.
11. Gautam, A.; Ahmed, T.; Batra, V.; Paliwal, J., Pharmacokinetics and Pharmacodynamics of Endoperoxide Antimalarials. *Curr. Drug Metab.* **2009**, 10 (3), 289-306.
12. Anderson, G. D., Pregnancy-Induced Changes in Pharmacokinetics. *Clin. Pharmacokinet.* **2005**, 44 (10), 989-1008.
13. Morris, C. A.; Duparc, S.; Borghini-Fuhrer, I.; Jung, D.; Shin, C. S.; Fleckenstein, L., Review of the Clinical Pharmacokinetics of Artesunate and Its Active Metabolite Dihydroartemisinin Following Intravenous, Intramuscular, Oral or Rectal Administration. *Malar. J.* **2011**, 10, 263.

14. Augustijns, P.; D'Hulst, A.; Van Daele, J.; Kinget, R., Transport of Artemisinin and Sodium Artesunate in Caco-2 Intestinal Epithelial Cells. *J. Pharm. Sci.* **1996**, *85* (6), 577-579.
15. Kauss, T.; Fawaz, F.; Guyot, M.; Lagueny, A. M.; Dos Santos, I.; Bonini, F.; Olliaro, P.; Caminiti, A.; Millet, P., Fixed Artesunate-Amodiaquine Combined Pre-Formulation Study for the Treatment of Malaria. *Int. J. Pharm.* **2010**, *395* (1-2), 198-204.
16. Lindegardh, N.; Hanpithakpong, W.; Kamanikom, B.; Singhasivanon, P.; Socheat, D.; Yi, P.; Dondorp, A. M.; McGready, R.; Nosten, F.; White, N. J.; Day, N. P., Major Pitfalls in the Measurement of Artemisinin Derivatives in Plasma in Clinical Studies. *J. Chromatogr. B Analyt. Technol. Biomed. Life Sci.* **2008**, *876* (1), 54-60.
17. Li, Q.; Xie, L. H.; Haeberle, A.; Zhang, J.; Weina, P., The Evaluation of Radiolabeled Artesunate on Tissue Distribution in Rats and Protein Binding in Humans. *Am. J. Trop. Med. Hyg.* **2006**, *75* (5), 817-826.
18. Xie, L. H.; Li, Q.; Zhang, J.; Weina, P. J., Pharmacokinetics, Tissue Distribution and Mass Balance of Radiolabeled Dihydroartemisinin in Male Rats. *Malar. J.* **2009**, *8*, 112.
19. Batty, K. T.; Ilett, K. F.; Davis, T. M., Protein Binding and Alpha : Beta Anomer Ratio of Dihydroartemisinin in vivo. *Br. J. Clin. Pharmacol.* **2004**, *57* (4), 529-533.
20. Batty, K. T.; Ilett, K. F.; Powell, S. M.; Martin, J.; Davis, T. M., Relative Bioavailability of Artesunate and Dihydroartemisinin: Investigations in the Isolated Perfused Rat Liver and in Healthy Caucasian Volunteers. *Am. J. Trop. Med. Hyg.* **2002**, *66* (2), 130-136.
21. Batty, K. T.; Le, A. T.; Ilett, K. F.; Nguyen, P. T.; Powell, S. M.; Nguyen, C. H.; Truong, X. M.; Vuong, V. C.; Huynh, V. T.; Tran, Q. B.; Nguyen, V. M.; Davis, T. M., A Pharmacokinetic and Pharmacodynamic Study of Artesunate for Vivax Malaria. *Am. J. Trop. Med. Hyg.* **1998**, *59* (5), 823-827.
22. Batty, K. T.; Thu, L. T.; Davis, T. M.; Ilett, K. F.; Mai, T. X.; Hung, N. C.; Tien, N. P.; Powell, S. M.; Thien, H. V.; Binh, T. Q.; Kim, N. V., A Pharmacokinetic and Pharmacodynamic Study of Intravenous vs Oral Artesunate in Uncomplicated Falciparum Malaria. *Br. J. Clin. Pharmacol.* **1998**, *45* (2), 123-129.
23. Binh, T. Q.; Ilett, K. F.; Batty, K. T.; Davis, T. M.; Hung, N. C.; Powell, S. M.; Thu, L. T.; Thien, H. V.; Phuong, H. L.; Phuong, V. D., Oral Bioavailability of Dihydroartemisinin in Vietnamese Volunteers and in Patients with Falciparum Malaria. *Br. J. Clin. Pharmacol.* **2001**, *51* (6), 541-546.
24. Byakika-Kibwika, P.; Lamorde, M.; Mayito, J.; Nabukeera, L.; Mayanja-Kizza, H.; Katabira, E.; Hanpithakpong, W.; Obua, C.; Pakker, N.; Lindegardh, N., Pharmacokinetics and Pharmacodynamics of Intravenous Artesunate During Severe Malaria Treatment in Ugandan Adults. *Malar. J.* **2012**, *11*, 132.

25. Davis, T. M.; Phuong, H. L.; Ilett, K. F.; Hung, N. C.; Batty, K. T.; Phuong, V. D.; Powell, S. M.; Thien, H. V.; Binh, T. Q., Pharmacokinetics and Pharmacodynamics of Intravenous Artesunate in Severe Falciparum Malaria. *Antimicrob. Agents Chemother.* **2001**, *45* (1), 181-186.
26. Ilett, K. F.; Batty, K. T.; Powell, S. M.; Binh, T. Q.; Thu le, T. A.; Phuong, H. L.; Hung, N. C.; Davis, T. M., The Pharmacokinetic Properties of Intramuscular Artesunate and Rectal Dihydroartemisinin in Uncomplicated Falciparum Malaria. *Br. J. Clin. Pharmacol.* **2002**, *53* (1), 23-30.
27. Krishna, S.; Planche, T.; Agbenyega, T.; Woodrow, C.; Agranoff, D.; Bedu-Addo, G.; Owusu-Ofori, A. K.; Appiah, J. A.; Ramanathan, S.; Mansor, S. M.; Navaratnam, V., Bioavailability and Preliminary Clinical Efficacy of Intrarectal Artesunate in Ghanaian Children with Moderate Malaria. *Antimicrob. Agents Chemother.* **2001**, *45* (2), 509-516.
28. Li, Q.; Cantilena, L. R.; Leary, K. J.; Saviolakis, G. A.; Miller, R. S.; Melendez, V.; Weina, P. J., Pharmacokinetic Profiles of Artesunate after Single Intravenous Doses at 0.5, 1, 2, 4, and 8 mg/kg in Healthy Volunteers: A Phase I Study. *Am. J. Trop. Med. Hyg.* **2009**, *81* (4), 615-621.
29. McGready, R.; Phyo, A. P.; Rijken, M. J.; Tarning, J.; Lindegardh, N.; Hanpithakpon, W.; Than, H. H.; Hlaing, N.; Zin, N. T.; Singhasivanon, P.; White, N. J.; Nosten, F., Artesunate/Dihydroartemisinin Pharmacokinetics in Acute Falciparum Malaria in Pregnancy: Absorption, Bioavailability, Disposition and Disease Effects. *Br. J. Clin. Pharmacol.* **2012**, *73* (3), 467-477.
30. Miller, R. S.; Li, Q.; Cantilena, L. R.; Leary, K. J.; Saviolakis, G. A.; Melendez, V.; Smith, B.; Weina, P. J., Pharmacokinetic Profiles of Artesunate Following Multiple Intravenous Doses of 2, 4, and 8 mg/kg in Healthy Volunteers: Phase 1b Study. *Malar. J.* **2012**, *11*, 255.
31. Nealon, C.; Dzeing, A.; Muller-Romer, U.; Planche, T.; Sinou, V.; Kombila, M.; Kremsner, P. G.; Parzy, D.; Krishna, S., Intramuscular Bioavailability and Clinical Efficacy of Artesunate in Gabonese Children with Severe Malaria. *Antimicrob. Agents Chemother.* **2002**, *46* (12), 3933-3939.
32. Newton, P. N.; Barnes, K. I.; Smith, P. J.; Evans, A. C.; Chierakul, W.; Ruangveerayuth, R.; White, N. J., The Pharmacokinetics of Intravenous Artesunate in Adults with Severe Falciparum Malaria. *Eur. J. Clin. Pharmacol.* **2006**, *62* (12), 1003-1009.
33. Hess, K. M.; Goad, J. A.; Arguin, P. M., Intravenous Artesunate for the Treatment of Severe Malaria. *Ann. Pharmacother.* **2010**, *44* (7-8), 1250-1258.
34. Ilett, K. F.; Ethell, B. T.; Maggs, J. L.; Davis, T. M.; Batty, K. T.; Burchell, B.; Binh, T. Q.; Thu le, T. A.; Hung, N. C.; Pirmohamed, M.; Park, B. K.; Edwards, G., Glucuronidation of Dihydroartemisinin in Vivo and by Human Liver Microsomes

- and Expressed UDP-Glucuronosyltransferases. *Drug Metab. Dispos.* **2002**, *30* (9), 1005-1012.
35. Newton, P.; Suputtamongkol, Y.; Teja-Isavadharm, P.; Pukrittayakamee, S.; Navaratnam, V.; Bates, I.; White, N., Antimalarial Bioavailability and Disposition of Artesunate in Acute Falciparum Malaria. *Antimicrob. Agents Chemother.* **2000**, *44* (4), 972-977.
 36. Ittarat, W.; Looareesuwan, S.; Pootrakul, P.; Sumpunsirikul, P.; Vattanavibool, P.; Meshnick, S. R., Effects of Alpha-Thalassemia on Pharmacokinetics of the Antimalarial Agent Artesunate. *Antimicrob. Agents Chemother.* **1998**, *42* (9), 2332-2335.
 37. Hien, T. T.; Davis, T. M.; Chuong, L. V.; Ilett, K. F.; Sinh, D. X.; Phu, N. H.; Agus, C.; Chiswell, G. M.; White, N. J.; Farrar, J., Comparative Pharmacokinetics of Intramuscular Artesunate and Artemether in Patients with Severe Falciparum Malaria. *Antimicrob. Agents Chemother.* **2004**, *48* (11), 4234-4239.
 38. Hendriksen, I. C.; Mtove, G.; Kent, A.; Gesase, S.; Reyburn, H.; Lemnge, M. M.; Lindegardh, N.; Day, N. P.; von Seidlein, L.; White, N. J., Population Pharmacokinetics of Intramuscular Artesunate in African Children with Severe Malaria: Implications for a Practical Dosing Regimen. *Clin. Pharmacol. Ther.* **2013**, *93* (5), 443-450.
 39. Olliaro, P. L.; Nair, N. K.; Sathasivam, K.; Mansor, S. M.; Navaratnam, V., Pharmacokinetics of Artesunate after Single Oral Administration to Rats. *BMC Pharmacol.* **2001**, *1*, 12.
 40. Haynes, R. K.; Chan, H. W.; Lung, C. M.; Ng, N. C.; Wong, H. N.; Shek, L. Y.; Williams, I. D.; Cartwright, A.; Gomes, M. F., Artesunate and Dihydroartemisinin (DHA): Unusual Decomposition Products Formed under Mild Conditions and Comments on the Fitness of DHA as an Antimalarial Drug. *ChemMedChem.* **2007**, *2* (10), 1448-1463.
 41. Diem Thuy, L. T.; Ngoc Hung, L.; Danh, P. T.; Na-Bangchang, K., Absence of Time-Dependent Artesunate Pharmacokinetics in Healthy Subjects During 5-Day Oral Administration. *Eur. J. Clin. Pharmacol.* **2008**, *64* (10), 993-998.
 42. Dondorp, A. M.; Nosten, F.; Yi, P.; Das, D.; Phyto, A. P.; Tarning, J.; Lwin, K. M.; Ariey, F.; Hanpithakpong, W.; Lee, S. J.; Ringwald, P.; Silamut, K.; Imwong, M.; Chotivanich, K.; Lim, P.; Herdman, T.; An, S. S.; Yeung, S.; Singhasivanon, P.; Day, N. P.; Lindegardh, N.; Socheat, D.; White, N. J., Artemisinin Resistance in Plasmodium falciparum malaria. *N. Engl. J. Med.* **2009**, *361* (5), 455-467.
 43. Karbwang, J.; Na-Bangchang, K.; Congpoung, K.; Thanavibul, A.; Harinasuta, T., Pharmacokinetics of Oral Artesunate in Thai Patients with Uncomplicated Falciparum Malaria. *Clin. Drug Investig.* **1998**, *15* (1), 37-43.

44. Na-Bangchang, K.; Karbwang, J.; Congpoung, K.; Thanavibul, A.; Ubalee, R., Pharmacokinetic and Bioequivalence Evaluation of Two Generic Formulations of Oral Artesunate. *Eur. J. Clin. Pharmacol.* **1998**, *53* (5), 375-376.
45. Navaratnam, V.; Mansor, S. M.; Mordi, M. N.; Akbar, A.; Abdullah, M. N., Comparative Pharmacokinetic Study of Oral and Rectal Formulations of Artesunic Acid in Healthy Volunteers. *Eur. J. Clin. Pharmacol.* **1998**, *54* (5), 411-414.
46. Krudsood, S.; Looareesuwan, S.; Tangpukdee, N.; Wilairatana, P.; Phumratanapapin, W.; Leowattana, W.; Chalermrut, K.; Ramanathan, S.; Navaratnam, V.; Olliaro, P.; Vaillant, M.; Kiechel, J. R.; Taylor, W. R., New Fixed-Dose Artesunate-Mefloquine Formulation against Multidrug-Resistant Plasmodium Falciparum in Adults: A Comparative Phase I/II Safety and Pharmacokinetic Study with Standard-Dose Nonfixed Artesunate Plus Mefloquine. *Antimicrob. Agents Chemother.* **2010**, *54* (9), 3730-3737.
47. Navaratnam, V.; Ramanathan, S.; Wahab, M. S.; Siew Hua, G.; Mansor, S. M.; Kiechel, J. R.; Vaillant, M.; Taylor, W. R.; Olliaro, P., Tolerability and Pharmacokinetics of Non-Fixed and Fixed Combinations of Artesunate and Amodiaquine in Malaysian Healthy Normal Volunteers. *Eur. J. Clin. Pharmacol.* **2009**, *65* (8), 809-821.
48. Orrell, C.; Little, F.; Smith, P.; Folb, P.; Taylor, W.; Olliaro, P.; Barnes, K. I., Pharmacokinetics and Tolerability of Artesunate and Amodiaquine Alone and in Combination in Healthy Volunteers. *Eur. J. Clin. Pharmacol.* **2008**, *64* (7), 683-690.
49. Ramharter, M.; Kurth, F.; Schreier, A. C.; Nemeth, J.; Glasenapp, I.; Belard, S.; Schlie, M.; Kammer, J.; Koumba, P. K.; Cisse, B.; Mordmuller, B.; Lell, B.; Issifou, S.; Ouevray, C.; Fleckenstein, L.; Kremsner, P. G., Fixed-Dose Pyronaridine-Artesunate Combination for Treatment of Uncomplicated Falciparum Malaria in Pediatric Patients in Gabon. *J. Infect. Dis.* **2008**, *198* (6), 911-919.
50. Teja-Isavadharm, P.; Watt, G.; Eamsila, C.; Jongsakul, K.; Li, Q.; Keeratithakul, G.; Sirisopana, N.; Luesutthiviboon, L.; Brewer, T. G.; Kyle, D. E., Comparative Pharmacokinetics and Effect Kinetics of Orally Administered Artesunate in Healthy Volunteers and Patients with Uncomplicated falciparum Malaria. *Am. J. Trop. Med. Hyg.* **2001**, *65* (6), 717-721.
51. Awad, M. I.; Eltayeb, I. B.; Baraka, O. Z.; Behrens, R. H.; Alkadru, A. M., Pharmacokinetics of Artesunate Following Oral and Rectal Administration in Healthy Sudanese Volunteers. *Trop. Doct.* **2004**, *34* (3), 132-135.
52. Benakis, A.; Paris, M.; Loutan, L.; Plessas, C. T.; Plessas, S. T., Pharmacokinetics of Artemisinin and Artesunate after Oral Administration in Healthy Volunteers. *Am. J. Trop. Med. Hyg.* **1997**, *56* (1), 17-23.
53. Chanthap, L.; Tsuyuoka, R.; Na-Bangchang, K.; Nivanna, N.; Suksom, D.; Sovannarith, T.; Socheat, D., Investigation of Bioavailability, Pharmacokinetics and

- Safety of New Pediatric Formulations of Artesunate and Mefloquine. *Southeast Asian J. Trop. Med. Public Health* **2005**, *36* (1), 34-43.
54. Davis, T. M.; England, M.; Dunlop, A. M.; Page-Sharp, M.; Cambon, N.; Keller, T. G.; Heidecker, J. L.; Ilett, K. F., Assessment of the Effect of Mefloquine on Artesunate Pharmacokinetics in Healthy Male Volunteers. *Antimicrob. Agents Chemother.* **2007**, *51* (3), 1099-1101.
 55. McGready, R.; Stepniewska, K.; Ward, S. A.; Cho, T.; Gilveray, G.; Looareesuwan, S.; White, N. J.; Nosten, F., Pharmacokinetics of Dihydroartemisinin Following Oral Artesunate Treatment of Pregnant Women with Acute Uncomplicated Falciparum Malaria. *Eur. J. Clin. Pharmacol.* **2006**, *62* (5), 367-371.
 56. Miller, A. K.; Bandyopadhyay, N.; Wootton, D. G.; Duparc, S.; Kirby, P. L.; Winstanley, P. A.; Ward, S. A., Pharmacokinetics of Chlorproguanil, Dapsone, Artesunate and Their Major Metabolites in Patients During Treatment of Acute Uncomplicated Plasmodium Falciparum Malaria. *Eur. J. Clin. Pharmacol.* **2009**, *65* (10), 977-987.
 57. Mwesigwa, J.; Parikh, S.; McGee, B.; German, P.; Drysdale, T.; Kalyango, J. N.; Clark, T. D.; Dorsey, G.; Lindegardh, N.; Annerberg, A.; Rosenthal, P. J.; Kanya, M. R.; Aweeka, F., Pharmacokinetics of Artemether-Lumefantrine and Artesunate-Amodiaquine in Children in Kampala, Uganda. *Antimicrob. Agents Chemother.* **2010**, *54* (1), 52-59.
 58. Na-Bangchang, K.; Krudsood, S.; Silachamroon, U.; Molunto, P.; Tasanor, O.; Chalermrut, K.; Tangpukdee, N.; Matangkasombut, O.; Kano, S.; Looareesuwan, S., The Pharmacokinetics of Oral Dihydroartemisinin and Artesunate in Healthy Thai Volunteers. *Southeast Asian J. Trop. Med. Public Health* **2004**, *35* (3), 575-582.
 59. Ramharter, M.; Kurth, F. M.; Belard, S.; Bouyou-Akotet, M. K.; Mamfoumbi, M. M.; Agnandji, S. T.; Missinou, M. A.; Adegnika, A. A.; Issifou, S.; Cambon, N.; Heidecker, J. L.; Kombila, M.; Kremsner, P. G., Pharmacokinetics of Two Paediatric Artesunate Mefloquine Drug Formulations in the Treatment of Uncomplicated falciparum Malaria in Gabon. *J. Antimicrob. Chemother.* **2007**, *60* (5), 1091-1096.
 60. Zhang, S. Q.; Hai, T. N.; Ilett, K. F.; Huong, D. X.; Davis, T. M.; Ashton, M., Multiple Dose Study of Interactions between Artesunate and Artemisinin in Healthy Volunteers. *Br. J. Clin. Pharmacol.* **2001**, *52* (4), 377-385.
 61. Fehintola, F. A.; Scarsi, K. K.; Ma, Q.; Parikh, S.; Morse, G. D.; Taiwo, B.; Akinola, I. T.; Adewole, I. F.; Lindegardh, N.; Phakderaj, A., Nevirapine-Based Antiretroviral Therapy Impacts Artesunate and Dihydroartemisinin Disposition in HIV-Infected Nigerian Adults. *AIDS Res. Treat.* **2012**, *2012*.
 62. Fortin, A.; Verbeeck, R. K.; Jansen, F. H., Comparative Oral Bioavailability of Non-Fixed and Fixed Combinations of Artesunate and Amodiaquine in Healthy Indian Male Volunteers. *Eur. J. Clin. Pharmacol.* **2011**, *67* (3), 267-275.

63. Morris, C. A.; Lopez-Lazaro, L.; Jung, D.; Methaneethorn, J.; Duparc, S.; Borghini-Fuhrer, I.; Pokorny, R.; Shin, C.-S.; Fleckenstein, L., Drug-Drug Interaction Analysis of Pyronaridine/Artesunate and Ritonavir in Healthy Volunteers. *Am. J. Trop. Med. Hyg.* **2012**, *86* (3), 489 – 495.
64. Onyamboko, M. A.; Meshnick, S. R.; Fleckenstein, L.; Koch, M. A.; Atibu, J.; Lokomba, V.; Douoguih, M.; Hemingway-Foday, J.; Wesche, D.; Ryder, R. W.; Bose, C.; Wright, L. L.; Tshefu, A. K.; Capparelli, E. V., Pharmacokinetics and Pharmacodynamics of Artesunate and Dihydroartemisinin Following Oral Treatment in Pregnant Women with Asymptomatic Plasmodium Falciparum Infections in Kinshasa Drc. *Malar. J.* **2011**, *10*, 49.
65. Saunders, D.; Khemawoot, P.; Vanachayangkul, P.; Siripokasupkul, R.; Bethell, D.; Tyner, S.; Se, Y.; Rutvisuttinunt, W.; Sriwichai, S.; Chanthap, L.; Lin, J.; Timmermans, A.; Socheat, D.; Ringwald, P.; Noedl, H.; Smith, B.; Fukuda, M.; Teja-Isavadharm, P., Pharmacokinetics and Pharmacodynamics of Oral Artesunate Monotherapy in Patients with Uncomplicated Plasmodium Falciparum Malaria in Western Cambodia. *Antimicrob. Agents Chemother.* **2012**, *56* (11), 5484-5493.
66. Sinou, V.; Malaika, L. T.; Taudon, N.; Lwango, R.; Alegre, S. S.; Bertaux, L.; Sugnaux, F.; Parzy, D.; Benakis, A., Pharmacokinetics and Pharmacodynamics of a New ACT Formulation: Artesunate/Amodiaquine (Trimalact) Following Oral Administration in African Malaria Patients. *Eur. J. Drug Metab. Pharmacokinet.* **2009**, *34* (3-4), 133-142.
67. Valea, I.; Tinto, H.; Traore, M.; Toe, L. C.; Lindegardh, N.; Tarning, J.; Van Geertruyden, J.-P.; D'Alessandro, U.; Davies, G. R.; Ward, S. A., Pharmacokinetics of Co-Formulated Mefloquine and Artesunate in Pregnant and Non-Pregnant Women with Uncomplicated Plasmodium falciparum Infection in Burkina Faso. *J. Antimicrob. Chemother.* **2014**, epub ahead of print
68. Newton, P. N.; van Vugt, M.; Teja-Isavadharm, P.; Siriyanonda, D.; Rasameesoraj, M.; Teerapong, P.; Ruangveerayuth, R.; Slight, T.; Nosten, F.; Suputtamongkol, Y.; Looareesuwan, S.; White, N. J., Comparison of Oral Artesunate and Dihydroartemisinin Antimalarial Bioavailabilities in Acute Falciparum Malaria. *Antimicrob. Agents Chemother.* **2002**, *46* (4), 1125-1127.
69. Bethell, D. B.; Teja-Isavadharm, P.; Cao, X. T.; Pham, T. T.; Ta, T. T.; Tran, T. N.; Nguyen, T. T.; Pham, T. P.; Kyle, D.; Day, N. P.; White, N. J., Pharmacokinetics of Oral Artesunate in Children with Moderately Severe Plasmodium Falciparum Malaria. *Trans. R. Soc. Trop. Med. Hyg.* **1997**, *91* (2), 195-198.
70. Tan, B.; Naik, H.; Jang, I. J.; Yu, K. S.; Kirsch, L. E.; Shin, C. S.; Craft, J. C.; Fleckenstein, L., Population Pharmacokinetics of Artesunate and Dihydroartemisinin Following Single- and Multiple-Dosing of Oral Artesunate in Healthy Subjects. *Malar. J.* **2009**, *8* (1), 304.
71. Stepniewska, K.; Taylor, W.; Sirima, S. B.; Ouedraogo, E. B.; Ouedraogo, A.; Gansane, A.; Simpson, J. A.; Morgan, C. C.; White, N. J.; Kiechel, J. R., Population

- Pharmacokinetics of Artesunate and Amodiaquine in African Children. *Malar. J.* **2009**, *8*, 200.
72. Sirivichayakul, C.; Sabchareon, A.; Pengsaa, K.; Thaiarporn, I.; Chaivisuth, A.; Na-Bangchang, K.; Wisetsing, P.; Chanthavanich, P.; Pojjaroen-Anant, C., Comparative Study of the Effectiveness and Pharmacokinetics of Two Rectal Artesunate/Oral Mefloquine Combination Regimens for the Treatment of Uncomplicated Childhood Falciparum Malaria. *Ann. Trop. Paediatr.* **2007**, *27* (1), 17-24.
 73. Halpaap, B.; Ndjave, M.; Paris, M.; Benakis, A.; Kremsner, P. G., Plasma Levels of Artesunate and Dihydroartemisinin in Children with Plasmodium Falciparum Malaria in Gabon after Administration of 50-Milligram Artesunate Suppositories. *Am. J. Trop. Med. Hyg.* **1998**, *58* (3), 365-368.
 74. Simpson, J. A.; Agbenyega, T.; Barnes, K. I.; Di Perri, G.; Folb, P.; Gomes, M.; Krishna, S.; Krudsood, S.; Looareesuwan, S.; Mansor, S.; McIlleron, H.; Miller, R.; Molyneux, M.; Mwenchanya, J.; Navaratnam, V.; Nosten, F.; Olliaro, P.; Pang, L.; Ribeiro, I.; Tembo, M.; van Vugt, M.; Ward, S.; Weerasuriya, K.; Win, K.; White, N. J., Population Pharmacokinetics of Artesunate and Dihydroartemisinin Following Intra-Rectal Dosing of Artesunate in Malaria Patients. *PLoS Med.* **2006**, *3* (11), e444.
 75. Karunajeewa, H. A.; Ilett, K. F.; Dufall, K.; Kemiki, A.; Bockarie, M.; Alpers, M. P.; Barrett, P. H.; Vicini, P.; Davis, T. M., Disposition of Artesunate and Dihydroartemisinin after Administration of Artesunate Suppositories in Children from Papua New Guinea with Uncomplicated Malaria. *Antimicrob. Agents Chemother.* **2004**, *48* (8), 2966-2972.
 76. van Vugt, M.; Edstein, M. D.; Proux, S.; Lay, K.; Ooh, M.; Looareesuwan, S.; White, N. J.; Nosten, F., Absence of an Interaction between Artesunate and Atovaquone--Proguanil. *Eur. J. Clin. Pharmacol.* **1999**, *55* (6), 469-474.
 77. Minzi, O. M.; Gupta, A.; Haule, A. F.; Kagashe, G. A.; Massele, A. Y.; Gustafsson, L. L., Lack of Impact of Artesunate on the Disposition Kinetics of Sulfadoxine/Pyrimethamine When the Two Drugs Are Concomitantly Administered. *Eur. J. Clin. Pharmacol.* **2007**, *63* (5), 457-462.
 78. Mercer, A. E.; Sarr Sallah, M., The Pharmacokinetic Evaluation of Artemisinin Drugs for the Treatment of Malaria in Paediatric Populations. *Expert Opin. Drug Metab. Toxicol.* **2011**, *7* (4), 427-39.
 79. Pawluk, S. A.; Wilby, K. J.; Ensom, M. H., Pharmacokinetic Profile of Artemisinin Derivatives and Companion Drugs Used in Artemisinin-Based Combination Therapies for the Treatment of Plasmodium Falciparum Malaria in Children. *Clin. Pharmacokinet.* **2013**, *52* (3), 153-67.
 80. Morris, C. A.; Tan, B.; Duparc, S.; Borghini-Fuhrer, I.; Jung, D.; Shin, C. S.; Fleckenstein, L., Effects of Body Size and Gender on the Population Pharmacokinetics of Artesunate and Its Active Metabolite Dihydroartemisinin in Pediatric Malaria Patients. *Antimicrob. Agents Chemother.* **2013**, *57* (12), 5889-900.

81. ICH Harmonized Tripartite Guidelines: Clinical Investigation of Medicinal Products in the Pediatric Population.
http://www.ich.org/fileadmin/Public_Web_Site/ICH_Products/Guidelines/Efficacy/E11/Step4/E11_Guideline.pdf (accessed July 16, 2014).
82. Kayentao, K.; Doumbo, O. K.; Penali, L. K.; Offianan, A. T.; Bhatt, K. M.; Kimani, J.; Tshefu, A. K.; Kokolomami, J. H.; Ramharter, M.; de Salazar, P. M.; Tiono, A. B.; Ouedraogo, A.; Bustos, M. D.; Quicho, F.; Borghini-Fuhrer, I.; Duparc, S.; Shin, C. S.; Fleckenstein, L., Pyronaridine-Artesunate Granules Versus Artemether-Lumefantrine Crushed Tablets in Children with Plasmodium Falciparum Malaria: A Randomized Controlled Trial. *Malar. J.* **2012**, *11* (1), 364.
83. Naik, H.; Murry, D. J.; Kirsch, L. E.; Fleckenstein, L., Development and Validation of a High-Performance Liquid Chromatography-Mass Spectroscopy Assay for Determination of Artesunate and Dihydroartemisinin in Human Plasma. *J. Chromatogr. B Analyt. Technol. Biomed. Life Sci.* **2005**, *816* (1-2), 233-242.
84. Bauer, R. J., NONMEM Users Guide: Introduction to NONMEM 7.2.0. **2011**
85. Lindbom, L.; Pihlgren, P.; Jonsson, E. N., Psn-Toolkit--a Collection of Computer Intensive Statistical Methods for Non-Linear Mixed Effect Modeling Using NONMEM. *Comput. Methods Programs Biomed.* **2005**, *79* (3), 241-57.
86. Keizer, R. J.; van Benten, M.; Beijnen, J. H.; Schellens, J. H.; Huitema, A. D., Pirana and Peluster: A Modeling Environment and Cluster Infrastructure for NONMEM. *Comput. Methods Programs Biomed.* **2011**, *101* (1), 72-79.
87. Beal, S. L., Ways to Fit a Pk Model with Some Data Below the Quantification Limit. *J. Pharmacokinet. Pharmacodyn.* **2001**, *28* (5), 481-504.
88. Haycock, G. B.; Schwartz, G. J.; Wisotsky, D. H., Geometric Method for Measuring Body Surface Area: A Height-Weight Formula Validated in Infants, Children, and Adults. *J. Pediatr.* **1978**, *93* (1), 62-66.
89. Bonate, P. L., *Pharmacokinetic-Pharmacodynamic Modeling and Simulation*. Springer: New York, 2011.
90. Gehan, E. A.; George, S. L., Estimation of Human Body Surface Area from Height and Weight. *Cancer Chemother. Rep.* **1970**, *54* (4), 225-235.
91. Mosteller, R., Simplified Calculation of Body-Surface Area. *N. Engl. J. Med.* **1987**, *317* (17), 1098.
92. Du Bois, D.; Du Bois, E. F., A Formula to Estimate the Approximate Surface Area If Height and Weight Be Known. *Arch. Intern. Med.* **1916**, *17*, 863-871.
93. Livingston, E. H.; Lee, S., Body Surface Area Prediction in Normal-Weight and Obese Patients. *Am. J. Physiol. Endocrinol. Metab.* **2001**, *281* (3), E586-E591.

94. Janmahasatian, S.; Duffull, S. B.; Ash, S.; Ward, L. C.; Byrne, N. M.; Green, B., Quantification of Lean Bodyweight. *Clin. Pharmacokinet.* **2005**, *44* (10), 1051-1065.
95. Foster, B. J.; Platt, R. W.; Zemel, B. S., Development and Validation of a Predictive Equation for Lean Body Mass in Children and Adolescents. *Ann. Hum. Biol.* **2012**, *39* (3), 171-182.
96. Peters, A. M.; Snelling, H. L.; Glass, D. M.; Bird, N. J., Estimation of Lean Body Mass in Children. *Br. J. Anaesth.* **2011**, *106* (5), 719-723.
97. Bird, N. J.; Henderson, B. L.; Lui, D.; Ballinger, J. R.; Peters, A. M., Indexing Glomerular Filtration Rate to Suit Children. *J. Nucl. Med.* **2003**, *44* (7), 1037-1043.
98. Boer, P., Estimated Lean Body Mass as an Index for Normalization of Body Fluid Volumes in Humans. *Am. J. Physiol.* **1984**, *247* (4 Pt 2), F632-6.
99. Gastonguay, M. R., A Full Model Estimation Approach for Covariate Effects: Inference Based on Clinical Importance and Estimation Precision. *AAPS J.* **2004**, *6* (Suppl 1), 3431.
100. Bergsma, T. T.; Knebel, W.; Fisher, J.; Gillespie, W. R.; Riggs, M. M.; Gibiansky, L.; Gastonguay, M. R., Facilitating Pharmacometric Workflow with the Metrumrg Package for R. *Comput. Methods Programs Biomed.* **2013**, *109* (1), 77-85.
101. Jonsson, E. N.; Karlsson, M. O., Xpose--an S-Plus Based Population Pharmacokinetic/Pharmacodynamic Model Building Aid for Nonmem. *Comput. Methods Programs Biomed.* **1999**, *58* (1), 51-64.
102. Evans, W. E.; Relling, M. V.; de Graaf, S.; Rodman, J. H.; Pieper, J. A.; Christensen, M. L.; Crom, W. R., Hepatic Drug Clearance in Children: Studies with Indocyanine Green as a Model Substrate. *J. Pharm. Sci.* **1989**, *78* (6), 452-456.
103. Oo, C.; Hill, G.; Dorr, A.; Liu, B.; Boellner, S.; Ward, P., Pharmacokinetics of Anti-Influenza Prodrug Oseltamivir in Children Aged 1-5 Years. *Eur. J. Clin. Pharmacol.* **2003**, *59* (5-6), 411-5.
104. Ross, A. K.; Davis, P. J.; Dear Gd, G. L.; Ginsberg, B.; McGowan, F. X.; Stiller, R. D.; Henson, L. G.; Huffman, C.; Muir, K. T., Pharmacokinetics of Remifentanyl in Anesthetized Pediatric Patients Undergoing Elective Surgery or Diagnostic Procedures. *Anesth. Analg.* **2001**, *93* (6), 1393-401.
105. de Wildt, S. N.; Kearns, G. L.; Leeder, J. S.; van den Anker, J. N., Glucuronidation in Humans. Pharmacogenetic and Developmental Aspects. *Clin. Pharmacokinet.* **1999**, *36* (6), 439-52.
106. Zaya, M. J.; Hines, R. N.; Stevens, J. C., Epirubicin Glucuronidation and Ugt2b7 Developmental Expression. *Drug Metab. Dispos.* **2006**, *34* (12), 2097-101.

107. Murry, D. J.; Crom, W. R.; Reddick, W. E.; Bhargava, R.; Evans, W. E., Liver Volume as a Determinant of Drug Clearance in Children and Adolescents. *Drug Metab. Dispos.* **1995**, *23* (10), 1110-6.
108. Urata, K.; Kawasaki, S.; Matsunami, H.; Hashikura, Y.; Ikegami, T.; Ishizone, S.; Momose, Y.; Komiyama, A.; Makuuchi, M., Calculation of Child and Adult Standard Liver Volume for Liver Transplantation. *Hepatology* **1995**, *21* (5), 1317-21.
109. Vallely, A.; Vallely, L.; Changalucha, J.; Greenwood, B.; Chandramohan, D., Intermittent Preventive Treatment for Malaria in Pregnancy in Africa: What's New, What's Needed? *Malar. J.* **2007**, *6*, 16.
110. Morris, C. A.; Onyamboko, M. A.; Capparelli, E.; Koch, M. A.; Atibu, J.; Lokomba, V.; Douoguih, M.; Hemingway-Foday, J.; Wesche, D.; Ryder, R. W.; Bose, C.; Wright, L.; Tshefu, A. K.; Meshnick, S.; Fleckenstein, L., Population Pharmacokinetics of Artesunate and Dihydroartemisinin in Pregnant and Non-Pregnant Women with Malaria. *Malar. J.* **2011**, *10*, 114.
111. Taylor, S. M.; Juliano, J. J.; Trotman, P. A.; Griffin, J. B.; Landis, S. H.; Kitsa, P.; Tshefu, A. K.; Meshnick, S. R., High-Throughput Pooling and Real-Time Pcr-Based Strategy for Malaria Detection. *J. Clin. Microbiol.* **2010**, *48* (2), 512-519.
112. Zhou, H., Pharmacokinetic Strategies in Deciphering Atypical Drug Absorption Profiles. *J. Clin. Pharmacol.* **2003**, *43* (3), 211-227.
113. Mandema, J. W.; Verotta, D.; Sheiner, L. B., Building Population Pharmacokinetic--Pharmacodynamic Models. I. Models for Covariate Effects. *J. Pharmacokinetic--Biopharm.* **1992**, *20* (5), 511-528.
114. Lindbom, L.; Ribbing, J.; Jonsson, E. N., Perl-Speaks-Nonmem (PsN)--a Perl Module for NONMEM Related Programming. *Comput. Methods Programs Biomed.* **2004**, *75* (2), 85-94.
115. Naik, H. Pharmacokinetics of Artesunate in Healthy Volunteers. University of Iowa, Iowa City, IA, USA, 2007.
116. Mennella, J. A.; Pepino, M. Y., Breast Pumping and Lactational State Exert Differential Effects on Ethanol Pharmacokinetics. *Alcohol (Fayetteville, N.Y.)* **2010**, *44* (2), 141-148.
117. Pepino, M. Y.; Steinmeyer, A. L.; Mennella, J. A., Lactational State Modifies Alcohol Pharmacokinetics in Women. *Alcohol. Clin. Exp. Res.* **2007**, *31* (6), 909-918.
118. Pepino, M. Y.; Mennella, J. A., Effects of Breast Pumping on the Pharmacokinetics and Pharmacodynamics of Ethanol During Lactation. *Clin. Pharmacol. Ther.* **2008**, *84* (6), 710-714

119. Ohman, I.; Luef, G.; Tomson, T., Effects of Pregnancy and Contraception on Lamotrigine Disposition: New Insights through Analysis of Lamotrigine Metabolites. *Seizure* **2008**, *17* (2), 199-202.
120. Pennell, P. B.; Newport, D. J.; Stowe, Z. N.; Helmers, S. L.; Montgomery, J. Q.; Henry, T. R., The Impact of Pregnancy and Childbirth on the Metabolism of Lamotrigine. *Neurology* **2004**, *62* (2), 292-295.
121. Mazzucchelli, I.; Onat, F. Y.; Ozkara, C.; Atakli, D.; Specchio, L. M.; Neve, A. L.; Gatti, G.; Perucca, E., Changes in the Disposition of Oxcarbazepine and Its Metabolites During Pregnancy and the Puerperium. *Epilepsia* **2006**, *47* (3), 504-509.
122. Papini, O.; da Cunha, S. P.; da Silva Mathes Ado, C.; Bertucci, C.; Moises, E. C.; de Barros Duarte, L.; de Carvalho Cavalli, R.; Lanchote, V. L., Kinetic Disposition of Lorazepam with Focus on the Glucuronidation Capacity, Transplacental Transfer in Parturients and Racemization in Biological Samples. *J. Pharm. Biomed. Anal.* **2006**, *40* (2), 397-403.
123. Nakai, A.; Sekiya, I.; Oya, A.; Koshino, T.; Araki, T., Assessment of the Hepatic Arterial and Portal Venous Blood Flows During Pregnancy with Doppler Ultrasonography. *Arch. Gynecol. Obstet.* **2002**, *266* (1), 25-29.
124. Bethell, D.; Se, Y.; Lon, C.; Socheat, D.; Saunders, D.; Teja-Isavadharm, P.; Khemawoot, P.; Darapiseth, S.; Lin, J.; Sriwichai, S., Dose-Dependent Risk of Neutropenia after 7-Day Courses of Artesunate Monotherapy in Cambodian Patients with Acute Plasmodium Falciparum Malaria. *Clin. Infect. Dis.* **2010**, *51* (12), e105-e114.
125. Angus, B. J.; Thaiaporn, I.; Chanthapadith, K.; Suputtamongkol, Y.; White, N. J., Oral Artesunate Dose-Response Relationship in Acute Falciparum Malaria. *Antimicrob. Agents Chemother.* **2002**, *46* (3), 778-782.
126. Barnes, K. I.; Watkins, W. M.; White, N. J., Antimalarial Dosing Regimens and Drug Resistance. *Trends Parasitol.* **2008**, *24* (3), 127-134.
127. Barnes, K. I.; Lindegardh, N.; Ogundahunsi, O.; Olliaro, P.; Plowe, C. V.; Randrianarivelojosa, M.; Gbotosho, G. O.; Watkins, W. M.; Sibley, C. H.; White, N. J., World Antimalarial Resistance Network (WARN) IV: Clinical Pharmacology. *Malar. J.* **2007**, *6* (1), 122.
128. Wilby, K. J.; Ensom, M. H., Pharmacokinetics of Antimalarials in Pregnancy: A Systematic Review. *Clin. Pharmacokinet.* **2011**, *50* (11), 705-723.
129. White, N. J.; Pongtavornpinyo, W.; Maude, R. J.; Saralamba, S.; Aguas, R.; Stepniewska, K.; Lee, S. J.; Dondorp, A. M.; White, L. J.; Day, N. P., Hyperparasitaemia and Low Dosing Are an Important Source of Anti-Malarial Drug Resistance. *Malar. J.* **2009**, *8*, 253.